Universidade de Aveiro Departamento de Química
2011

ANA SOFIA PEREIRA MOREIRA

ESTUDO DE ALTERAÇÕES ESTRUTURAIS EM MODELOS DE GALACTOMANANAS DO CAFÉ

STUDY OF STRUCTURAL CHANGES IN MODELS OF COFFEE GALACTOMANNANS

Universidade de Aveiro Departamento de Química
2011

ANA SOFIA PEREIRA MOREIRA

ESTUDO DE ALTERAÇÕES ESTRUTURAIS EM MODELOS DE GALACTOMANANAS DO CAFÉ

STUDY OF STRUCTURAL CHANGES IN MODELS OF COFFEE GALACTOMANNANS

Dissertação apresentada à Universidade de Aveiro para cumprimento dos requisitos necessários à obtenção do grau de Mestre em Química Analítica e Qualidade, realizada sob a orientação científica da Doutora Maria do Rosário Domingues, Professora Auxiliar do Departamento de Química da Universidade de Aveiro, e do Doutor Manuel António Coimbra Rodrigues da Silva, Professor Associado com Agregação do Departamento de Química da Universidade de Aveiro.

Apoio financeiro da FCT no âmbito do projecto PTDC/QUI-QUI/100044/2008.

Dedico este trabalho aos meus pais, aos meus irmãos e ao Vasco.

o júri

presidente

Prof. Doutor Artur Manuel Soares da Silva
professor catedrático da Universidade de Aveiro

Prof. Doutor Fernando Hermínio Ferreira Milheiro Nunes
professor auxiliar da Universidade de Trás-os-Montes e Alto Douro

Prof. Doutor Manuel António Coimbra Rodrigues da Silva
professor associado com agregação da Universidade de Aveiro

Prof. Doutora Maria do Rosário Gonçalves Reis Marques Domingues
professora auxiliar da Universidade de Aveiro

agradecimentos

Gostaria de expressar um especial e sincero agradecimento à Professora Maria Rosário Domingues e ao Professor Manuel António Coimbra, orientadores deste trabalho, pela constante motivação e pela disponibilidade revelada para a discussão e esclarecimento de quaisquer dúvidas.

Aos Professores Armando Duarte e Valdemar Esteves agradeço a disponibilidade de utilização da termobalança.

Ao Professor Carlos Silva e à Doutora Cláudia Passos agradeço a disponibilidade de utilização do laboratório para a realização das análises termogravimétricas.

Ao Professor Fernando Nunes da Universidade de Trás-os-Montes e Alto Douro agradeço a colaboração prestada.

Gostaria também de agradecer a todos os colegas do laboratório do Professor Manuel António e do grupo de espectrometria de massa que me receberam da melhor forma e me ajudaram sempre que necessário. Um especial agradecimento à Joana Simões, pela sua amizade e por estar sempre pronta para me ajudar, e à Cristina Barros, pelo seu apoio nos espectrómetros de massa.

Aos amigos, em especial à Vera, à Marina e à Ana, agradeço as suas palavras de incentivo e todos os momentos de alegria e pura descontracção.

Aos meus pais, aos meus irmãos e ao Vasco agradeço o apoio incondicional em todos os momentos da minha vida.

palavras-chave

Café, processamento térmico, galactomananas, oligossacarídeos modelo, espectrometria de massa, electrospray, MALDI

resumo

O processo de torra induz alterações estruturais nas galactomananas do café, os polissacarídeos mais abundantes nos grãos de café. Com o objectivo de saber mais sobre os produtos que são formados a partir das galactomananas em consequência do processo de torra, neste trabalho foi desenvolvida uma metodologia que usou oligossacarídeos modelo que foram submetidos a diferentes tratamentos térmicos utilizando uma termobalança. Esta metodologia permitiu a análise de compostos que se podem formar no processo de torra. A análise foi feita por espectrometria de massa (ESI-MS, MALDI-MS e ESI-MS^n), sendo os dados de MS complementados pela análise de açúcares por metilação.

Numa primeira fase foram estudados quatro oligossacarídeos estruturalmente relacionados com as galactomananas: β-(1→4)-D-manotriose, [α-(1→6)-D-galactosil]^{I}-β-(1→4)-D-manobiose, β-(1→4)-D-manotetraose e [α-(1→6)-D-galactosil]^{I}-β-(1→4)-D-manotriose. A metodologia desenvolvida permitiu verificar para todos os oligossacarídeos, a formação de produtos provenientes de reacções de despolimerização, desidratação, isomerização e polimerização. Destas, a polimerização por reacções de transglicosilação nunca foi reportada ocorrer durante a torra do café.

Com a metodologia desenvolvida foram ainda analisados os produtos das reacções promovidas pela torra de α-(1→5)-L-arabinotriose (estruturalmente relacionada com as cadeias laterais das arabinogalactanas, o segundo polissacarídeo mais abundante nos grãos de café) e de uma mistura de β-(1→4)-D-manotriose e α-(1→5)-L-arabinotriose. A menor estabilidade térmica da arabinotriose comparativamente aos oligossacarídeos de hexose foi evidenciada pela formação de novos tipos de produtos resultantes de quebras do anel da pentose e de reacções de oxidação. A análise da mistura de oligossacarídeos mostrou a formação de vários oligossacarídeos constituídos por resíduos de arabinose e manose. Esta observação reforça a hipótese de que os resíduos de arabinose libertados a partir das cadeias laterais das arabinogalactanas durante a torra podem estar ligados às galactomananas.

Os resultados obtidos mostraram que a utilização de uma termobalança para torra de oligossacarídeos modelo e a análise dos compostos formados por espectrometria de massa e análise de açúcares por metilação permitem identificar alterações estruturais que provavelmente também ocorrem nas galactomananas do café durante a torra e inferir muitas das reacções que ocorrem durante este processamento térmico.

keywords

Coffee, thermal processing, galactomannans, model oligosaccharides, mass spectrometry, electospray, MALDI

abstract

The roasting process induces structural changes in coffee galactomannans, the most abundant polysaccharide in coffee beans. Aiming to know more about the products generated from galactomannans as consequence of coffee roasting, in this work was developed a methodology using model oligosaccharides that were subjected to different thermal treatments using a thermobalance. This methodology allowed the analysis of compounds that can be formed during coffee roasting. The analysis was performed by (ESI-MS, MALDI-MS, and ESI-MS^n), being the MS data complemented by methylation analysis.

First, four oligosaccharides structurally related with galactomannans were studied: β-(1→4)-D-mannotriose, [α-(1→6)-D-galactosyl]^1-β-(1→4)-D-mannobiose, β-(1→4)-D-mannotetraose and [α-(1→6)-D-galactosyl]^1-β-(1→4)-D-mannotriose. The developed methodology allowed to observe for all oligosaccharides, the formation of products resulting from depolymerization, dehydration, isomerization, and polymerization reactions. The polymerization reactions occurring via transglycosylation reactions were never reported to occur during the coffee roasting.

With the developed methodology were also analysed the products resulting from the roasting of α-(1→5)-L-arabinotriose (structurally related with side chains of arabinogalactans, the second most abundant polysaccharide in coffee beans) and the mixture of β-(1→4)-D-mannotriose and α-(1→5)-L-arabinotriose. The lower thermal stability of arabinotriose was showed for the formation of new types of products, resulting from ring cleavages and oxidation reactions. The analysis of the oligosaccharide mixture showed the formation of oligosaccharides composed by arabinose and mannose residues. This observation supports the hypothesis that the arabinose residues lost from arabinogalactans during roasting can be linked to galactomannans.

The obtained results showed that the use of a thermobalance for roasting of model oligosaccharides and the analysis of the compounds formed by mass spectrometry and methylation analysis allow to identify structural changes that probably also occur in coffee galactomannans during roasting and to infer several reactions that occur during this thermal processing.

Contents

List of figures

List of tables

Abbreviations

Ara_3	α-(1→5)-L-arabinotriose
CAD	Collisionally activated dissociation
CI	Chemical ionization
CID	Collision-induced dissociation
CRM	Charge residue model
DHB	2,5-dihydroxybenzoic acid
DMSO	Dimethylsulfoxide
DP	Degree of polymerization
DTG	Derivative thermogravimetric (curve)
EI	Electron impact
ESI	Electrospray ionization
FT-ICR	Fourier transform ion cyclotron resonance
$GalMan_2$	[α-(1→6)-D-galactosyl]^{I}-β-(1→4)-D-mannobiose
$GalMan_3$	[α-(1→6)-D-galactosyl]^{I}-β-(1→4)-D-mannotriose
GC/MS	Gas chromatography/mass spectrometry
GG	Guar gum
Hex_{res}	Hexose residue
IEM	Ion evaporation model
LBG	Locust bean gum
m/z	Mass-to-charge ratio
$[M+H]^+$	Proton adduct ion
$[M+K]^+$	Potassium adduct ion
$[M+Na]^+$	Sodium adduct ion
MALDI	Matrix assisted laser desorption/ ionization
Man_3	β-(1→4)-D-mannotriose
Man_4	β-(1→4)-D-mannotetraose
MS	Mass spectrometry
MS^n	Tandem mass spectrometry
$Pent_{res}$	Pentose residue
PMAA	Partially *O*-methylated alditol acetates
TG	Tara gum
TG	Thermogravimetric (curve)
TOF	Time-of-flight

I. General introduction and aims of the work

Polysaccharides are biopolymers widely distributed in nature, being found in animals, plants, and microorganisms (1). These polymers are important in biological point of view, but also in many industrial applications. During the industrial processing, the polysaccharides can undergo structural modifications that can affect their properties and, consequently, the quality of the final product. In general, these structural changes occurring as consequence of industrial processing are largely unknown and, therefore, they continue to be of a great interest for research works.

Thermal processing is a form of industrial processing widely used within different industry sectors. Particularly in food industry, thermal processing (drying, frying, pasteurizing, roasting, sterilizing, etc) persists as the most widely used industrial procedure (2). However, no matter how minimal the heating source is, thermal processing can promote reactions that change the constituents of foods. Some substances arising from the heating processes can play a positive role on human health. The melanoidins formed during the coffee roasting process are an example of substances that are developed during thermal processing and that show positive effects on human health having antioxidant, antimicrobial, and antihypertensive properties (3). Nevertheless, the major concern arising from heating processes comes from the formation of compounds that can reveal a negative role on human health. Well known examples of these compounds are acrylamide and 5-hydroxymethylfurfural. These compounds, occurring mainly in bread and bakery products, are considered as probably carcinogenic to humans or might be

metabolized by humans to potentially carcinogenic compounds (4). The identification of these harmful compounds reinforces the need for studies to identify and characterize structural changes promoted by thermal processing.

Galactomannans are one of the most abundant polysaccharides in nature and they are the major polysaccharides present in coffee infusions prepared from roasted coffee beans (*5, 6*). It is well known that the roasting process promotes structural changes on the structure of coffee galactomannans (*5-11*). However, the reactions that occur inside the coffee bean during this thermal processing as well as the structural modifications that these reactions can induce in coffee galactomannans are far from being completely elucidated. This is probably due, on the one hand, to the complexity of the coffee bean and, on the other hand, to the diversity and complexity of the new structures formed. In consequence, the work presented in this dissertation aims to contribute to the identification of the reactions that occur during the coffee roasting process and that are responsible for changing the structural features of coffee galactomannans. The knowledge of the global changes that occur in the structure of coffee galactomannans during the roasting process can be crucial for future developments in coffee industry, namely in the area of quality control. For example, the new structures identified can be useful as chemical markers to control of the degree of roasting of coffee beans. This knowledge can also be useful for the implementation of new quality control protocols in other carbohydrate-based industries, namely other food industries.

A significant information concerning the specific reactions that can take place inside the coffee bean during roasting, modifying the structure of their components, can be obtained using model systems comprising a single (or few) class(es) of components. Based on this consideration, in this work a new methodology was developed using model systems comprising oligosaccharides structurally related with coffee galactomannans that were subjected to dry thermal processing mimicking the coffee roasting conditions and the resulting materials were then analysed. Mass spectrometry (MS) is a highly sensitive analytical technique, allowing the identification of structural modifications in compounds present at the picomole level, even when they are present in mixtures. Aiming to identify the structural changes on the structure of the model oligosaccharides promoted by the

thermal processing, the roasted materials were directly analysed by MS. The direct analysis by MS was complemented with the specific labelling of oligosaccharides before MS analysis and the glycosidic linkage composition determined by the preparation of partially *O*-methylated alditol acetates (PMAA) that were separated and analysed by gas chromatography/mass spectrometry (GC/MS).

Before presenting the results obtained, a literature review focusing the current knowledge as well as relevant studies that support the relevance of the developed work is presented in **section II** of the present dissertation. This literature review is divided into two main parts. In the first part, important aspects about galactomannans in general and coffee galactomannans in particular are described. In the second part of the literature review are presented the basic principles and practical aspects having in mind during the analysis of oligo- and polysaccharides by mass spectrometry, the main analytical technique used in this work. The experimental work, results, and discussions are then presented in **section III** of this dissertation, subdivided according to two different studies performed in order to accomplish the main objective of this work. Finally, in the **section IV** the main conclusions and perspectives for future work are presented.

II. Literature review

II.A. Galactomannans

II.A.1. Occurrence and general structure of galactomannans

Galactomannans are polysaccharides mainly found in the seed endosperm of many plant species (*12*). However, there are other sources of galactomannans, such as fungi (*13*) and lichens (*14, 15*). Seed galactomannans are the most reported in the literature, and are these that are also described in this literature review.

Most galactomannans studied were isolated from the endosperm of seeds belonging to the Leguminosae family. However, galactomannans have also been found in species of other families such as Annonaceae, Convolvulaceae, Palmae, and Rubiaceae. Some examples of seeds containing galactomannans are listed in **Table II.A.1**. The soybean seed (*Glycine max*) is an exception because their galactomannans do not appear located in seed endosperm and appear in seed hull.

The occurrence of galactomannans in seed endosperms has two main physiological functions. On one hand, they serve as an energy source for seed germination. On other hand, they interact with water molecules, preventing the complete dehydration of the seed that would lead to protein denaturation, especially of those enzymes essential for seed germination (*12, 16, 17*).

Table II.A.1. Examples of seeds containing galactomannans.

Family	Species	Reference(s)
Annonaceae	*Annona muricata*	*(18)*
Convolvulaceae	*Convolvulus tricolor*	*(18)*
Leguminosae	*Adenanthera pavonina*	*(19, 20)*
	Caesalpina spinosa	*(21)*
	Caesalpinia pulcherrima	*(19, 20)*
	Cassia angustifolia	*(22)*
	Cassia saltiana	*(23)*
	Cassia siamea	*(24)*
	Cassia javahikai	*(25)*
	Cassia pleurocarpa	*(26)*
	Cassia spectabilis	*(27)*
	Ceratonia siliqua	*(21)*
	Cyamopsis tetragonoloba	*(21)*
	Dimorphandra gardneriana	*(28)*
	Gleditsia triacanthos	*(19, 20, 29)*
	Glycine Max	*(30)*
	Glycyrrhiza uralensis	*(31)*
	Leucaena leucocephala	*(30)*
	Medicago sativa	*(23)*
	Mimosaceae spp.	*(32)*
	Parkinsonia aculeata	*(33)*
	Prosopis juliflora	*(21)*
	Retama raetam	*(34)*
	Senna obtusifolia	*(35)*
	Sophora japonica	*(18, 19, 29)*
	Trifolium alexandrinum	*(23)*
	Trigonella foenum-graecum	*(36)*
Palmae	*Arenga saccharifera*	*(18)*
	Cocos nucifera	*(18)*
	Phoenix dactylifera	*(30, 37)*
Rubiaceae	*Coffea arabica*	*(7, 9)*
	Coffea canephora (*Coffea* Robusta)	*(5, 38)*

Structurally, galactomannans have been classically described as linear polysaccharides with a main chain of β-(1→4)-linked D-mannose residues substituted at *O*-6 with side chains of a single α-D-galactose residue (*39*). However, galactomannans with a structure that differs from this fundamental structure have also been reported. For example, Ishurd et al. (*34*) studied the galactomannans isolated from *Retama raetam* seeds, extensively used by the Libyan population to control diabetes mellitus and for

treatment of hypertension, and concluded that these galactomannans have a backbone of β-(1→3)- and occasional β-(1→4)-linked D-mannose residues, and side chains, at positions *O*-6, of a single α-D-galactose residue. Also, studies for structural characterization of the galactomannans extracted with hot water from green coffee beans, the seeds of the coffee tree, showed the presence of acetyl groups (*40*), containing doubly acetylated hexose residues and contiguously acetylated hexose residues (*41*). Furthermore, arabinose and glucose residues were also found as structural features of hot water soluble green coffee galactomannans (*41*).

Also, the galactomannans from different species differ from one another in their mannose/galactose ratios as well as in the distribution of α-(1→6)-linked D-galactose residues along the mannan backbone (*21, 42*). In the Leguminosae family, the mannose/galactose ratio can even be used as a taxonomic marker. The three subfamilies (Caesalpinioideae, Mimosoideae, and Faboideae) of the Leguminosae differ in the mannose/galactose ratios of their galactomannans. The galactomannans of Caesalpinioideae present higher mannose/galactose ratios, whereas lower mannose/galactose ratios are characteristics of the Faboideae (*42*). For example, the galactomannans extracted from carob (*Ceratonia siliqua*) seeds (**Figure II.A.1**), belonging to the Caesalpinioideae subfamily, have mannose and galactose residues in the ratio of about 4. The galactomannans extracted from fenugreek (*Trigonella foenum-graecum*) seeds (**Figure II.A.1**), belonging to the Faboideae subfamily, present a mannose/galactose ratio of about 1, having all mannose residues in the backbone substituted at *O*-6 with a single galactose residue (*12*).

The differences in the degree of galactose substitution as well as in the distribution of galactose residues along the mannan backbone reported for galactomannans from different sources are reflected in their physicochemical properties, including, among others, the solubility in water. The molecules with larger mannose/galactose ratios can form intermolecular hydrogen bonds between unsubstituted regions in the mannan backbone. The presence of galactose side chains can prevent the formation of these hydrogen bonds. Thus, an increase in the degree of substitution leads to higher water solubility of the galactomannans (*36, 43*).

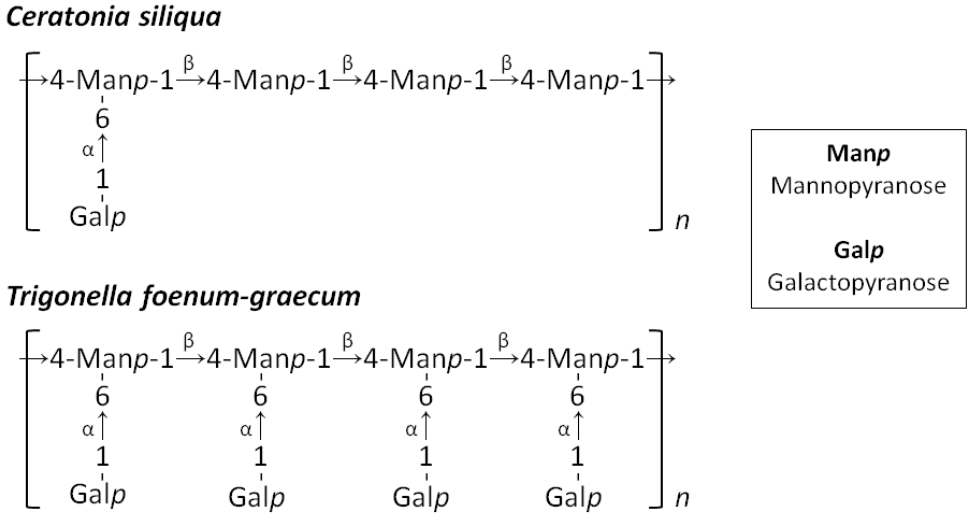

Figure II.A.1. Schematic representation of the structure of galactomannans from *Ceratonia siliqua* and *Trigonella foenum-graecum*.

II.A.2. Industrial applications of galactomannans

The galactomannans extracted from seeds are used in various industries worldwide and in various applications. Because of their high water binding capacity, galactomannans can form highly viscous solutions at low concentrations, making them useful as thickeners or stabilizers agents (*12*).

Due to their abundance in nature and relatively low cost as well as absence of toxicity, seed galactomannans are widely used in food industry, but they are also used in other industries, such as paper, cosmetic, pharmaceutical, and textile. In the food industry, the galactomananas extracted from seed sources are used as ingredients to food products, such as cream desserts, cheeses, sauces, soups, and frozen meats (*16*). These polysaccharides are used in the cosmetic industry as an ingredient for skin creams and body lotions. The galactomannans are used as additives in papermaking to improve the mechanical properties of paper sheets (*44*). In the pharmaceutical industry, the galactomannans are used as excipients in the preparation of solid dosage forms as well as an active ingredient in a variety of laxative formulations (*45*). These polysaccharides are also used for the treatment of coloured effluents from the textile industry (*46, 47*). Apart

from the current applications described above, potential applications for galactomannans have been reported in the literature. For example, studies have shown the suitability of galactomannans to produce edible coatings for cheese (*48*) and tropical fruits (*19*), aiming shelf life extension of these products.

The galactomannans, either as natural components of food or as additives, contribute significantly to the human intake of dietary fiber (*16*). The term dietary fiber is used as a collective term to designate indigestible carbohydrates of plant origin. The consumption of dietary fiber has come to be associated with beneficial effects on human health (*49*). Particularly for coffee galactomannans, recent studies have reported some of their beneficial effects. Srichamroen et al. (*50*) conducted an in vitro study to determine if galactomannans from fenugreek seeds affect intestinal glucose uptake in genetically determined lean and obese rats and concluded that the uptake of glucose is reduced in the presence of galactomannans. These results suggested that the galactomannans have the potential to reduce intestinal absorption of glucose and hence for the benefit of blood glucose management. Jaquet et al. (*51*) studied the impact of a moderate consumption of an instant coffee (galactomannans are the major polysaccharide of coffee brews) on the general composition of the human intestinal bacterial population of sixteen healthy adults. The results obtained showed that the moderate consumption of the coffee promotes an increase in the metabolic activity and/or numbers of the *Bifidobacterium* spp. population. Also, Simões et al. (*52*) showed that the galactomannans from roasted coffee infusions present immunostimulatory activity. Due to their indigestibility, galactomannans are not absorbed in the gastrointestinal tract but can stimulate the immune system.

Currently, the galactomannans of major commercial importance are extracted from *Cyamopsis tetragonoloba*, *Ceratonia siliqua*, and *Caesalpinia spinosa*, being commercially designated as guar gum (GG), locust bean gum (LBG), and tara gum (TG). Also, the seeds of the coffee tree (coffee beans), containing galactomannans in their composition, are commercially very important (*16*). Coffee, prepared from the roasted coffee beans, is one of the most popular beverages in the world (*53, 54*).

II.A.3. Structural features of coffee galactomannans and effects of the roasting process

Green coffee beans (**Figure II.A.2**) are the seeds from the fruit of coffee trees (called the coffee cherry), belonging to the Rubiaceae family and the *Coffea* genus. There are many species belonging to the genus *Coffea*, but only two are economically important: *Coffea arabica* and *Coffea canephora*, commonly designated as Arabica coffee and Robusta coffee, respectively. The coffee beans are mainly used in the preparation of the coffee beverage, obtained by hot water extraction from roasted and ground coffee beans (*54*).

Figure II.A.2. Cherry and beans (*54*).

The quality of the coffee beverage is influenced for all steps that occur between the seed maturation and the preparation of the beverage. All of these steps – the seed maturation, harvesting, drying, hulling, storage and transportation, roasting, grinding and brewing – have an impact on the sensory qualities of the coffee beverage; in particular, the roasting is a fundamental step in the development of the flavours. During the roasting process, many physical and chemical changes occur in the coffee beans (*54*).

The coffee roasting process involves submitting the beans to a high temperature for a certain period of time. In most of the conventional roasters, hot air is used to roast the coffee beans. The air is heated in a combustion unit and then sent to a roasting unit where the beans are roasted (*2*). The temperature inside the beans rises to about 200 °C during roasting. The roasting time may take as long as 40 minutes or as short as 90

seconds, depending on the degree of roasting desired. The roasting process is finished by rapid cooling of the beans, using air or water as cooling agent. The roasting process can be broken into three phases: drying phase, during which moisture is eliminated; roasting phase, where a number of complex reactions take place changing the composition of the beans; cooling phase, where the roasted coffee beans are quickly cooled down to the room temperature (*54*).

Polysaccharides are the major constituents of coffee beans, comprising almost half of its dry weight. Galactomannans are the predominant polysaccharides (22%), followed by type II arabinogalactans (14-17%) and then cellulose (7-9%) (*38, 53*). The total polysaccharide content is similar between Arabica and Robusta coffees; however, these coffee varieties differ in properties and relative proportions of their galactomannans and arabinogalactans (*5, 38, 55*).

Only 7% of the polysaccharides are extracted from green coffee beans by sequential extraction with water (90 °C, 1h), EDTA, 0.05M NaOH, 1M NaOH, and 4M NaOH. After roasting, 29% of the polysaccharides are extracted by using the same sequential extraction procedure (*8*). The increase of the extractable polysaccharides after roasting has been related to the changes in the bean microstructure produced by the roasting process, such as the increase in bean volume and the appearance of larger micropores in the cell walls (*56*). Also, structural changes in coffee polysaccharides have been associated with the increase on their extractability after roasting (*53*).

Galactomannans are the major polysaccharides in coffee infusions prepared from roasted coffee beans (69%), followed by arabinogalactans (28%). Contrarily, arabinogalactans are the main extractable polysaccharides from green coffee beans (*5, 6*). Structurally, the galactomannans from roasted coffee infusions, as well as those from green coffee, are composed by a backbone of β-(1→4)-linked D-mannose residues substituted at *O*-6 with side chains of single α-D-galactose residues (*8, 38*). These galactomannans also contain acetyl groups (*40*), being located at *O*-2 and/or *O*-3 position of the mannose residues (*41*). Single and doubly acetylated hexose residues as well as consecutively acetylated hexose residues are present in coffee galactomannans. Also, coffee galactomannans are composed by single arabinose residues as side chains and

contain glucose residues. In green coffee, glucose residues are a constituent of the mannan backbone, and in the roasted coffee, they are located only at the reducing end of the mannan backbone (*41*).

The roasting of coffee beans promotes the decrease of the degree of polymerization (DP) and branching of the extractable galactomannans (*6, 8*). These decreases of the DP as well as the degree of branching are more pronounced with the increase of the degree of roasting (*5, 8*). Also, Nunes et al. (*7*) identified several modifications induced by coffee roasting process in digests of galactomannans from roasted coffee infusions obtained by *endo-β-(1→4)-mannanase* treatment and analysed by mass spectrometry (MS). The detection of Amadori compounds, 1,6-anhydromannose, fructose, glucose, mannonic acid, 2-ketogluconic acid, and arabinonic acid in the reducing end of the obtained oligosaccharides allowed to infer that Maillard reaction as well as caramelization, isomerization, oxidation and decarboxylation reactions occur during coffee roasting. During the coffee roasting process, galactomannans are also involved in melanoidins formation. Melanoidins are heterogeneous polymers characterized by brown colour and high molecular weight. The structure of coffee melanoidins is still largely unknown, but it is recognized that they contain thermally transformed galactomannans (*11, 57*).

Although some structural changes promoted by roasting have already been identified, more studies are necessary to better understand the reactions that take place inside of the coffee beans during the roasting process and that promote changes in the structure of the galactomannans. Mass spectrometry (MS), as exemplified by the study of Nunes et al. (*7*), is a promising technique for identification of structural changes promoted by roasting in coffee galactomannans, thus being the methodology of choice in the present work. The results presented in this dissertation were obtained subjecting model oligosaccharides (structurally related with coffee galactomannans) to dry thermal processing mimicking coffee roasting conditions and MS was the main analytical tool used for the analysis of these oligosaccharides. Thus, a brief description of MS applied to the analysis of polysaccharides as well as oligosaccharides is presented in following sections.

II.B. Mass spectrometry in the analysis of oligo- and polysaccharides

Mass spectrometry (MS) has played an important role in the field of structural characterization and identification of oligo- and polysaccharides. Over the last decade, several studies using MS in the analysis of these compounds has been published (*7, 20, 41, 58-66*). The analysis of oligo- and polysaccharides by MS allows to obtain information about monosaccharide composition and sequence, branching pattern, type of linkage and presence of modifying chemical groups. Apart from the diversity of structural information that can be obtained by MS, a main advantage of this analytical tool is its very high sensitivity allowing the analysis of oligo- and polysaccharides even when they are present in mixtures and with low abundance (*67*). Nevertheless, the coupling of a separation technique with MS can be advantageous in the analysis of complex mixtures (*68*).

In the following sections, basic concepts of MS and important aspects having in mind during the application of this technique to the analysis of oligo- and polysaccharides are presented.

II.B.1. Basic principles of mass spectrometry

The mass spectrometer is an instrument designed to separate ions in the gas phase according to their mass-to-charge ratios (*m/z*), where *m* is the ion mass in atomic mass units (Dalton) and *z* is the number of elementary charges carried by the ion (*68, 69*). The first step in the mass spectrometric analysis is therefore the production of gas phase ions from the sample. All these ions are then separated in the mass spectrometer according to their *m/z* values. The last step in the mass spectrometric analysis is the detection, the ion current due to these mass-separated ions is measured and displayed in the form of a mass spectrum (*68*).

A simplistic view of the components of a mass spectrometer is illustrated in **Figure II.B.1**.

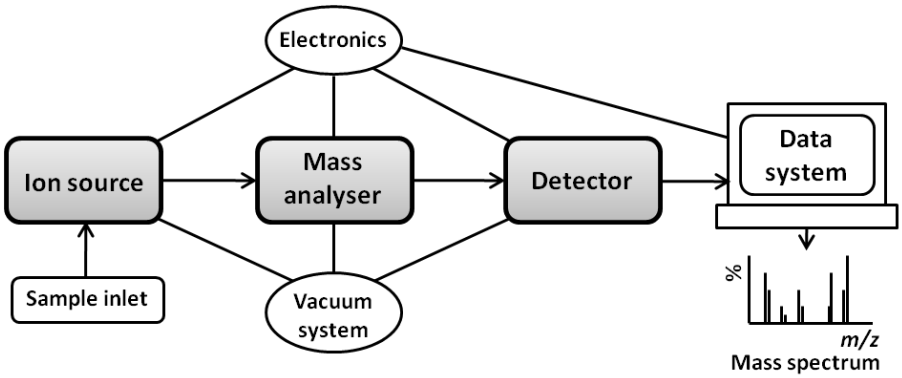

Figure II.B.1. Schematic representation of a mass spectrometer. Adapted from reference (*68*).

The main components of a mass spectrometer include:

• An inlet system to introduce the sample into the ionization source. This system can be conducted through direct injection or using a coupling of a separation instrument like a chromatograph.

• An ionization source to produce gas phase ions from the sample. Many ionization techniques, such as chemical ionization (CI), electron impact (EI), electrospray ionization (ESI), and matrix assisted laser desorption/ionization (MALDI), have been developed for this purpose. The ionization method to be used depends largely on the nature of the sample under investigation and the type of information desired.

• One or several mass analysers to separate the various ions according to their *m/z* values. Several different types of mass analysers are currently used, namely magnetic sector, quadrupole, time-of-flight (TOF), ion trap, and Fourier transform ion cyclotron resonance (FT-ICR).

• A detector to measure and amplify the ion current of mass-resolved ions.

• A data system to record, process, store, and display data, typically in the form of a mass spectrum.

• A vacuum system to maintain the analyser and detector of the mass spectrometer, and often the ionization source too, under a very low pressure avoiding collisions between ions and air molecules.

• Electronics to control the operation of various units.

A mass spectrum is a plot of ion abundance versus mass-to-charge ratio (*m/z*). Typically, the peak resulting from the most intense ion is assigned an arbitrary intensity of 100 and the relative abundance of all other ions is reported as percentage of the most intense peak. The acquisition of a mass spectrum can be made in positive or negative mode depending if the sample ionizes preferentially forming positively or negatively charged ions, respectively (*68*).

II.B.2. Ionization of oligo- and polysaccharides

In the analysis of oligo- and polysaccharides by mass spectrometry (MS), two ionization methods are commonly used: electrospray ionization (ESI) and matrix-assisted laser desorption/ionization (MALDI) (*67*).

ESI and MALDI are designated as soft ionization techniques. As the name suggests, the formation of the ions from the sample occurs without giving it too much energy and therefore preventing the fragmentation of the sample ions during the ionization process (*70, 71*). Consequently, the resulting ESI-MS and MALDI-MS spectra are relatively easy to interpret, being these ionization techniques suitable for analysis of mixtures.

Although both ESI and MALDI represent soft ionization techniques, there are distinct differences between these techniques. One of the main differences between ESI and MALDI is the state in which the sample is introduced into the ion source. In ESI-MS, the sample is in solution, and in MALDI-MS, the sample is in solid state.

A brief description of these ionization techniques, ESI and MALDI, is presented in the following sections.

II.B-2.1. Electrospray ionization

In electrospray ionization (ESI), the production of gas phase ions can be subdivided into three main steps: the formation of a spray of highly charged droplets, the decrease of droplet size, and the desorption of ions from charged droplets into the gas phase (*68*).

A schematic representation of an ESI source is shown in **Figure II.B.2**. The sample solution in a suitable solvent mixture is continuously pumped through the stainless steel capillary at a flow rate of between 1 µL/min and 10 µL/min. A voltage of 3-6 kV is applied to the capillary tip, located 0.3–2 cm from the counter electrode. The potential difference between the tip of the capillary and the counter electrode produces an electrostatic field that is sufficiently strong to disperse the emerging solution into an aerosol of highly charged droplets. The size of these droplets is continuously diminished by solvent evaporation, assisted by a flow of hot gas (usually nitrogen). When the charge density at the droplet surface reaches a critical value (the Rayleigh limit), a so called Coulomb explosion occurs and several even smaller droplets are formed. Two mechanisms have been proposed to explain ion desorption from these droplets: the ion-desorption model (IDM) and the charge-residue model (CRM). The IDM predicts the direct ion emission from the droplets when the droplets reach a critical size (10-20 nm in radius). According with the CRM, the sequence of solvent evaporation and droplet fission is repeated several times, until the drop size becomes so small that it contains only one molecule. As the last of the solvent is then evaporated, the molecule is dispersed into the ambient gas retaining the charge of the droplets (*68, 70-72*). Some studies have demonstrated that the IDM is dominant in the case of hydrophobic species, whereas the CRM is dominant in the case of hydrophilic species (*68*).

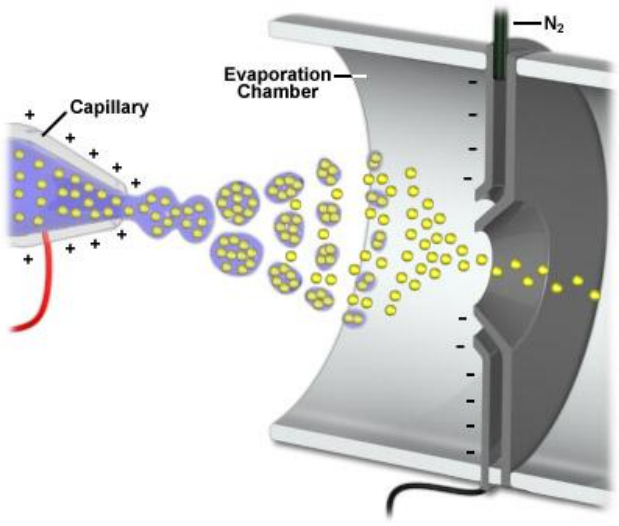

Figure II.B.2. Schematic representation of an electrospray ionization source (*73*).

Mass spectrometry with electrospray ionization (ESI-MS) has been used in the analysis of oligo- and polysaccharides. Nevertheless, multiple charged ions are commonly observed in the ESI-MS spectra of high molecular weight compounds, difficulting MS spectra interpretation. Thus, ESI-MS is more suitable for the analysis of oligosaccharides with low molecular weight. Aiming to obtain lower molecular weight oligosaccharides, polysaccharides and oligosaccharides with higher molecular weight are usually subjected to partial hydrolysis prior to ESI-MS analysis, using acidic conditions or enzymatic procedures (*68*).

Under ESI-MS conditions, oligosaccharides ionize preferentially as sodium adducts ($[M+Na]^+$); however, ions corresponding to their proton ($[M+H]^+$) and potassium ($[M+K]^+$) adduct ions can also be observed in the MS spectra acquired in positive mode (*64*).

II.B-2.2. Matrix-assisted laser desorption/ionization

In matrix-assisted laser desorption/ionization (MALDI), the production of gas phase ions can be subdivided into two main steps: the sample preparation using a compound called matrix and the irradiation by laser of the sample/matrix mixture (*71*). An illustration of a MALDI source is shown in **Figure II.B.3**.

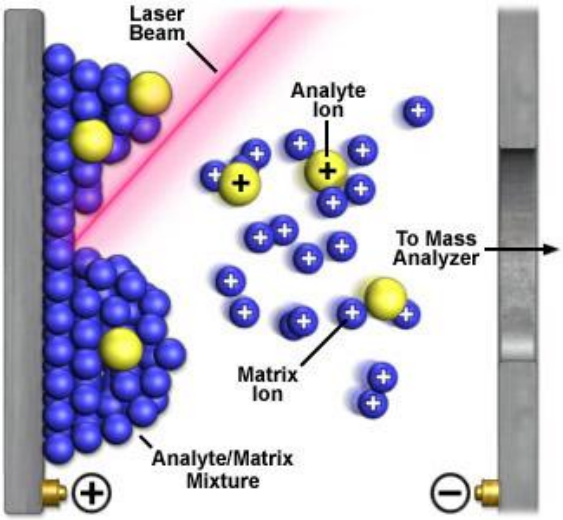

Figure II.B.3. Schematic representation of a matrix-assisted laser desorption/ionization source (*73*).

The mixture of the sample and matrix is first deposited upon a MALDI sample plate. After solvents evaporation, the sample/matrix mixture is irradiated with light emitted from a laser, often a nitrogen laser emitting in the ultraviolet range at 337 nm. During the irradiation process, sample and matrix molecules are vaporized. The ionized sample molecules are then accelerated towards the analyser. The origin of the ions produced in MALDI is not yet clear. According to the proposed mechanisms, the ions may be pre-formed in the solid state or may be formed in the gas phase by ion-molecule reactions immediately following desorption by the laser. Alternatively, both processes can occur simultaneously (*68, 71, 74*).

The quality of MALDI-MS spectra depends greatly of the matrix selection as well as sample preparation. The use of a matrix has two main purposes. The matrix, chosen to absorb at the wavelength of the laser, absorbs most of the incident laser energy and gradually transfers this energy to the sample, avoiding the decomposition of the sample. The matrix also serves as a solvent for the sample, preventing the formation of sample aggregates. The matrix selection is, firstly, based on the laser wavelength used. However, this selection is also related to the sample nature (*71*). In the analysis of oligo- and polysaccharides, the most frequently used matrix is 2,5-dihydroxybenzoic acid (DHB, **Figure II.B.4**) (*74*).

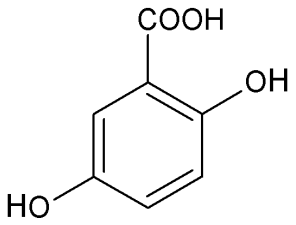

Figure II.B.4. Structure of 2,5-dihydroxybenzoic acid (DHB).

The sample preparation is an important step in MALDI-MS analysis. Sample preparation promoting a homogeneous crystal formation is essential to obtain a spectrum with a good signal-to-noise ratio (*68*). There are several methods of sample preparation described in the literature, including the dried-droplet, fast evaporation, and sandwich methods as well as many variations of these methods (*75*). The dried-droplet method was the first method to be developed and still is widely used. This method consists of mixing

some saturated matrix solution (5–10 μL) with a smaller volume (1–2 μL) of the sample solution; both solutions prepared using an appropriate volatile solvent mixture. An aliquot (0.5-2 μL) of the resulting mixture is then applied on the MALDI plate, where solvent evaporation occurs under ambient conditions or by a gentle stream of cold air. In respect to the sample preparation, it is also important to refer that there is no universal method to be used for each type of sample and, in particular, in the analysis of oligo- and polysaccharides (*68, 71*).

Under MALDI-MS conditions, oligo- and polysaccharides are detected predominantly as sodium adduct ions ($[M+Na]^+$); however, minor ions corresponding to their proton ($[M+H]^+$) and potassium ($[M+K]^+$) adduct ions as well as adducts with the matrix of type $[M+DHB+X]^+$ (X=Na or K) can also be observed in the MS spectra acquired in positive mode (*76, 77*).

II.B.3. Tandem mass spectrometry of oligo- and polysaccharides

Tandem mass spectrometry (MS^n) is an extraordinarily useful tool for structural elucidation of unknown compounds. In a simplistic way, it can be understood as the coupling of *n* stages of mass analysis. The MS^n experiment designated as MS^2 (**Figure II.B.5**), also abbreviated as MS/MS, relies on the isolation of a specific ion (designated as precursor ion) that is then fragmented and the resulting fragments (designated as fragment ions) are identified by their *m/z* values. These fragment ions, displayed in the form of a MS^2 spectrum, can reveal valuable information about the structure of the analysed compound. For higher order MS^n experiments ($n>2$), the sequence of analysis described for the MS^2 experiment is consecutively repeated. For example, MS^3 involves the isolation and fragmentation of an ion resulting from the fragmentation of the precursor ion (*68, 71*).

The mass spectrometers available for MS^n experiments are classified into two broad categories: tandem in-space and tandem in-time. In tandem in-space mass spectrometers, the different steps of the analysis (ion isolation, ion dissociation, and mass analysis of the fragment ions) are carried out in different regions of the spectrometer. In

this category, one of the commonly used mass spectrometers is the triple quadrupole mass spectrometer, suited to MS^2 experiments. This instrument, abbreviated as QqQ, is equipped with three quadrupole mass analysers, where the first and third quadrupoles act as mass analysers and the second quadrupole serves as a fragmentation chamber. In tandem in-time spectrometers, all steps of the analysis are carried out in a single mass analyser using a temporal sequence. The ion trap mass spectrometers, suited to perform multiple stages of tandem mass spectrometry, fall into this latter category of tandem spectrometers (*68, 70, 71*).

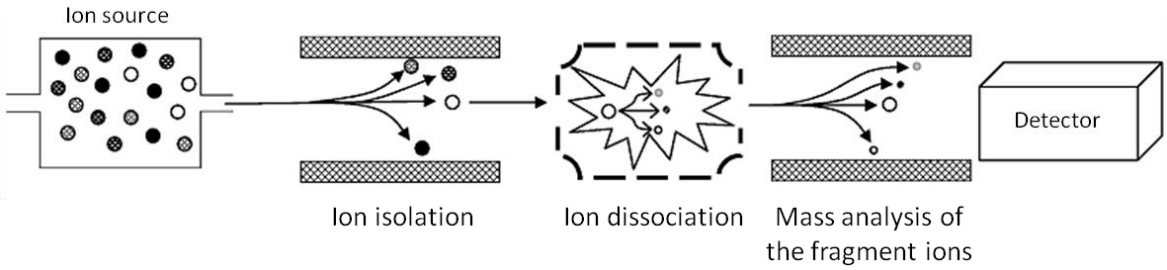

Figure II.B.5. Schematic representation of a MS^2 experiment. Modified from reference (*70*).

The dissociation of the precursor ion can be promoted using different techniques, but collision-induced dissociation (CID) is by far the most commonly used. In this technique, also known as collisionally activated dissociation (CAD), the precursor ion is fragmented by collisions with atoms of an inert gas, such as helium, nitrogen, or argon (*68*).

Tandem mass spectrometry (MS^n) using collision-induced dissociation (CID) has been successfully applied in the structural characterization of oligosaccharides (*67*), including oligosaccharides obtained by hydrolysis of polysaccharides (*7, 63, 65, 78*). The major fragmentation pathways of oligosaccharides under CID conditions can be classified into two groups: glycosidic cleavages and cross-ring cleavages. The glycosidic cleavages, resulting from the cleavage of a bond between two adjacent sugar residues, provide information about the monosaccharide composition, sequence and branching. The cross-ring cleavages, resulting from the cleavage of two bonds within the sugar ring, provide additional information about the type of glycosidic linkages in the oligosaccharide (*74, 79*).

Apart from the oligosaccharide structure, the abundance of the different fragment ions is also influenced by the state of the precursor ion. For example, the abundance of ions resulting from cross-ring cleavages was observed to be higher for sodiated ions ($[M+Na]^+$) relative to protonated ions ($[M+H]^+$). Thus, the resulting CID spectra of $[M+H]^+$ ions provide less information about the glycosidic linkages than those of $[M+Na]^+$ ions (*67, 80*).

The fragment ions resulting from oligosaccharide fragmentation are usually named according to the nomenclature introduced by Domon and Costello (*81*). As shown in **Figure II.B.6**, fragment ions that contain the non-reducing end of the oligosaccharide are labelled with uppercase letters from the beginning of the alphabet (A, B, C), and those that contain the reducing end are labelled with letters from the end of the alphabet (X, Y, Z). The A and X ions result from cross-ring cleavages, and are labelled with superscript numbers showing the bonds cleaved. The other ions (B, C, Y, Z) result from glycosidic cleavages. All fragment ions are labelled with a subscript number identifying the number of sugar residues retained in the fragment ion.

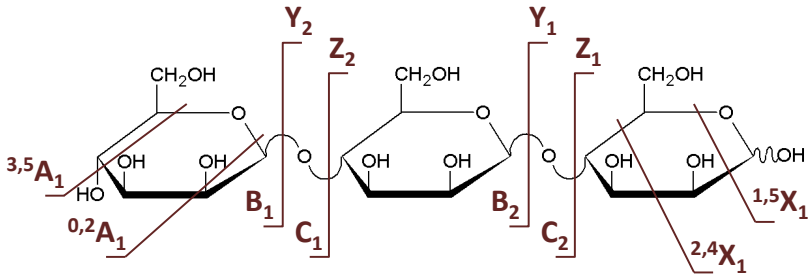

Figure II.B.6. Nomenclature for oligosaccharide fragment ions according to Domon and Costello (*81*).

Tandem mass spectrometry, particularly using electrospray ionization (ESI-MS^n), has been used for structural characterization of coffee galactomannans (*7, 41, 82*). This methodology was also used in the present work performed using model oligosaccharides structurally related with coffee galactomannans. The obtained results are showed in section III of the present dissertation. This section is divided into two main parts (A and B). The effects of dry thermal processing on the structure of mannosyl and galactomannosyl oligosaccharides are presented in part A. The results obtained with arabinotriose and a mixture of arabinotriose and mannotriose are presented in part B.

III. Experimental work, results and discussions

III.A. Effects of dry thermal processing on the structure of mannosyl and galactomannosyl oligosaccharides

III.A.1. Background and aims

Although it is recognized that the coffee galactomannans undergo structural modifications during the roasting process, the chemical reactions that occur during the coffee roasting changing the structural features of these polysaccharides are not yet completely elucidated. In order to know more about the consequences of the roasting process on the structure of coffee galactomannans, in this study a dry thermal processing was applied independently in four oligosaccharides structurally related with coffee galactomannans: two isomeric trisaccharides (**Figure III.A.1**), β-(1→4)-D-mannotriose (Man_3) and [α-(1→6)-D-galactosyl]^{I}-β-(1→4)-D-mannobiose ($GalMan_2$), and two isomeric tetrasaccharides (**Figure III.A.2**), β-(1→4)-D-mannotetraose (Man_4) and [α-(1→6)-D-galactosyl]^{I}-β-(1→4)-D-mannotriose ($GalMan_3$). This thermal processing was performed using a thermogravimetric analyser (also designated as thermobalance). The use of a thermogravimetric analyser instead of a conventional laboratory oven has the advantage of allowing the continuous weighing of the oligosaccharide while it is subjected to a controlled temperature program.

The roasted materials resulting from thermal processing of the different oligosaccharides used in this study were analysed by mass spectrometry using electrospray ionization (ESI-MS and ESI-MS^n) and matrix-assisted laser desorption/ionization (MALDI). MS data were complemented by information concerning glycosidic linkage composition obtained by methylation analysis.

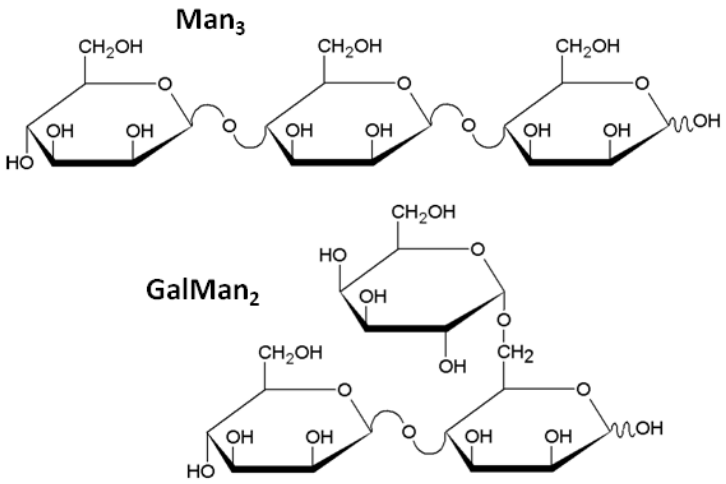

Figure III.A.1. Structures of β-(1→4)-D-mannotriose (Man_3) and [α-(1→6)-D-galactosyl]^I-β-(1→4)-D-mannobiose ($GalMan_2$).

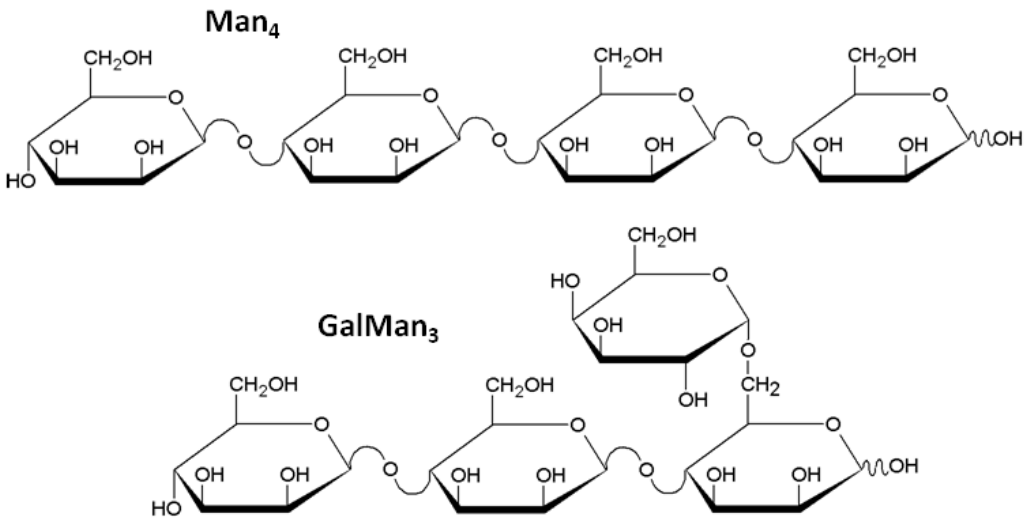

Figure III.A.2. Structures of β-(1→4)-D-mannotetraose (Man_4) and [α-(1→6)-D-galactosyl]^I-β-(1→4)-D-mannotriose ($GalMan_3$).

III.A.2. Material and methods

III.A-2.1. Samples

Oligosaccharide samples, β-(1→4)-D-mannotriose, [α-(1→6)-galactosyl]^{I}-β-(1→4)-D-mannobiose, β-(1→4)-D-mannotetraose and [α-(1→6)-galactosyl]^{I}-β-(1→4)-D-mannotriose, having a white crystalline powder appearance and a purity ≥ 95% were obtained from Megazyme (County Wicklow, Ireland).

III.A-2.2. Thermal treatment of samples

The thermal treatments were performed with a thermogravimetric analyser (**Figure III.A.3**), model TGA-50 (Shimadzu, Kyoto, Japan), operating with a controlled air flow of 20 mL/min and a heating rate of 10 °C/min. All the experiments were conducted using a platinum sample cell and an initial sample mass of 4-5 mg. Thermogravimetric (TG) curves as well as their first derivatives (DTG) were analysed using Shimadzu TASYS software. In order to improve signal-to-noise ratio, the first derivatives of the original TG curves were smoothed using 100-point smoothing.

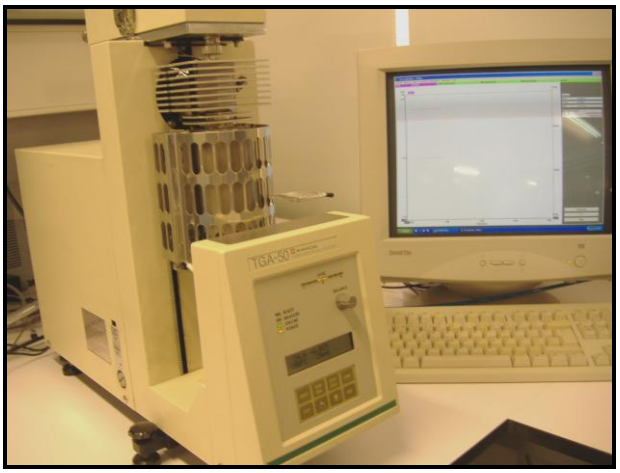

Figure III.A.3. Thermogravimetric analyser (TGA-50, Shimadzu).

At the end of temperature programs (described in the section III.A-3.1), samples were left to cool down to the room temperature inside the furnace. The materials resulting from the thermal treatments of oligosaccharides studied were then recuperated, weighed and dissolved with Milli-Q high-purity water to give a concentration of about 5 mg/mL. In order to ensure the complete dissolution of these samples, they were stirred at 37 °C for 3h and kept frozen at -20 °C until analysis. Solutions (approx. 1 mg/mL) of individual oligosaccharides without thermal treatment were prepared and stored by the same procedure.

III.A-2.3. Preparation of oligosaccharide alditols

The mannotriose alditol derivatives were prepared according to the procedure described by Reis et al. (*64*). The sample (2 mg) was dissolved in ultrapure water (200 µL) and 100 µL of sodium borohydride solution (15% in 3M NH_3) were added. The reaction mixture was heated in a heating block at 30 °C for 1h. Then, the excess of borohydride was removed by successive addition of aliquots (5 µL) of glacial acetic acid until no bubbles were observed. Borate was then removed by four additions of methanol (2 mL) and evaporation using a rotary evaporator (30 °C).

Removal of sample contaminants is essential to successful mass spectrometry analysis (*79*). To remove the excess of sodium ions, the dried material was dissolved in 1 mL of ultrapure water and the solution was then exposed to Dowex® 50W-X8 cation exchange resin (Bio-Rad Laboratories, Hercules, CA). Upon 30 min of incubation at room temperature, the solution was recovered, frozen, and freeze-dried.

III.A-2.4. Preparation of deuterium-labelled oligosaccharides

To replace the hydrogen atom of hydroxyl groups by deuterium, 40 µL of thermally treated trisaccharides (Man_3 and $GalMan_2$), previously dissolved in water, were dried in a SpeedVac Plus SC210A (Thermo Savant, Holbrook, NY) and then dissolved in deuterated water (40 µL) immediately before MS analysis.

III.A-2.5. Electrospray ionization mass spectrometry

ESI-MS and ESI-MS^n spectra of untreated and thermally treated oligosaccharides, as well as the deuterium-labelled ones, were carried out on a LXQ linear ion trap mass spectrometer (Thermo Fisher Scientific Inc., Waltham, MA). Typical operating conditions were as follow: electrospray voltage was 5 kV; capillary temperature was 275 °C; capillary voltage 1 V and tube lens voltage 40 V. Samples were introduced at a flow rate of 8 µL/min into the source. Nitrogen was used as nebulising and drying gas. In the MS^n experiments, the collision energy used was set between 18 and 31 (arbitrary units). Data acquisitions were carried out on an Xcalibur data system.

ESI-MS and ESI-MS^2 spectra of thermally treated mannotriose alditols were carried out on a Q-TOF2 hybrid tandem mass spectrometer (Micromass, Manchester, UK). The cone voltage was set at 35 V and the capillary voltage was maintained at 3 kV. The source temperature was 80 °C and the desolvation temperature was 150 °C. MS^2 spectra were obtained using argon as the collision gas and the collision energy used was set between 25 and 30 eV. The raw data were processed using a MassLynx software (version 4.0).

For all ESI analyses, samples dissolved in water were diluted in methanol/formic acid (99:1, v/v) and the spectra were acquired in the positive mode, scanning the mass range from *m/z* 100 to 1500.

III.A-2.6. Matrix-assisted laser desorption/ionization spectrometry

Sample preparation for MALDI analysis was performed by deposition of 0.5 µL of sample dissolved in water on top of a layer of crystals of 2,5-dihydroxybenzoic acid (DHB) formed by deposition of 0.5 µL of DHB solution on the MALDI plate and letting it to dry at room temperature. The matrix solution was prepared by dissolving 5 mg of DHB in a 1 mL mixture of acetonitrile: methanol: aqueous trifluoroacetic acid (1%, v/v) (1:1:1, v/v/v).

MALDI-MS spectra of untreated and thermally treated oligosaccharides were acquired using a MALDI-TOF/TOF Applied Biosystems 4800 Proteomics Analyser (Applied Biosystems, Framingham, MA) equipped with a nitrogen laser emitting at 337 nm and

operating in a reflectron mode. Full scan mass spectra ranging from *m/z* 500 to 4000 were acquired in the positive mode.

III.A-2.7. Methylation analysis

Both the untreated and thermally treated trisaccharides (Man_3 and $GalMan_2$) were converted to partially *O*-methylated alditol acetates (PMAA) via successive methylation, hydrolysis, reduction, and acetylation reactions by the method described by Nunes and Coimbra (*6*) with only slight variations.

Each sample was methylated using methyl iodide (*83*). The sample (1 mg) was dispersed in 1 mL of anhydrous dimethylsulfoxide (DMSO) and stirred continuously until fully dissolution. NaOH pellets (40 mg) were powdered under argon and added to the solution. After 30 min at room temperature with continuous agitation, CH_3I (80 µL) was added and allowed to react 20 min under vigorous stirring. Distilled water (2 mL) was then added, and the solution was neutralized using 1M HCl. Dichloromethane (3 mL) was added and, upon vigorous shaking, the dichloromethane phase was recovered and washed three times with distilled water (2 mL). The organic phase was evaporated to dryness and, to ensure complete methylation, the material was remethylated using the same procedure.

The remethylated material was hydrolyzed with 2M trifluoroacetic acid (500 µL) at 121 °C for 1h (*84*), and the acid was then evaporated to dryness.

For carboxyl-reduction, the partially methylated sugars were suspended in 300 µL of 3M NH_3 and 20 mg of sodium borodeuteride were added. The reaction mixture was incubated at 30 °C for 1h. After cooling, the excess of borodeuteride was removed by the addition of 100 µL of glacial acetic acid. The partially methylated alditols were acetylated by adding 1-methylimidazole (450 µL) and acetic anhydride (3 mL) and allowing reacting 30 min at 30 °C (*85*). This solution was treated with water (3 mL) to decompose the excess of acetic anhydride, and the PMAA were extracted with dichloromethane (5 mL). The dichloromethane phase was washed and evaporated to dryness. The dried material was dissolved with anhydrous acetone (2 x 1 mL) followed by evaporation of acetone to dryness.

The PMAA were dissolved in anhydrous acetone and identified by gas chromatography/mass spectrometry (GC/MS) on an Agilent Technologies 6890N Network (Santa Clara, CA). The GC was equipped with a 400-1HT (Quadrex Corp., Woodbridge, CT) capillary column (25 m length, 0.23 mm of internal diameter, and 0.05 μm of film thickness). The samples were injected in splitless mode (a splitless time of 6 min), with the injector operating at 220 °C, and using the following temperature program: initial temperature 50 °C, a rise in temperature at a rate of 8 °C/min until 140 °C, standing for 5 min at this temperature, followed by a rate of 0.5 °C/min until 150 °C and then followed by a rate of 40 °C/min until 300 °C, with further 1 min at 300 °C. The helium carrier gas had a flow rate of 0.2 mL/min and a column head pressure of 12.95 psi. The GC was connected to an Agilent 5973 mass quadrupole selective detector operating with an electron impact mode at 70 eV and scanning the *m/z* range of 40–500 in a 1s cycle in a full scan mode acquisition.

III.A.3. Results and discussion

III.A-3.1. Thermal stability of the oligosaccharides

Thermogravimetric analysis (TG and DTG curves, **Figure III.A.4a**) of mannotriose (Man_3) was carried out from room temperature to 600 °C in order to determine the thermal stability of this oligosaccharide. In the DTG curve it is possible to observe three main mass loss stages. The first mass loss (8.8%) occurring from room temperature to 150 °C should be associated to the evaporation of water molecules adsorbed to the oligosaccharide, as reported in other TG studies (*86, 87*). The two other main mass loss stages, observed for temperatures higher than 200 °C, are indication of the occurrence of thermal reactions that are accompanied by mass changes. Taking into account that the coffee roasting process is usually performed at temperatures around 200 °C (*54*) and that at this temperature Man_3 seems to be thermally stable, the temperature programs used for thermal treatment of the oligosaccharides in this study took into account this maximum.

As illustrated in **Figure III.A.4b**, Man_3 was heated from room temperature up to 200 °C (approx. 18 min), being maintained at 200 °C for different periods of time (0, 30, and 60 min). These different thermal treatments are designated as T1, T2 and T3, respectively; while the thermally untreated sample is designated as T0. After 18 min, when the temperature reached 200 °C (T1), the loss of material was 7.7%, which is in accordance with the amount of water loss observed in **Figure III.A.4a**, although a light brown coloured material was recorded. When the oligosaccharide remains at 200 °C during 30 min (T2), it was observed a loss of an extra 8.1% of material. Based on the brown colour of the sample, it can be inferred that this mass loss may be due to the occurrence of thermal reactions that are accompanied by mass changes. The same can be inferred when the material was heated during 60 min at 200 °C (T3) as a loss of an extra 4.2% of material was observed and the material was darker than the previous one. The appearance of the brown coloration is consistent with the formation of brown-colour compounds observed in heated sugar-rich foods as a result of caramelization reactions (*88*) that were shown to occur during the roasting process of coffee beans (*7*).

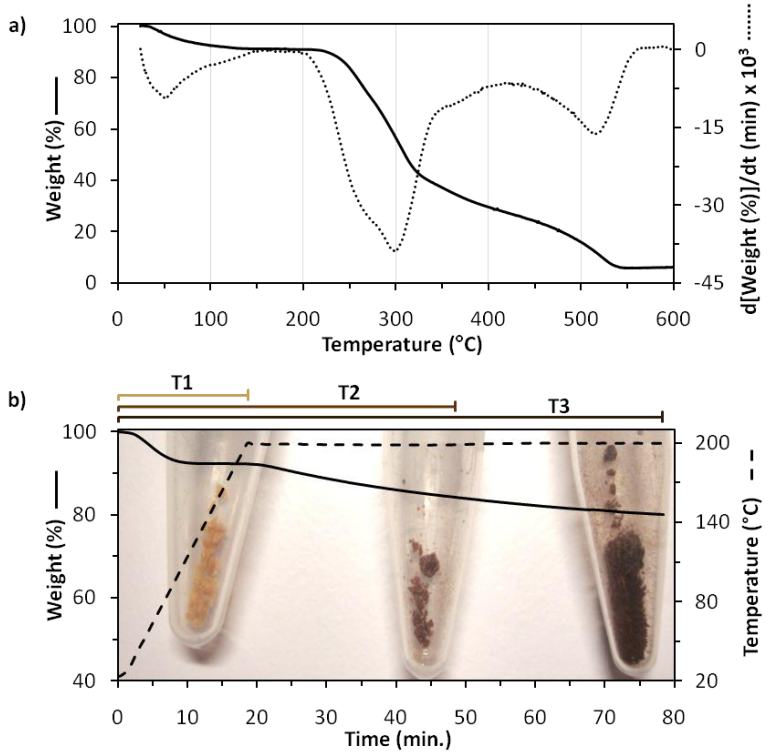

Figure III.A.4. a) TG and DTG curves of mannotriose (Man_3) obtained from room temperature to 600 °C and **b)** TG curve of Man_3 with illustration of the different thermal treatments (T1, T2, and T3).

The thermal treatments performed for Man_3 were also carried on for the other oligosaccharides structurally related with coffee galactomannans, namely $GalMan_2$, Man_4, and $GalMan_3$. All these samples acquired the brown coloration reported for Man_3 along the thermal treatment. For all oligosaccharides in study, the total mass loss percentages determined from TG curves were: 4-10% for T1, 12-16% for T2, and 16-20% for T3. In order to further characterize the structural changes associated with these thermal treatments, the materials resulting from T1, T2, and T3 of all oligosaccharides under study were analysed by MS using ESI and MALDI ionization techniques.

III.A-3.2. ESI-MS analysis of thermally treated oligosaccharides

In the ESI-MS spectrum of thermally untreated Man_3 (**Figure III.A.5a**) were observed the ions at *m/z* 527 and 543, attributed to the sodium ($[Hex_3+Na]^+$) and potassium ($[Hex_3+K]^+$) adduct ions, respectively. Furthermore, an adduct ion formed by two oligosaccharides and one sodium ion ($[2Hex_3+Na]^+$) at *m/z* 1031 was also observed. The same *m/z* ions were observed for $GalMan_2$ (data not shown). In the ESI-MS spectra of untreated Man_4 and $GalMan_3$ (data not shown) were observed the ions at *m/z* 689 and 705, attributed to $[Hex_4+Na]^+$ and $[Hex_4+K]^+$, respectively. All oligosaccharides under study ionized predominately as sodium adducts, in accordance with the previous studies on mannosyl oligosaccharides (*7, 41, 82*).

In the ESI-MS spectrum acquired for Man_3 after the thermal treatment at 200 °C during 30 min (T2) (**Figure III.A.5b**) were observed the ions at *m/z* 203, 365, 527, 689, 851, 1013, 1175, and 1337, attributed to the sodium adducts of a series from a single hexose up to eight hexose residues ($[Hex_{1-8}+Na]^+$). Also, in this spectrum were observed the ions at *m/z* 347, 509, 671, 833, 995, and 1157, attributed to the sodium adducts of a series of hexose residues presenting a loss of one water molecule ($[Hex_{2-7}-H_2O+Na]^+$), as well as the ions at *m/z* 311, 473, 635, 797, 959, and 1121, attributed to the sodium adducts of a series of hexose residues presenting a loss of three water molecules ($[Hex_{2-7}-3H_2O+Na]^+$). The corresponding potassium adducts of some of these ions were also observed, as for example the ion at *m/z* 489 ($[Hex_3-3H_2O+K]^+$).

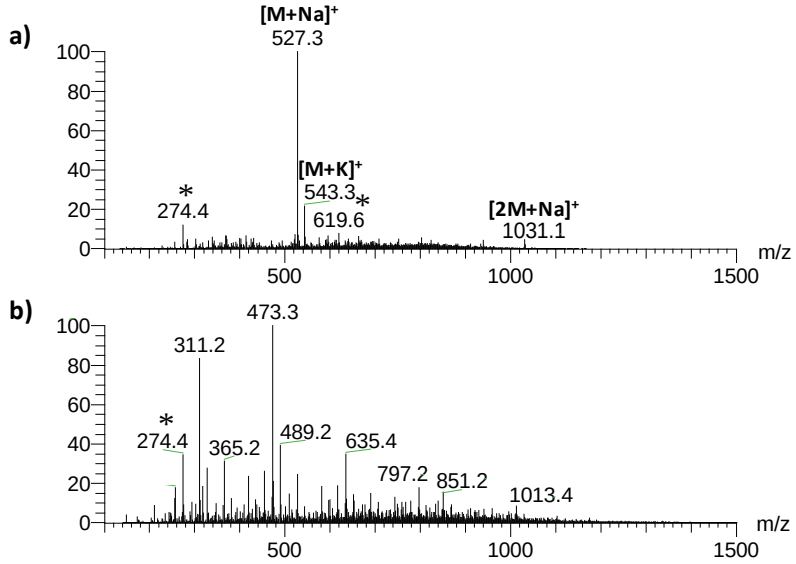

Figure III.A.5. ESI-MS spectra obtained for mannotriose (Man_3): **a)** thermally untreated (T0) and **b)** after thermal treatment at 200 °C for 30 min (T2). Ions marked with an asterisk (∗) are attributed to impurities.

Figure III.A.6a shows the relative abundances of $[M+Na]^+$ ions identified in the ESI-MS spectra acquired for Man_3 after the thermal treatments (T1, T2, and T3). It is possible to observe that, with the exception of the ion at *m/z* 1337 ($[Hex_8+Na]^+$), the same ions were observed for T2 and T3. For these two treatments, the most intense ions were observed at *m/z* 311 and 473, attributed to $[Hex_{2-3}\text{-}3H_2O+Na]^+$. Also, it is possible to observe the decrease in the relative abundance of the ion correspondent to Man_3, from an average of 54.1% for T2 to 37.8% for T3. For the lightest treatment (T1), the only ion identified beyond the ion at *m/z* 527 was the ion at *m/z* 365, attributed to $[Hex_2+Na]^+$.

The relative abundances of $[M+Na]^+$ ions identified in the ESI-MS spectra acquired for $GalMan_2$, Man_4, and $GalMan_3$ are shown in **Figure III.A.6b-d**. As observed for Man_3, few products were identified when these oligosaccharides were heated from room temperature up to 200 °C (T1). After this thermal treatment, the predominant ion observed in the mass spectra occurs at *m/z* 527 for trisaccharides and *m/z* 689 for tetrasaccharides, attributed to $[Hex_3+Na]^+$ and $[Hex_4+Na]^+$, respectively. Also, products having a lower degree of polymerization (DP) in comparison with the starting material were observed for Man_4 and $GalMan_3$, inferred by the presence of the ions at *m/z* 365 and 527, attributed to $[Hex_{2-3}+Na]^+$. Contrary to that observed for Man_3, in the ESI-MS spectrum of $GalMan_2$ did not show the ion corresponding to the product with DP 2 but showed the presence of the

ions with a higher DP than that of the starting oligosaccharide, occurring at *m/z* 689 ($[Hex_4+Na]^+$) and 1013 ($[Hex_6+Na]^+$). For longer times of thermal treatment (T2 and T3), in the ESI-MS spectra were observed ions corresponding to products with lower and higher DP than those of the untreated oligosaccharides, as well as the respective ions resulting from the loss of one or three water molecules. The predominant ions observed in the ESI-MS spectra acquired after these thermal treatments, except for the T2 treatment of Man_4, were the ions at *m/z* 311 or 473, attributed to $[Hex_{2-3}\text{-}3H_2O+Na]^+$. For Man_4 treated during 30 min at 200 °C (T2), the predominant ion was observed at *m/z* 527, attributed to $[Hex_3+Na]^+$.

The identification of products having a lower DP in comparison with the starting material is in accordance with the decrease of the molecular weight and the degree of branching of roasted coffee extractable galactomannans (*5, 6, 8, 9*). The loss of one water molecule was also identified in roasted coffee galactomannans by the detection of 1,6-anhydromannose at the reducing end of these polysaccharides (*7*). However, the occurrence of polymerization was never reported to occur in coffee polysaccharides during the roasting process. This may be due to the complexity of the coffee matrix and to the fact that still a high fraction of galactomannans remained in the residue after aqueous extraction. This insoluble material, usually associated with the high molecular weight polysaccharides, can have a contribution from the polymerization reactions similar to those observed in this model system. Nevertheless, the formation of oligosaccharides having a higher DP in comparison with the starting oligosaccharide was already reported for dry heating of maltotriose at 200 °C for 30 min (*89*). Thermal polymerization was also reported to occur during the heating of glucose at 150 °C for 2.5h under vacuum conditions (*90*). Also, tri-dehydrated galactomannans from roasted coffee infusions were never identified. However, a revisiting of the pyrolysis-mass spectrometry experiments carried out on amylose and dextran (*91*) allowed to observe the possible occurrence of tri-dehydrated oligosaccharides.

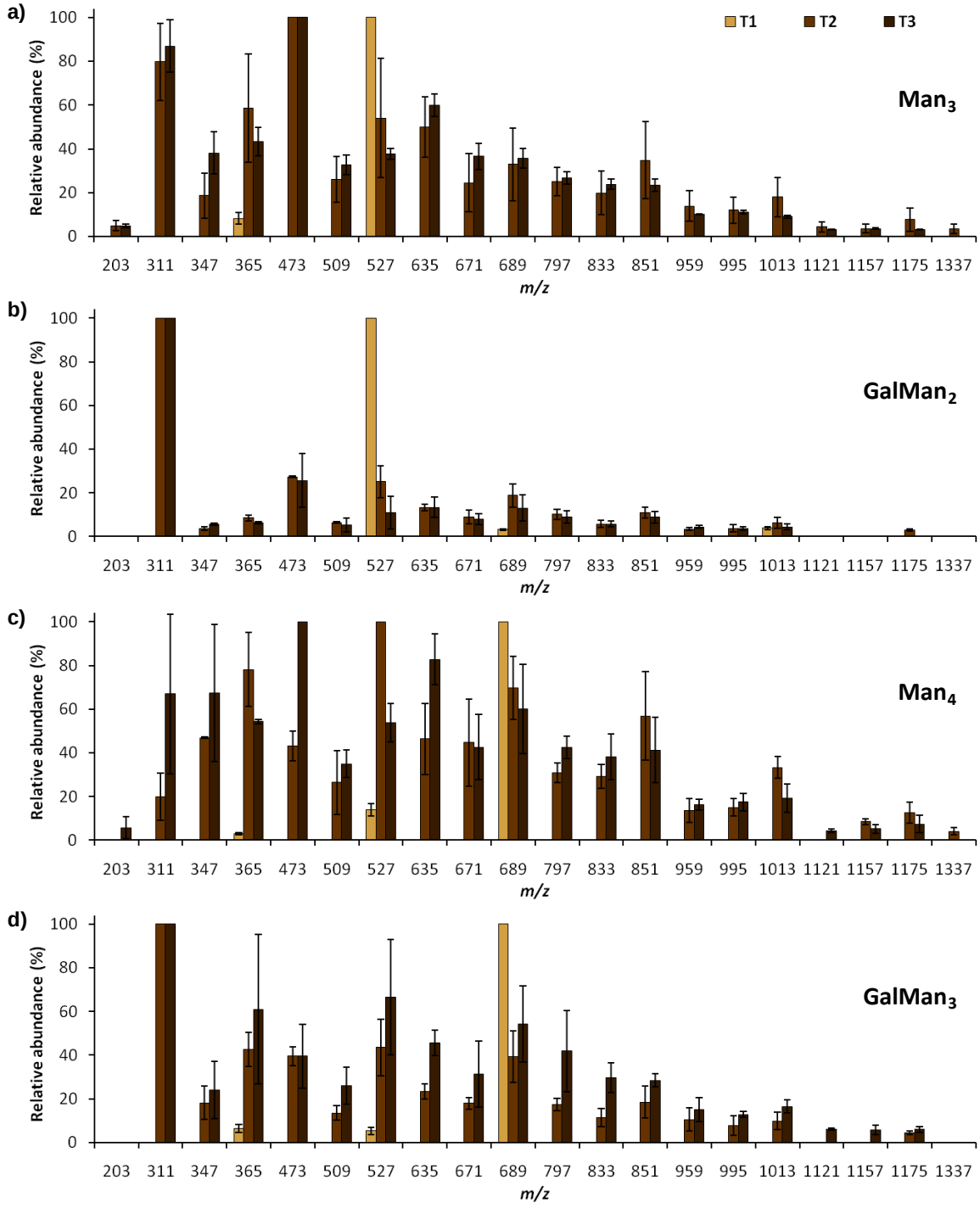

Figure III.A.6. Relative abundances of $[M+Na]^+$ ions observed in the ESI-MS spectra acquired for **a)** Man_3, **b)** $GalMan_2$, **c)** Man_4, and **d)** $GalMan_3$ dry heated from room temperature up to 200 °C and maintaining at 200 °C for 0 min (T1), 30 min (T2) and 60 min (T3). Values are given as mean ± standard deviation of three replicate spectra acquisitions made in different days. Ions with a mean relative abundance less than 3 % were not considered.

III.A-3.3. MALDI-MS analysis of thermally treated oligosaccharides

In order to investigate the presence of oligosaccharides with a higher degree of polymerization (DP) than those detected by ESI-MS, a MALDI-MS analysis was performed for all data set.

Comparing MALDI-MS spectra obtained before (**Figure III.A.7a**) and after thermal treatment during 30 min at 200 °C (T2) (**Figure III.A.7b**) of Man_3, it is possible to identify in the spectrum of thermally treated sample other ions beyond the ion at *m/z* 527. The identification of the ions at *m/z* 689, 851, 1013, 1175, 1337, 1499, and 1661, attributed to $[Hex_{4\text{-}10}+Na]^+$, confirms the formation of oligosaccharides with a higher DP than that of the starting material. This MS spectrum also showed mono- and tri- dehydrated products, identified as $[Hex_{3\text{-}10}\text{-}H_2O+Na]^+$ and $[Hex_{4\text{-}10}\text{-}3H_2O+Na]^+$, respectively. The ions corresponding to the sodium adduct ions of oligosaccharides with 9 and 10 hexose residues were not identified by ESI-MS.

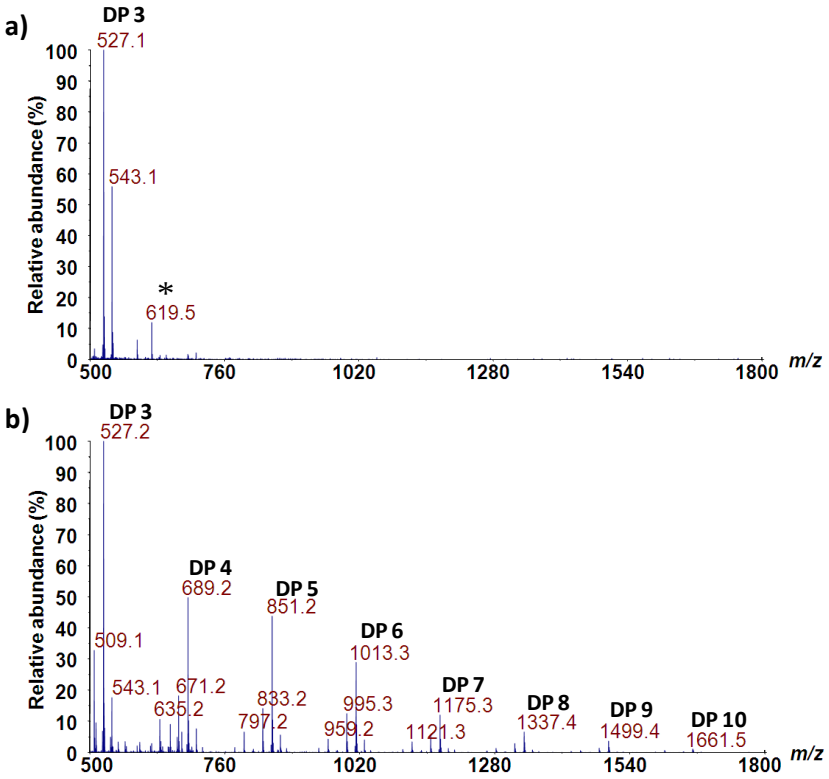

Figure III.A.7. MALDI-MS spectra obtained for mannotriose: **a)** thermally untreated (T0) and **b)** after thermal treatment at 200 °C for 30 min (T2). The ion marked with an asterisk (*) is attributed to an impurity.

The MALDI-MS spectra obtained for all samples (data not shown) allowed to confirm the previous findings obtained by ESI-MS, that are, the polymerization of the oligosaccharides when heated at 200 °C for 30 and 60 min (T2 and T3), and the occurrence of mono- and tri-dehydrated derivatives of all oligosaccharides formed. Also, MALDI-MS spectra allowed to identify in the samples subjected to T2 and T3 treatments the ions occurring at *m/z* 1499 and 1661 ($[Hex_{9-10}+Na]^+$), that were not detected by ESI-MS.

III.A-3.4. ESI-MS^n analysis of thermally treated oligosaccharides

In order to confirm the assignments of all sodium adduct ions identified in the ESI-MS spectra as well as to find additional details about their structures, MS^2 spectra (and casually MS^n spectra with *n* upper to 2) of these ions were acquired. Although MS^2 spectra have been acquired for all ions identified in the ESI-MS spectra, only a spectrum for one product of each series of ions identified after thermal treatment of mannotriose (Man_3) at 200 °C during 30 min (T2) will be explained in detail. MS^2 spectra obtained for the other thermal treatments as well as the other model oligosaccharides provided the same information.

Previous studies performed on the fragmentation of $[M+Na]^+$ ions of mannosyl oligosaccharides under ESI-MS^n conditions exhibited a characteristic predominant loss of a hexose residue (Hex_{res}, -162 Da) due to glycosidic bond cleavage, and fragment ions resulting from cross-ring cleavages (cleavage of two bonds within the sugar ring) as well as losses of water (-18 Da) (*7, 41*). The cross-ring cleavages are referred as neutral losses of $C_2H_4O_2$ (-60 Da), $C_3H_6O_3$ (-90 Da), and $C_4H_8O_4$ (-120 Da), being their occurrence variable with the type of glycosidic linkage (*92, 93*). Furthermore, there is a strong preference for glycosidic bond cleavage on the non-reducing side of the glycosidic oxygen (*93*).

Figure III.A.8a shows the MS^2 spectrum of the ion at *m/z* 527, attributed to $[Hex_3+Na]^+$, presenting a fragmentation pattern characteristic of β-(1→4)-linked hexose oligosaccharides (*92, 93*). It is possible to observe the fragment ions at *m/z* 365 ($[Hex_2+Na]^+$) and 203 ($[Hex+Na]^+$) formed by glycosidic bond cleavage with loss of one and two Hex_{res} (-162 Da) from the precursor ion. The fragment ions at *m/z* 509, resulting from a loss of water (-18 Da) from the precursor ion, and at *m/z* 467 and 407, resulting

from cross-ring cleavages (-60 and -120 Da, respectively) from the precursor ion, are also observed in the spectrum. The fragment ions observed in this spectrum and their relative abundances were the same than those observed in the MS^2 spectrum obtained for the thermally untreated Man_3 (data not shown), indicating that the remaining trisaccharide was not structurally changed.

Figure III.A.8b shows the MS^2 spectrum of the ion at *m/z* 365, attributed to $[Hex_2+Na]^+$. In this spectrum, an important point to note is the occurrence of the fragment ion at *m/z* 275, formed by a mass loss of 90 Da ($C_3H_6O_3$) from the precursor ion, which is not expected to occur for β-(1→4)-linked oligosaccharides. Because the loss of $C_3H_6O_3$ was reported for (1→3)- and (1→6)-linked oligosaccharides (*92, 93*), this observation suggests the formation of (1→3) and/or (1→6) glycosidic linkages during the thermal processing of the oligosaccharide under study, resulting from depolymerization and transglycosylation reactions. Transglycosylation reactions are known to occur during the dry thermal processing of oligo- and polysaccharides (*94, 95*).

Figure III.A.8c shows the MS^2 spectrum of the ion at *m/z* 689, attributed to $[Hex_4+Na]^+$. This spectrum shows the similar fragmentation pattern described for $[Hex_3+Na]^+$, presenting fragment ions that result of glycosidic cleavages (-162 Da), water losses (-18 Da), and cross-ring cleavages (-60 Da and -120 Da).

Figure III.A.8d shows the MS^2 spectrum of the ion at *m/z* 509, attributed to $[Hex_3-H_2O+Na]^+$. The fragment ion occurring at *m/z* 365, attributed to $[Hex_2+Na]^+$ and formed by loss of an anhydrohexose residue (-144 Da) from precursor ion, indicates that there are two hexoses linked to each other and that the dehydration occurs in a terminal residue. Comparing this fragmentation pattern with the non-modified correspondent oligosaccharide ($[Hex_3+Na]^+$, **Figure III.A.8a**), the predominance of the ion at *m/z* 347 suggests that the anhydrohexose is preferentially positioned at the reducing end of the oligosaccharide. A similar MS^2 spectrum was obtained by Nunes et al. *(7)* after enzymatic hydrolysis of galactomannans from roasted coffee infusions, being the precursor ion assigned as a oligosaccharide with reducing end sugar unit modified in the form of 1,6-β-anhydromannose.

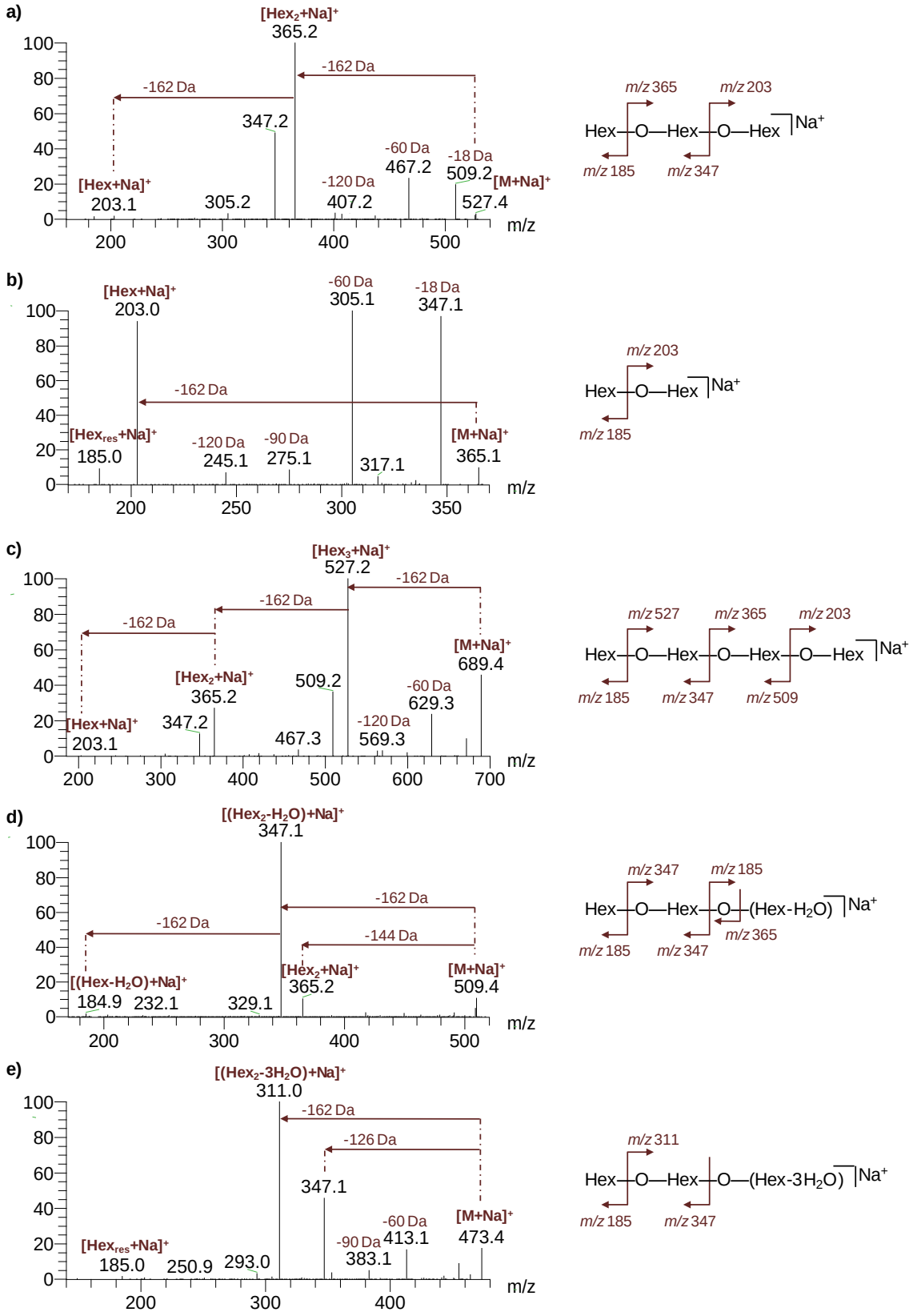

Figure III.A.8. ESI-MS^2 spectra and schematic fragmentation pathways of sodium adduct ions identified after thermal treatment of the mannotriose at 200 °C for 30 min (T2): **a)** $[Hex_3+Na]^+$ (*m/z* 527), **b)** $[Hex_2+Na]^+$ (*m/z* 365), **c)** $[Hex_4+Na]^+$(*m/z* 689), **d)** $[Hex_3-H_2O+Na]^+$ (*m/z* 509), and **e)** $[Hex_3-3H_2O+Na]^+$ (*m/z* 473).

Furthermore, 1,6-β-anhydro-oligosaccharides have also been identified when oligo- and polysaccharides, namely maltooligosaccharides with a degree of polymerization (DP) between 2-5 (*94*) and cellulose (*96-98*), were submitted on dry heating conditions. The $[Hex_n\text{-}H_2O+Na]^+$ ions identified in the ESI-MS spectra of thermally treated samples can correspond to oligosaccharides with reducing end sugar unit modified in the form of 1,6-anhydrohexose. However, dehydration occurring from other position of the reducing end hexose cannot be excluded.

Figure III.A.8e shows the MS^2 spectrum of the ion at *m/z* 473, attributed to $[Hex_3\text{-}3H_2O+Na]^+$. The glycosidic bond cleavage from the non-reducing end was the predominant fragmentation pathway, with the loss of a Hex_{res} (-162 Da) to give a predominant fragment ion at *m/z* 311, attributed to $[Hex_2\text{-}3H_2O+Na]^+$, being an indication that the sugar unit at the non-reducing end is a non-modified hexose residue. The fragment ion at *m/z* 347, formed by loss of a trianhydrohexose (-126 Da) from precursor ion, suggests that the losses of water molecules occur in the hexose residue located at the reducing end of the oligosaccharide. Furthermore, the MS^3 fragmentation of the fragment ion at *m/z* 311 (**Figure III.A.9**) gave predominant ions at *m/z* 149 and 185 resulting from the loss of a Hex_{res} (-162 Da) and a trianhydrohexose (-126 Da), respectively. If the reducing end sugar unit was not modified, the predominant fragment ion formed by glycosidic cleavage would be the ion at *m/z* 203, attributed to $[Hex+Na]^+$. The fragmentation pattern observed in this MS^3 spectrum supports that the loss of three water molecules occurs at the reducing end sugar unit of the oligosaccharide.

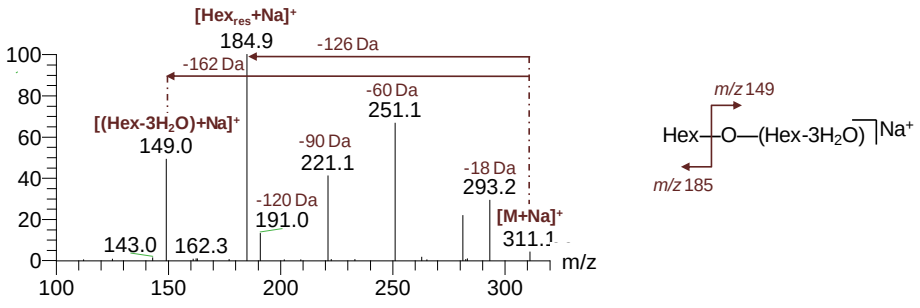

Figure III.A.9. ESI-MS^3 spectrum and schematic fragmentation pathway of the ion at *m/z* 311 ($[Hex_2\text{-}3H_2O+Na]^+$) formed by MS^2 fragmentation of the ion at *m/z* 473 ($[Hex\text{-}3H_2O+Na]^+$).

III.A-3.5. Deuterium-labelling and alditol derivatization experiments

Although MS^n experiments suggest that the loss of three water molecules in the $[Hex_{2-7}-3H_2O+Na]^+$ ions occurs at the reducing end sugar unit of the oligosaccharides, additional experiments were undertaken to unambiguously demonstrate this evidence, namely, deuterium-labelling and alditol derivatization experiments.

A portion of the dissolved material resultant from the thermal treatment for 30 min at 200 °C (T2) of mannotriose (Man_3) and galactosyl-mannobiose ($GalMan_2$) was dried and then dissolved in deuterated water for replacement of the hydrogen atom of hydroxyl groups by deuterium. The ESI-MS^2 spectrum of the ion at *m/z* 480, corresponding to the ion at *m/z* 473 ($[Hex_3-3H_2O+Na]^+$, **Figure III.A.8e**) in the unlabelled Man_3 sample, is shown in **Figure III.A.10**. The difference between the *m/z* values of 480 ($[M-7H+7D+Na]^+$) and 473 ($[M+Na]^+$) indicates that this tri-dehydrated product has seven hydroxyl groups in its structure. The main fragment ion occurs at *m/z* 315, formed by loss of 165 Da from precursor ion, by glycosidic bond cleavage according to the mechanism proposed by Hofmeister et al. (*99*). This mechanism involves the transference of a deuterium atom from an oxygen linked to a carbon from the sugar ring to the glycosidic oxygen as is shown in **Figure III.A.11** for the formation of the fragment ions occurring at *m/z* 315 and 188. The two consecutive losses of 165 Da from precursor ion allows to conclude that this tri-dehydrated product has no hydroxyl groups other that those present in the two non-modified hexose residues. Furthermore, the fragmentation pattern obtained, similar to that observed for the ion at *m/z* 473 in the unlabelled sample, allows to confirm that the loss of three water molecules occurred at the reducing end residue. For $GalMan_2$, the ESI-MS^2 spectrum of the ion at *m/z* 315, corresponding to the ion at *m/z* 311 ($[Hex_2-3H_2O+Na]^+$) in the unlabelled sample (data not shown) allowed to achieve the same conclusions. Some studies showed that glucosylisomaltol is formed by heat treatment of foods rich in sugars (*100*). Because no hydroxyl protons are present in the reducing end sugar unit of the tri-dehydrated oligosaccharides identified in this work, it can be suggested that these tri-dehydrated products have an isomaltol moiety at the reducing end, as illustrated in **Figures III.A.10-11**. Nevertheless, for branched oligosaccharides ($GalMan_2$ and $GalMan_3$), this structure is not possible to occur without the loss of

galactose residue prior to the formation of the tri-anhydrous derivative. Alternatively, a different structure may be formed at the reducing mannose residue in branched oligosaccharides.

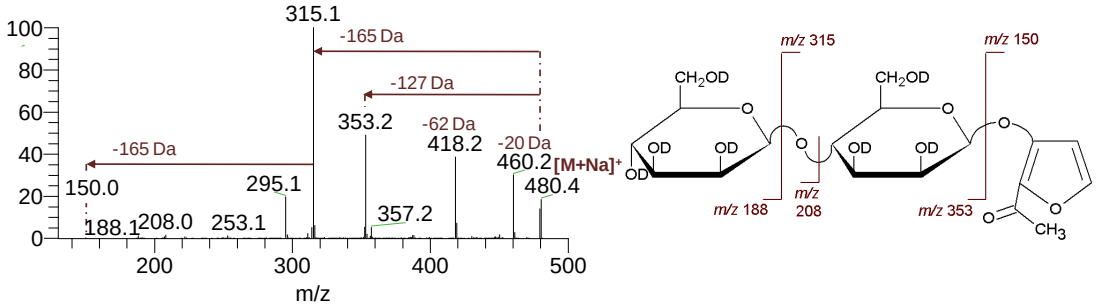

Figure III.A.10. ESI-MS^2 spectrum and schematic fragmentation pathways of the deuterium-labelled $[M+Na]^+$ ion at *m/z* 480 corresponding to the ion at *m/z* 473 in unlabelled sample.

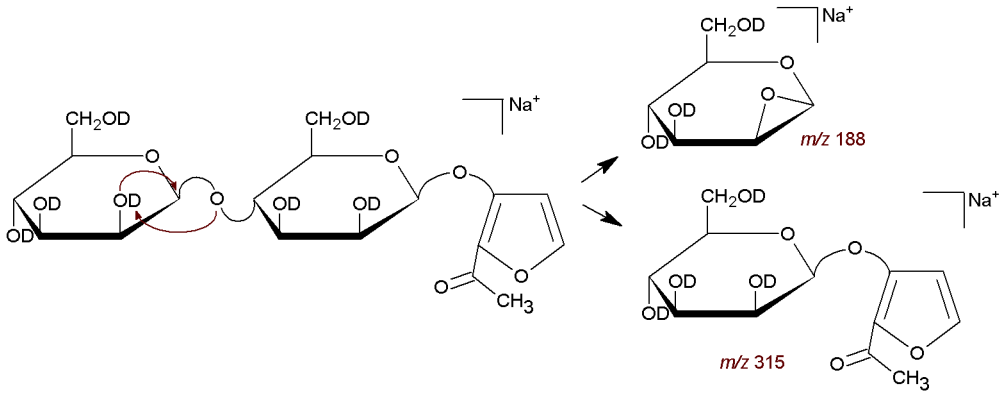

Figure III.A.11. Mechanism of glycosidic bond cleavage according to Hofmeister et al. (*99*).

To evaluate the relevance of the anomeric carbon for the formation of the modifications at the reducing end residue, Man_3 oligosaccharides were converted into their alditol derivatives upon reduction with sodium borohydride and were thermally treated from room temperature to 200 °C (T1) and left at 200 °C during 30 min (T2). For T1, the ESI-MS spectrum (**Figure III.A.12a**) shows the ions at *m/z* 529 and 367, corresponding to $[M+Na]^+$ adducts of Hex_3 and Hex_2 alditols (Hex_2Hexol and HexHexol, respectively). The presence of the ion at *m/z* 367 ($[HexHexol+Na]^+$) and the absence of the ion at *m/z* 365 ($[Hex_2+Na]^+$) indicates that the formation of this product with a lower DP than that of the starting material occurs by loss of the non-reducing end hexose residue.

On the other hand, the presence of the ions at *m/z* 511 and 349, attributed to $[Hex_{2\text{-}1}Hexol\text{-}H_2O+Na]^+$, indicates that the alditol derivatization allows the formation of anhydrous products not observed in the ESI-MS spectrum of non-reduced sample subjected to the same thermal treatment (T1). MS^2 spectra of these ions (data not shown) showed that the loss of the water molecule occurs exclusively at the hexitol residue. The ESI-MS spectrum obtained for treatment T2 (**Figure III.A.12b**) shows an ion at *m/z* 493, attributed to $[Hex_2Hexol\text{-}2H_2O+Na]^+$, a di-dehydrated derivative not observed in the ESI-MS spectrum of non-reduced sample (**Figure III.A.5b**). MS^2 spectrum of this ion (data not shown) suggests the presence of two structural isomers, one formed by the loss of two water molecules at the hexitol residue and the other formed by the loss of one water molecule at both sides, at the terminal non-reducing residue and at the hexitol residue. Furthermore, an important point to note is the absence of the tri-dehydrated products, confirming the loss of three water molecules at the reducing end sugar unit of the oligosaccharides. The MALDI-MS spectrum of the alditol derivative of mannotriose (Man_3) treated at 200 °C during 30 min (T2) (data not shown) allowed to observe the ions at *m/z* 511 and 529, attributed to $[Hex_2Hexol\text{-}H_2O+Na]^+$ and $[Hex_2Hexol+Na]^+$, as already observed by ESI-MS.

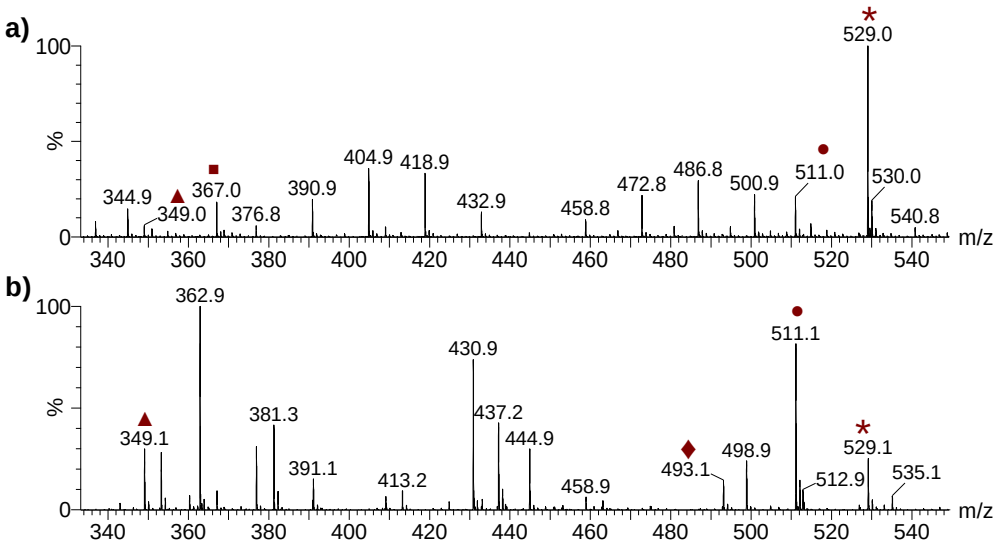

Figure III.A.12. ESI-MS spectra of mannotriose (Man_3) after reduction and thermal treatment at 200 °C for **a)** 0 min (T1) and **b)** 30 min (T2). *: $[M+Na]^+$ adduct of Hex_3 alditol; ●: $[M+Na]^+$ adduct of $Hex_3\text{-}H_2O$ alditol; ♦: $[M+Na]^+$ adduct of $Hex_3\text{-}2H_2O$ alditol; ■: $[M+Na]^+$ adduct of Hex_2 alditol; ▲: $[M+Na]^+$ adduct of $Hex_2\text{-}H_2O$ alditol. Ions non-marked by a symbol are due to contaminants arising from alditol synthesis procedure.

These analyses confirm that under the conditions used, neither tri-dehydrated products nor polymerization products are formed during the thermal processing of the Man_3 alditols, highlighting the relevance of the presence of an anomeric carbon for the formation of these products. In fact, as the polymerization observed occurred via transglycosylation, the absence of the anomeric carbon prevents its occurrence. Nevertheless, the depolymerization of these alditol structures would result in the formation of new anomeric carbons able to undergo polymerization. However, this was not observed, allowing to suggest that the extent of the depolymerization reactions is not enough to promote the occurrence of the high abundant polymerized oligosaccharides observed in thermal treated non-reduced samples. Although the polymerization reactions were shown to be more frequent than depolymerization in these oligosaccharides, their extent should be lower when considering polysaccharides because of the lower proportion of reducing ends in relation to the number of glycosidic linkages that can be cleaved by thermal processing. This is an aspect that deserves research in a near future.

III.A-3.6. Methylation analysis

In order to compare the type of glycosidic linkages present in mannotriose (Man_3) and galactosyl-mannobiose ($GalMan_2$) before and after thermal treatments of these oligosaccharides, a methylation analysis was performed (**Table III.A.1**).

For thermally untreated Man_3 (T0), terminally linked mannopyranosyl residues (T-Man*p*, 41.8%) and (1→4)-linked Man*p* (54.8%) were the most abundant residues. As (1→4)-Man*p* can arise from the reducing end as well as from the middle chain residue, no quantitative analysis was achieved. A small amount of (1→4)-linked mannose in the open-chain form (4-Man_{red}), 2.2%, was also identified. The presence of (1→4,6)-Man*p* (0.6%), and terminally linked galactopyranosyl (Gal*p*) residues (2.0%) as well as terminally linked glucopyranosyl (Glc*p*) residues (0.1%) and (1→4)-Glc*p* (0.7%) show that, although in small amounts, oligosaccharides other than β-(1→4)-D-mannotriose are also present in this sample. The percentage of T-Man*p* from thermal treated samples was higher for longer times of thermal treatment (40.7% for T1, 43.5% for T2, and 51.5% for T3). The percentage

of (1→4)-Man*p* decreased from untreated sample to thermally treated samples and from the shorter treatment time to the longest treatment (51.7, 29.4, and 22.4%, respectively). A decrease of T-Gal*p* residues was also observed, varying from 1.9% for T1 to 0.9% for T3. The amount of (1→4,6)-Man*p* increased from the untreated sample to the thermally treated ones (1.5-7.8%). In all thermal treatments, methylation analysis revealed the presence (1→2)- and (1→6)-Man*p* residues, varying in the range of 0.1-2.6% and 1.2-15.7%, respectively. These results show that new types of glycosidic linkages are formed during the thermal processing. The identification of (1→6)-Man*p* residues is in agreement with the cross-ring cleavage fragment ions formed by loss of $C_3H_6O_3$ (-90 Da) observed in the MS^n experiments previous described. An increase of (1→4)-Glc*p* residues was also observed from untreated sample to thermally treated samples (2.2-3.4%). This increase of (1→4)-Glc*p* residues can result of the occurrence of isomerization reactions during thermal processing, promoting the conversion of mannose into glucose. In chair conformation, β-D-glucose has all of its substituents in equatorial positions, and is thus the most stable hexopyranose (*101*). This fact can explain the specific formation of Glc*p* residues during the thermal processing of this model oligosaccharide (Man_3).

For thermally untreated $GalMan_2$ (T0), T-Man*p* (36.8%) and (1→4,6)-Man*p* (26.5%) as well as T-Gal*p* (33.5%) were the most abundant residues. Small amounts of (1→4)- and (1→6)-Man*p* (1.6 and 0.4%, respectively) as well as (1→2)-Gal*p* (0.3%) and T- and (1→4)-Glc*p* (0.8 and 0.2%, respectively) were also identified, showing that this sample is not composed exclusively by [α-(1→6)-D-galactosyl]^{I}-β-(1→4)-D-mannobiose. The percentage of T-Man*p* from thermal treated samples, contrary to that observed for Man_3, was lower for longer times of thermal treatment (32.5% for T2 and 29.0% for T3), while for the lightest treatment (T1) the percentage of T-Man*p* (40.8 %) increase in relation to thermally untreated sample. The percentage of (1→4)-Man*p* residues identified for T1 (1.3%) was approximately the same to that the observed for T0. However, an increase of (1→4)-Man*p* was observed for longer thermal treatments (5.2% for T2 and 4.6% for T3). A similar behaviour was observed for (1→2)-Gal*p*, varying in the range of 0.2-3.7% for thermally treated samples. Also, the percentage of (1→4,6)-Man*p* as well as T-Gal*p* decreased from untreated sample to the thermally treated ones. As observed for Man_3, (1→2)- and (1→6)-

Man*p* were formed as consequence of thermal processing, varying in the range of 0.2-2.4 and 0.6-10.7%, respectively. For longer thermal treatments (T2 and T3), methylation analysis also revealed the presence of (1→6)-Gal*p* residues. An increase of T- and (1→4)-Glc*p* was observed from untreated sample to thermally treated samples, varying in the range of 1.1-3.6 and 0.6-11.6%, respectively.

Table III.A.1. Glycosidic linkage composition (% area) of the mannotriose (Man_3) and galactosyl-mannobiose ($GalMan_2$) before (T0) and after their thermal processing (T1, T2 and T3).

Linkage	Man_3				$GalMan_2$			
	T0	**T1**	**T2**	**T3**	**T0**	**T1**	**T2**	**T3**
4-Man_{red}[a]	2.2	0.5	-	-	-	-	-	-
T-Man*p*	41.8	40.7	43.5	51.5	36.8	40.8	32.5	29.0
2-Man*p*	-	0.1	2.6	2.0	-	0.2	2.3	2.4
4-Man*p*	54.8	51.7	29.4	22.4	1.6	1.3	5.2	4.6
6-Man*p*	-	1.2	11.5	15.7	0.4	0.6	8.4	10.7
4,6-Man*p*	0.6	1.5	7.8	5.2	26.5	23.7	7.7	6.1
T-Gal*p*	2.0	1.9	1.5	0.9	33.5	31.5	24.6	21.7
2-Gal*p*	-	-	-	-	0.3	0.2	3.7	3.4
6-Gal*p*	-	-	-	-	-	-	5.9	7.1
T-Glc*p*	0.1	0.2	0.4	-	0.8	1.1	3.6	3.5
4-Glc*p*	0.7	2.6	3.4	2.2	0.2	0.6	6.0	11.6

[a] Reducing terminal residue detected as 1,4-di-O-acetyl-1-deuterio-2,3,5,6-tetra-O-methyl-mannitol. Other abbreviations used: T-Man*p*, terminally linked mannopyranosyl residues; 2-Man*p*, (1→2)-linked mannopyranosyl residues; 4-Man*p*, (1→4)-linked mannopyranosyl residues; 6-Man*p*, (1→6)-linked mannopyranosyl residues; 4,6-Man*p*,(1→4,6)-linked mannopyranosyl residues; T-Gal*p*, terminally linked galactopyranosyl residues; 2-Gal*p*, (1→2)-linked galactopyranosyl residues; 6-Gal*p*, (1→6)-linked galactopyranosyl residues; T-Glc*p*, terminally linked glucopyranosyl residues; 4-Glcp, (1→4)-linked glucopyranosyl residues.

The formation of (1→2)- and (1→6)-Man*p* during the thermal processing, occurring in both oligosaccharides, confirms the occurrence of transglycosylation reactions. The formation of (1→6) glycosidic linkages was previously reported for starch heat treated at low moisture content (*95*). Also, an increase of (1→4)-Glc*p* was observed for thermally treated Man_3 and $GalMan_2$. In a previous work, it was shown that the galactomannans of the roasted coffee infusions contained (1→4)-Glc residues at the reducing end, contrary to what was observed for green coffee infusions (*7, 41*). The results obtained in this work suggest that these Glc residues at the reducing end can be formed by an isomerization reaction. The isomerization reaction was already described to occur

during the roasting of the coffee by detection of fructose at the reducing end of the galactomannans of coffee infusions (*7*). Furthermore, the isomerization process has been observed in various model oligosaccharides heated under dry conditions (*94, 102*).

III.A.4. Conclusions

The methodology used for analysis of thermally treated oligosaccharides allowed to observe that the dry thermal processing of mannosyl and galactomannosyl oligosaccharides from room temperature to 200 °C had almost no effect on their structures. However, when these oligosaccharides were heated from room temperature to 200 °C and maintained at 200 °C by 30 and 60 minutes, several structural modifications were identified allowing to infer the occurrence of depolymerization, dehydration, isomerization, and transglycosylation reactions. Transglycosylation reactions can, however, be prevented when the anomeric carbon of the oligosaccharides is reduced, highlighting the relevance of the presence of an anomeric carbon for the occurrence of these reactions. Also, tri-dehydrated products are not formed by reduction of the anomeric carbon, indicating that the loss of three water molecules occurs in the sugar unit located at the reducing end. This finding is also reinforced by deuterium-labelling experiments.

Although this study has been performed using model oligosaccharides, it is expected that similar reactions occur during the roasting of coffee beans and similarly modify the structure of the coffee galactomannans. In particular, the occurrence of transglycosylation reactions and the formation of tri-dehydrated products were never reported to occur during the roasting coffee process. Nevertheless, the hypothesis of the occurrence of these reactions/modifications during the coffee roasting may not be excluded. There is always a fraction of galactomannans in the roasted coffee beans that is not extractable and this fraction can be structurally modified.

III.B. Effects of dry thermal processing on the structural characteristics of arabinotriose and on the mixture of arabinotriose and mannotriose

III.B.1. Background and aims

The two most abundant polysaccharides in green coffee beans are galactomannans and type II arabinogalactans (*6, 38*). These latter polysaccharides are composed by a main backbone of β-(1→3)-linked D-galactose residues, some of them substituted at *O*-6 with short chains of β-(1→6)-linked D-galactose residues. The galactose residues of these short chains are substituted with various combinations of arabinose, rhamnose, and glucuronic acid residues. In particular, side chains composed by α-(1→5)-linked L-arabinose residues are present (*78*). During the roasting process, between 50 and 80% of the arabinose residues present in coffee arabinogalactans are lost and its fate is largely unknown (*6, 10*).

The use of a thermobalance in the dry heating of mannosyl and galactomannosyl oligosaccharides proved to be a useful methodology to study the effects of dry thermal processing on the structure of these compounds. Also, the results obtained in this study with mannosyl and galactomannosyl oligosaccharides (presented in the section III.A) suggested the possibility of the occurrence of transglycosylation reactions during the coffee roasting process. This suggestion raises a hypothesis concerning the fate of the arabinose residues that are lost from arabinogalactans during the roasting process. These arabinose residues could be linked to other coffee polysaccharides such as galactomannans. The galactomannans extracted with hot water from roasted coffee beans were found to contain less arabinose residues than those extracted from green coffee (*41*). This finding, however, does not exclude the presented hypothesis, because galactomannans containing a higher amount of arabinose residues can occur in the unextractable polysaccharide fraction. Thus, in order to investigate the presented hypothesis, a mixture of β-(1→4)-D-mannotriose (Man_3) and α-(1→5)-L-arabinotriose (Ara_3, **Figure III.B.1**) was subjected to the same thermal treatments used in the previous

study with mannosyl and galactomannosyl oligosaccharides. Prior to the study of the oligosaccharide mixture and in order to compare with the results obtained for mannosyl and galactomannosyl oligosaccharides, the effects of the thermal treatments on the structure of the Ara_3 were also investigated. The thermally treated Ara_3 as well as Ara_3 and Man_3 mixture were firstly analysed by methylation analysis in order to obtain information concerning their glycosidic linkage compositions. A more detailed analysis of the structural modifications promoted by thermal processing was made by mass spectrometry using electrospray ionization (ESI-MS and ESI-MS^n) and matrix-assisted laser desorption/ionization (MALDI).

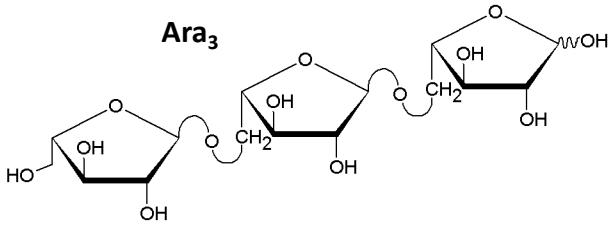

Figure III.B.1. Structure of α-(1→5)-L-arabinotriose (Ara_3).

III.B.2. Material and methods

III.B-2.1. Samples

The following samples were analysed for the present study: arabinotriose and arabinotriose and mannotriose mixture. α-(1→5)-L-arabinotriose (syrup) and β-(1→4)-D-mannotriose (powder), having a purity ≥ 95%, were purchased from Megazyme (County Wicklow, Ireland). The syrup sample was diluted with Milli-Q high-purity water and freeze-dried. The resulting material, having a hydrated appearance, was homogenized using an agate mortar and pestle and then stored in a desiccator until used.

A solution of arabinotriose (10.01 mg, $2.416x10^{-2}$ mmol) and mannotriose (12.18 mg, $2.409x10^{-2}$ mmol) in 100 mL of ultrapure water was prepared. After freeze-drying, the solid mixture was powdered with an agate mortar and pestle and then stored in a desiccator until used.

III.B-2.2. Thermal treatment of samples

Each sample in study was submitted to the same temperature programs used in the previous study with mannosyl and galactomannosyl oligosaccharides (section III.A) using a thermobalance. The thermal stability of the samples was studied submitting them to a temperature program from ambient temperature to 600 °C. The samples were also submitted to three different temperature programs, achieving the maximum temperature of 200 °C. Samples were heated from room temperature up to 200 °C (approx. 18 min), being maintained at 200°C for different periods of time (0, 30, and 60 min). After finishing these temperature programs, samples were left to cool down to the room temperature inside the furnace. The thermally treated samples were then recuperated, weighed and dissolved with ultrapure water to give a concentration of about 5 mg/mL. In order to facilitate the dissolution of these samples, they were stirred at 37 °C for 3h. The water-soluble fractions were separated and kept frozen at -20 °C until analysis. The insoluble fractions were dried under nitrogen flow, weighed and frozen at -20 °C for analysis in a future work. Solutions (approx. 1 mg/mL) of thermally untreated samples were prepared and stored by the same procedure described for thermally treated samples.

III.B-2.3. Methylation analysis

The methylation procedure to obtain the partially *O*-methylated alditol acetates (PMAA) and the analysis of PMAA by gas chromatography/mass spectrometry were performed as previously described (section III.A-2.7).

III.B-2.4. ^{18}O-labelling of the carbonyl oxygen of reducing sugar residues

To label with oxygen-18 (^{18}O) the carbonyl oxygen of reducing residues, 50 µL of the thermally untreated arabinotriose and the mixture of arabinotriose and mannotriose after thermal treatment until 200 °C (T1), previously dissolved in water, were dried and redissolved in 50 µL of ^{18}O-enriched water ($H_2{}^{18}O$, 97 %, Sigma-Aldrich, St. Louis, MO). These solutions were kept frozen at -20 °C during 4 days until analysis.

III.B-2.5. ESI-MS, ESI-MS^n and MALDI-MS analyses

Electrospray ionization mass spectra (ESI-MS) and tandem mass spectra (ESI-MS^n) were carried out on a LXQ linear ion trap mass spectrometer (Thermo Fisher Scientific Inc., Waltham, MA), using the operating conditions previously described (Section III.A-2.5). ESI-MS^n spectra were acquired with the energy collision set between 21 and 37 (arbitrary units). Data acquisitions were carried out on an Xcalibur data system. For all ESI analyses, samples were diluted in methanol/formic acid (99.9:0.1, v/v) prior to analysis and spectra were acquired scanning the mass range from *m/z* 100 to 1500.

Matrix assisted laser desorption/ionization mass spectra (MALDI-MS) were acquired in the *m/z* range of 500-4000 using the MALDI-TOF/TOF Applied Biosystems 4800 Proteomics Analyser (Applied Biosystems, Framingham, MA, USA) instrument equipped with a nitrogen laser emitting at 337 nm and operating in a reflectron mode. The sample preparation for MALDI analysis was performed as previously described (Section III.A-2.6).

III.B.3. Results and discussion

III.B-3.1. Thermal stability of the arabinotriose and the mixture of arabinotriose and mannotriose

TG and DTG curves obtained for arabinotriose (Ara_3) as well as for the mixture of arabinotriose and mannotriose (Ara_3 and Man_3 mix.) at a heating rate of 10 °C/min from room temperature to 600 °C are shown in **Figure III.B.2** in comparison with TG and DTG curves obtained for mannotriose (previously showed in section III.A-2.1). For both samples (Ara_3 and oligosaccharide mixture), the loss of weight until around 100 °C should be associated to the loss of adsorbed water, as previously described for Man_3. The observed weight losses at higher temperatures should be related to the thermal degradation of these samples. The analysis of DTG curves (**Figure III.B.2b**) allowed concluding that the degradation of the Ara_3 as well as the mixture of Ara_3 and Man_3 starts at a temperature

below 200 °C, while the DTG curve of Man_3 showed that the degradation of this oligosaccharide starts after 200 °C. For Man_3, there was almost no weight loss (0.3%) between 150 °C and 200 °C. In the same range of temperatures, the percentage of weight loss observed for Ara_3 and for the oligosaccharide mixture was 4.4% and 2.7%, respectively. These differences in the percentage of weight loss within the same temperature range (150-200 °C) suggest that the arabinotriose as well as the mixture of arabinotriose and mannotriose have a lower thermal stability than that of mannotriose.

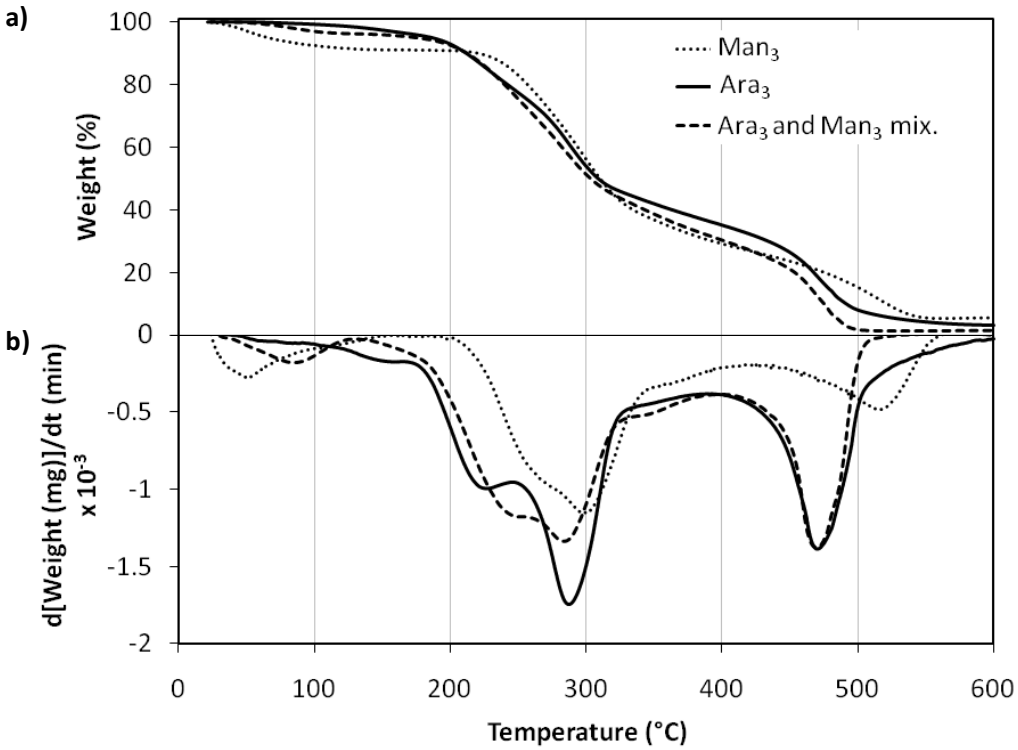

Figure III.B.2. a) TG and **b)** DTG curves obtained for mannotriose, arabinotriose, and for the mixture of these oligosaccharides from room temperature to 600 °C.

The total mass loss percentages determined from TG curves obtained for Ara_3 and for Ara_3 and Man_3 mixture when heated from room temperature up to 200 °C and maintained at 200°C for different periods of time (0, 30, and 60 min, designated as T1, T2, and T3, respectively) were: 6.0% and 6.3% for T1; 19.4% and 19.8% for T2; 21.7% and 27.4% for T3. The materials resulting from the T1 treatment were completely solubilised in water. Nevertheless, the materials resultants from T2 and T3 treatments were only partially dissolved in water. For Ara_3, the percentage of water-soluble residue was 35.3% and 24.6%

for T2 and T3, respectively. For the mixture, the percentage of water-soluble residue was 45.5% for T2 and 31.0% for T3. In accordance with that previously observed for the mannosyl and galactomannosyl oligosaccharides (section III.A), Ara_3 and the oligosaccharide mixture also acquired a brown coloration, more intense the longer the thermal treatment was. Nevertheless, the materials resulting from T2 and T3 treatments of Ara_3 and oligosaccharide mixture became darker than those obtained for the mannosyl and galactomannosyl oligosaccharides. These colour differences reflect differences in the structure of products formed and, consequently, can explain the observed differences in water solubility of the materials resulting from T2 and T3 treatments of Ara_3 and oligosaccharide mixture in comparison than those obtained for Man_3 subjected to the same thermal treatments.

III.B-3.2. Glycosidic-linkage composition

In order to verify if the thermal treatments promoted changes in glycosidic linkage compositions, methylation analysis was performed for both untreated and thermally treated samples.

The results of methylation analysis of the arabinotriose (Ara_3) before (T0) and after its thermal processing (T1, T2, and T3) are shown in **Table III.B.1**. For thermally untreated Ara_3 (T0), terminally linked arabinofuranosyl residues (T-Ara*f*, 29.2%) and (1→5)-linked Ara*f* (69.1%) were found approximately in the proportion of 1 to 2. Nevertheless, small amounts of (1→3,5)- and (1→2,5)-Ara*f* (0.1%), terminally linked xylopyranosyl residues (T-Xyl*p*, 0.4%) and (1→4)-Xyl*p* (0.5%) as well as (1→4)-linked glucopyranosyl residues (4-Glc*p*, 0.6%) were also identified, showing that this sample is not composed exclusively by α-(1→5)-L-arabinotriose. The percentage of T- and (1→5)-Ara*f* (12.4% and 67.7%, respectively) decreased from T0 to T1. Contrarily, an increase of (1→4)-Xyl*p* (3.7%) and (1→4)-Glc*p* (7.9%) as well as (1→3,5)- and (1→2,5)-Ara*f* (2.3% and 2.7%, respectively) was observed. Also, the appearance of (1→2)- and (1→3)-Ara*f* (1.0% and 2.3%, respectively) was observed from T0 to T1. Because only the material resulting from T1 was completely water soluble, the glycosidic linkage composition of the water soluble fraction of the materials resulting from different thermal treatments (T1, T2, and T3) is not comparable.

Table III.B.1. Glycosidic linkage composition (% area) of the arabinotriose (Ara_3) before (T0) and after its thermal processing (T1, T2 and T3).

Linkage[a]	T0	T1	T2	T3
T-Ara*f*	29.2	12.4	16.6	24.5
2-Ara*f*	-	1.0	4.3	8.5
3-Ara*f*	-	2.3	8.4	11.0
5-Ara*f*	69.1	67.7	37.1	32.5
3,5-Ara*f*	0.1	2.3	12.5	7.1
2,5-Ara*f*	0.1	2.7	13.6	8.6
T-Xyl*p*	0.4	-	1.2	1.9
4-Xyl*p*	0.5	3.7	1.4	2.0
4-Glc*p*	0.6	7.9	4.6	3.9

[a]Abbreviations used: T-Ara*f*, terminally linked arabinofuranosyl residues; 2-Ara*f*, (1→2)-linked arabinofuranosyl residues; 3-Ara*f*, (1→3)-linked arabinofuranosyl residues; 5-Ara*f*, (1→5)-linked arabinofuranosyl residues; 3,5-Ara*f*,(1→3,5)-linked arabinofuranosyl residues; 2,5-Ara*f*,(1→2,5)-linked arabinofuranosyl residues; T-Xyl*p*, terminally linked xylopyranosyl residues; 4-Xyl*p*, (1→4)-linked xylopyranosyl residues; 4-Glc*p*, (1→4)-linked glucopyranosyl residues.

Table III.B.2. Glycosidic linkage composition (% area) of the mixture of arabinotriose (Ara_3) and mannotriose (Man_3) before (T0) and after its thermal processing (T1, T2 and T3).

Linkage[a]	T0	T1	T2	T3
T-Ara*f*	7.1	11.4	24.4	28.8
2-Ara*f*	-	0.5	3.5	5.4
3-Ara*f*	-	0.7	4.9	5.0
5-Ara*f*	17.4	15.6	16.7	16.2
3,5-Ara*f*	-	0.4	1.2	0.9
2,5-Ara*f*	-	0.5	1.5	1.7
T-Xyl*p*	0.1	0.2	1.5	1.8
4-Xyl*p*	-	0.6	1.0	1.1
T-Man*p*	28.1	29.7	25.0	25.0
2-Man*p*	-	0.3	0.7	0.7
4-Man*p*	44.2	31.9	9.8	5.2
6-Man*p*	-	2.5	5.2	5.1
4,6-Man*p*	1.2	2.2	1.4	1.4
T-Gal*p*	1.7	1.1	0.4	-
T-Glc*p*	0.1	-	-	-
4-Glc*p*	-	2.2	2.8	1.7

[a]Abbreviations used: T-Ara*f*, terminally linked arabinofuranosyl residues; 2-Ara*f*, (1→2)-linked arabinofuranosyl residues; 3-Ara*f*, (1→3)-linked arabinofuranosyl residues; 5-Ara*f*, (1→5)-linked arabinofuranosyl residues; 3,5-Ara*f*,(1→3,5)-linked arabinofuranosyl residues; 2,5-Ara*f*,(1→2,5)-linked arabinofuranosyl residues; T-Xyl*p*, terminally linked xylopyranosyl residues; 4-Xyl*p*, (1→4)-linked xylopyranosyl residues; T-Man*p*, terminally linked mannopyranosyl residues; 2-Man*p*, (1→2)-linked mannopyranosyl residues; 4-Man*p*, (1→4)-linked mannopyranosyl residues; 6-Man*p*, (1→6)-linked mannopyranosyl residues; 4,6-Man*p*,(1→4,6)-linked mannopyranosyl residues; T-Gal*p*, terminally linked galactopyranosyl residues; T-Glc*p*, terminally linked glucopyranosyl residues; 4-Glc*p*, (1→4)-linked glucopyranosyl residues.

Nevertheless, the water soluble fractions of T2 and T3 also showed, comparatively with the untreated sample (T0), a decrease of T- and (1→5)-Ara*f* and an increase of (1→4)-Xyl*p*, (1→4)-Glc, and (1→3,5)- and (1→2,5)-Ara*f* as well as the appearance of (1→2)- and (1→3)-Ara*f*. Also, an increase of T-Xyl*p* was observed from T0 to T2 and T3. Overall, the formation of new types of glycosidic linkages, inferred by the appearance of (1→2)- and (1→3)-Ara*f*, allowed to infer the occurrence of transglycosylation reactions during the thermal treatments. On other hand, because this methylation analysis is not quantitative, the increase of the relative abundance of 4-Xyl*p* and 4-Glc*p* residues present in the thermally treated Ara_3 in comparison with the untreated Ara_3 can be due to the decrease in the abundance of other residues. To confirm this suggestion explaining the increase of these residues, a quantitative analysis of sugars need to be performed in a near future.

The results of methylation analysis of the oligosaccharide mixture before (T0) and after its thermal processing (T1, T2, and T3) are shown in **Table III.B.2**. For thermally untreated sample (T0), the observed percentages of T-Ara*f* (7.1 %), (1→5)-Ara*f* (17.4 %), T-Man*p* (28.1%), and (1→4)-Man*p* (44.2 %) suggested that Ara_3 and Man_3 were not mixed in equimolar proportions, but in the proportion of 1 to 3. This result can be explained by the hydrated appearance of the arabinotriose used for the preparation of the oligosaccharide mixture. Small amounts of T-Xyl*p* (0.1%), (1→4,6)-Man*p* (1.2%), T-Gal*p* (1.7%), and T-Glc*p* (0.1%) were also identified for T0. An increase of T-Ara*f* (11.4%), T-Man*p* (29.7%), and (1→4,6)-Man*p* (2.2%) was observed from T0 to T1. Also, a decrease of (1→5)-Ara*f* (15.6%), (1→4)-Man*p* (31.9%), and T-Gal*p* (1.1%) was observed. For T1, methylation analysis also revealed the presence of small amounts of (1→2)-, (1→3)-, (1→3,5)- and (1→2,5)-Ara*f* (0.5%, 0.7%, 0.4%, and 0.5%, respectively), T- and (1→4)-Xyl*p* (0.6% and 0.2%, respectively), (1→4)-Glc*p* (2.2%) as well as (1→2)- and (1→6)-Man*p* (0.3% and 2.5%, respectively). The water soluble fractions of T2 and T3 showed, comparatively with the untreated sample (T0), an increase (or the formation) of T-Ara*f*, T- and (1→4)-Xyl*p*, and (1→4)-Glc*p* as well as (1→2)-, (1→6)-, and (1→4,6)-Man*p*. The percentage of (1→5)-Ara*f*, T- and (1→4)-Man*p*, T-Gal*p*, and T-Glc*p* decreased from T0 to T2 and T3. Overall, the identification of (1→2)- and (1→3)-Ara*f* as well as (1→2)- and (1→6)-Man*p* in the thermally treated samples, indicating the occurrence of transglycosylation reactions, is

consistent with the results obtained for Ara_3 and Man_3 when these oligosaccharides were independently subjected to the same thermal treatments. Also, the appearance of 4-Glc*p* residues in the thermally treated samples suggests the occurrence of isomerization reactions.

III.B-3.3. ESI-MS analysis

In order to identify the products formed as consequence of the dry thermal processing, the untreated samples (T0) as well as the thermally treated samples completely soluble in water, obtained when the temperature reached 200 °C (T1), were analysed by ESI-MS.

Figure III.B.3 shows the positive ion ESI-MS spectra acquired for arabinotriose (Ara_3) before and after T1 thermal treatment. The spectrum of thermally untreated Ara_3 (**Figure III.B.3a**) showed a predominant ion at *m/z* 437, attributed to $[Ara_3+Na]^+$, and minor ions at *m/z* 453 and 851, attributed to $[Ara_3+K]^+$ and $[2Ara_3+Na]^+$, respectively. After heating to 200 °C (**Figure III.B.3b**), the ion at *m/z* 437 remained predominant, but a wide series of new ions was identified. All series of the ions identified are resumed in **Table III.B.3**, being presented the *m/z* values of the ions and their relative abundances.

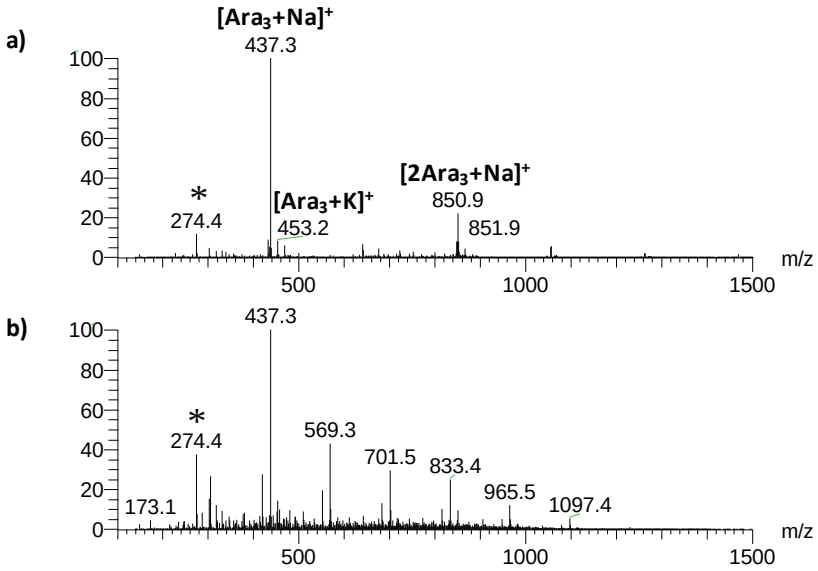

Figure III.B.3. Positive ion ESI-MS spectra of arabinotriose (Ara_3): **a)** thermally untreated (T0) and **b)** heated from room temperature to 200 °C (T1). The ion marked with an asterisk (∗) is attributed to an impurity.

Table III.B.3. Summary of the ions observed in the ESI-MS spectrum of arabinotriose (Ara_3) heated to 200 °C (T1).

n	1	2	3	4	5	6	7	8
$[Pent_n+Na]^+$	**173**[a] 5.2 ± 1.9[b]	**305** 26.5 ± 1.1	**437** 100 %	**569** 43.2 ± 1.4	**701** 33.5 ± 3.2	**833** 23.7 ± 3.4	**965** 10.2 ± 3.3	**1097** 4.8 ± 0.8
$[Pent_n-H_2O+Na]^+$		**287** 8.4 ± 0.8	**419** 26.4 ± 3.8	**551** 21.2 ± 2.9	**683** 12.5 ± 1.0	**815** 9.3 ± 1.4	**947** 4.6 ± 0.5	
$[Pent_n-2H_2O+Na]^+$			**401** 5.5 ± 0.7	**533** 6.3 ± 0.7	**665** 3.9 ± 0.2	**797** 3.1 ± 0.9	**929** 2.7 ± 0.6	
$[Pent_n-3H_2O+Na]^+$				**515** 3.5 ± 0.3	**647** 4.2 ± 0.7	**779** 2.7 ± 0.8	**911** 2.6 ± 0.9	
$[Pent_n-2Da+Na]^+$		**303** 6.2 ± 1.3	**435** 7.7 ± 1.5	**567** 5.8 ± 1.6	**699** 5.1 ± 1.5	**831** 4.4 ± 2.5	**963** 2.9 ± 0.8	
$[Pent_n-60Da+Na]^+$		**245** 2.45 ± 0.8	**377** 8.1 ± 1.8	**509** 10.0 ± 2.2	**641** 7.1 ± 1.3	**773** 6.1 ± 2.2	**905** 4.3 ± 1.9	
$[Pent_n-72Da+Na]^+$				**497** 3.4 ± 0.8	**629** 3.7 ± 1.0	**761** 3.2 ± 0.4	**893** 3.0 ± 0.6	
$[Pent_n-90Da+Na]^+$			**347** 6.3 ± 1.5	**479** 10.3 ± 0.9	**611** 6.9 ± 1.0	**743** 5.3 ± 0.7	**875** 3.6 ± 0.7	
$[Pent_n+16Da+Na]^+$ $[Pent_n+K]^+$		**321** 4.4 ± 1.4	**453** 16.8 ± 5.4	**585** 7.5 ± 2.0	**717** 6.0 ± 1.1	**849** 5.2 ± 1.6	**981** 3.1 ± 1.0	
$[Pent_n+20Da+Na]^+$		**325** 3.2 ± 0.7	**457** 10.5 ± 0.7	**589** 4.3 ± 0.6	**721** 3.6 ± 0.3			
$[Pent_n+28Da+Na]^+$		**333** 2.8 ± 0.5	**465** 5.1 ± 0.7	**597** 6.9 ± 1.0	**729** 3.4 ± 0.8	**861** 3.3 ± 0.5		

[a] *m/z* values of the ions are depicted in bold.

[b] Mean ± standard deviation of three replicate spectra acquisitions made in different days. Ions with a mean relative abundance less than 3 % were not considered.

ESI-MS analysis of arabinotriose (Ara_3) heated to 200 °C (T1) allowed to observe the presence of a series of ions, present at *m/z* 173, 305, 437, 569, 701, 833, 965, and 1097, that can be attributed to the sodium adduct ions of pentose residues with a degree of polymerization (DP) ranging from 1 to 8 ($[Pent_{1-8}+Na]^+$). The presence of these ions is an indication of the occurrence of depolymerization and polymerization reactions during the thermal processing. On other hand, three series of ions can be assigned to the sodiated ions of pentose oligosaccharides modified by dehydration, presenting a loss of one, two or three water molecules, respectively. Belonging to the first series were identified the ions at *m/z* 287, 419, 551, 683, 815, and 947, attributed to $[Pent_{2-7}-H_2O+Na]^+$. In the second series of sodium adduct ions were identified the ions at *m/z* 401, 533, 665, 797, and 929, attributed to $[Pent_{3-7}-2H_2O+Na]^+$. In the third series were identified the ions at *m/z* 515, 647, 779, and 911, attributed to $[Pent_{4-7}-3H_2O+Na]^+$. Also, a series of ions with less two atomic mass units when compared with the ions of $[Pent_n+Na]^+$ series, occurring at *m/z* 303, 435, 567, 699, 831, and 963, was identified. This series of ions can correspond to the sodium adduct ions of pentose oligosaccharides with DP ranging from 2 to 7 containing a keto group, $[Pent_{2-7}-2Da+Na]^+$. According to their *m/z* values, this series of ions could also be attributed to potassium adducts ions of pentose oligosaccharides presenting a loss of one water molecule, $[Pent_{2-7}-H_2O+K]^+$. Nevertheless, the corresponding $[M-H]^-$ ions of this series of ions were identified in the ESI-MS spectrum of thermally treated Ara_3 (T1) acquired in negative mode (data not shown), presenting the ion-intensity ratio between $[Pent_n-H]^-$ and $[Pent_n-2Da-H]^-$ similar to that observed between $[Pent_n+Na]^+$ and $[Pent_n-2Da+Na]^+$. Thus, despite the two possible assignments for this series of ions, the first seems to be the right. Other three series of ions were identified and attributed to sodium adduct ions of pentose oligosaccharides that were cleaved during the thermal treatment, presenting less 60, 72, and 90 Da, respectively, when compared with the corresponding sodium adduct ion of the intact oligosaccharide. Belonging to the first series were identified the ions at *m/z* 245, 377, 509, 641, 773, and 905, attributed to $[Pent_{2-7}-60Da+Na]^+$. In the second series were identified the ions at *m/z* 497, 629, 761, and 893, attributed to $[Pent_{4-7}-72Da+Na]^+$. In the third series were identified the ions at *m/z* 347, 479, 611, 743, and 875, attributed to $[Pent_{3-7}-90Da+Na]^+$. A series of ions with more

16 atomic mass units when compared with the series of pentose oligosaccharides, occurring at *m/z* 321, 453, 585 717, 849, and 981, can be assigned to potassium adducts ions of pentose oligosaccharides with DP ranging from 2 to 7 ($[Pent_{2-7}+K]^+$). Nevertheless, these ions can also be attributed to the sodium adduct ions of pentose oligosaccharides modified by oxidation ($[Pent_{2-7}+16Da+Na]^+$). The analysis of the ESI-MS spectrum acquired in negative mode (data not shown) allowed confirming that these two ion assignments are possible. Also, two series of ions with *m/z* values higher 20 Da and 28 Da than the sodiated ions of the pentose oligosaccharides series were identified. Belonging to the first series were identified the ions at *m/z* 325, 457, 589, and 721 ($[Pent_{2-5}+20Da+Na]^+$), and in the second series were identified the ions at *m/z* 333, 465, 527, 729, 861 ($[Pent_{2-6}+28Da+Na]^+$).

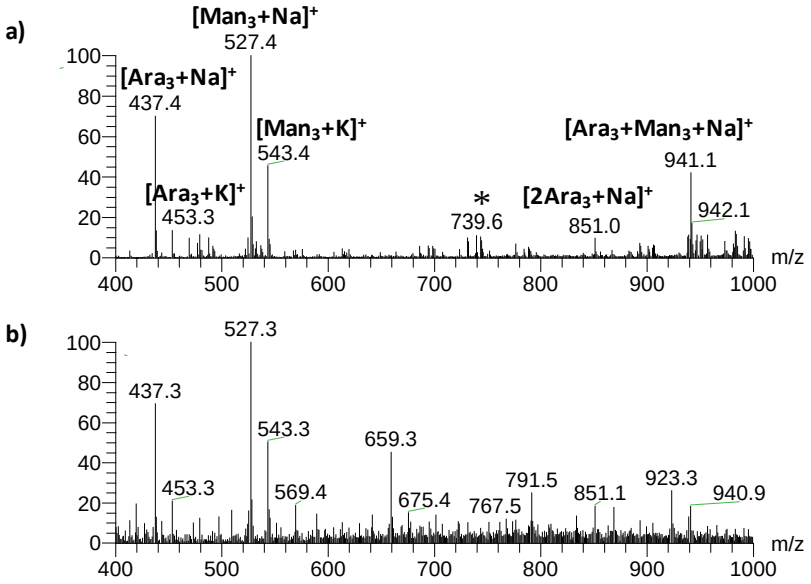

Figure III.B.4. Positive ion ESI-MS spectra of arabinotriose and mannotriose mixture: **a)** thermally untreated (T0) and **b)** heated from room temperature to 200 °C (T1). The ion marked with an asterisk (*) is attributed to an impurity.

Figure III.B.4 shows the positive ion ESI-MS spectra acquired for arabinotriose (Ara_3) and mannotriose (Man_3) mixture before and after T1 thermal treatment. The spectrum of thermally untreated mixture (**Figure III.B.4a**) showed two predominant ions at *m/z* 437 and 527, attributed to $[Ara_3+Na]^+$ and $[Man_3+Na]^+$, respectively. The corresponding potassium adduct of these ions, occurring at *m/z* 453 ($[Ara_3+K]^+$) and 543

($[Man_3+K]^+$), were also observed. Also, it was possible to observe ions at *m/z* 851, 941, and 1031, attributed to $[2Ara_3+Na]^+$, $[Ara_3+Man_3+Na]^+$ and $[2Man_3+Na]^+$, respectively. As shown in **Figure III.B.4b**, other ions than those observed for untreated sample were observed in the ESI-MS spectrum obtained for the oligosaccharide mixture heated from room temperature to 200 °C (T1). All the ions identified in this spectrum are summarised in **Table III.B.4**.

Table III.B.4. Summary of the ions observed in the ESI-MS spectrum of arabinotriose and mannotriose mixture heated to 200 °C (T1).

n	1	2	3	4	5	6
$[Pent_n+Na]^+$		**305** 15.9 ± 1.6	**437** 64.3 ± 3.2	**569** 20.8 ± 4.7	**701** 13.4 ± 0.9	
$[Hex_n+Na]^+$		**365** 33.6 ± 2.0	**527** 100%			**1013** 12.0 ± 3.7
$[Pent_nHex+Na]^+$		**467** 5.2 ± 1.5	**599** 5.5 ± 1.4	**731** 5.3 ± 0.5	**863** 4.3 ± 0.8	**995** 3.9 ± 1.9
$[Pent_nHex-H_2O+Na]^+$		**449** 3.8 ± 0.7	**581** 6.0 ± 1.6	**713** 3.7 ± 0.1	**845** 2.7 ± 0.5	
$[Pent_nHex-3H_2O+Na]^+$		**413** 10.2 ± 1.3	**545** 14.1 ± 3.7	**677** 7.9 ± 1.0	**809** 6.1 ± 1.2	**941** 14.3 ± 5.4
$[Pent_nHex_2+Na]^+$	**497**[a] 14.4 ± 2.1[b]	**629** 11.4 ± 2.5	**761** 8.9 ± 0.3	**893** 6.7 ± 1.5		
$[Pent_nHex_2-H_2O+Na]^+$	**479** 9.4 ± 0.7	**611** 7.0 ± 1.1	**743** 6.6 ± 0.7	**875** 3.1 ± 0.8		
$[Pent_nHex_2-3H_2O+Na]^+$	**443** 8.5 ± 1.5	**575** 6.3 ± 1.4	**707** 8.8 ± 2.9	**839** 5.8 ±1.4		
$[Pent_nHex_3+Na]^+$	**659** 45.8 ± 5.7	**791** 26.1 ± 3.1	**923** 18.3 ± 6.7	**1055** 4.6 ± 1.0		
$[Pent_nHex_3-H_2O+Na]^+$	**641** 6.4 ± 1.0	**773** 8.0 ± 1.0	**905** 6.0 ± 1.9	**1037** 2.6 ± 1.1		
$[Pent_nHex_3-3H_2O+Na]^+$	**605** 7.7 ± 2.0	**737** 4.1 ± 0.8	**869** 14.9 ± 2.2			

[a] *m/z* values of the ions are depicted in bold; [b] Mean ± standard deviation of three replicate spectra acquisitions made in different days. Ions with a mean relative abundance less than 3 % were not considered.

As shown in **Table III.B.4**, ESI-MS analysis of Ara_3 and Man_3 mixture heated to 200 °C (T1) allowed to observe a series of ions, occurring at *m/z* 305, 437 and 569, that can correspond to sodium adduct ions of pentose oligosaccharides with a degree of polymerization (DP) ranging from 2 to 4 ($[Pent_{2-4}+Na]^+$). Also, the ions observed at *m/z* 365, 527 and 1013 can be attributed to sodium adducts of oligosaccharides composed only by hexose residues, $[Hex_2+Na]^+$, $[Hex_3+Na]^+$, and $[Hex_6+Na]^+$, respectively. The

identification of these two series of ions allowed to conclude that each component of the oligosaccharide mixture (Ara_3 and Man_3) undergoes separately depolymerization and polymerization/transglycosylation reactions. Three series of ions that can be attributed to sodiated ions of oligosaccharides containing pentose and hexose residues were also identified, indicating that transglycosylation reactions also occur between Ara_3 and Man_3. One of these series, present at *m/z* 467, 599, 731, 863, and 995, can be attributed to the oligosaccharides formed by one hexose residue and a variable number (2-6) of pentose residues ($[Pent_{2-6}Hex+Na]^+$). Other of these series, present at *m/z* 497, 629, 761, and 893, can be attributed to sodium adducts of oligosaccharides formed by two hexose residues and a number of pentose residues ranging from 1 to 4 ($[Pent_{1-4}Hex_2+Na]^+$). The third of these series, present at *m/z* 659, 791, 923, and 1055, can correspond to sodium adducts of oligosaccharides formed by three hexose residues and a number of pentose residues between 1 and 4 ($[Pent_{1-4}Hex_3+Na]^+$). The ESI-MS analysis also allowed to observe two series of ions that can be attributed to sodium adducts of oligosaccharides formed by pentose and hexose residues presenting a loss of one and three water molecules, respectively. The $[M-H_2O+Na]^+$ ions observed were as follows: $[Pent_{2-5}Hex-H_2O+Na\ ]^+$, present at *m/z* 449, 581, 713, and 845; $[Pent_{1-4}Hex_2-H_2O+Na\ ]^+$, present at *m/z* 479, 611, 743, and 875; and $[Pent_{1-4}Hex_3-H_2O+Na\ ]^+$, present at *m/z* 641, 773, 905, and 1037. The $[M-3H_2O+Na]^+$ ions observed were as follows: $[Pent_{2-6}Hex-3H_2O+Na\ ]^+$, present at *m/z* 413, 545, 677, 809, and 941; $[Pent_{1-4}Hex_2-54+Na\ ]^+$, present at *m/z* 443, 575, 707, and 839; and $[Pent_{1-3}Hex_3-3H_2O+Na\ ]^+$, present at *m/z* 605, 737, and 869. The formation of the products resulting from the loss of one and three water molecules is consistent with what was observed for thermally treated Man_3. However, the products resulting from the oxidation and cleavage of Ara_3 observed for thermally treated Ara_3 were not observed.

In summary, ESI-MS analysis complemented with the information concerning the glycosidic linkages obtained by methylation analysis allowed to infer that during the thermal processing of Ara_3 as well as of Ara_3 and Man_3 mixture, several reactions take place, such as depolymerization, dehydration, transglycosylation, and eventually isomerization reactions. The same reactions were identified to occur during the thermal treatment of mannosyl and galactomannosyl oligosaccharides (section III.A). The results

obtained for thermally treated Ara_3 allowed to suggest the occurrence of oxidation reactions as well as the occurrence of cleavages in the sugar rings. These reactions/modifications identified exclusively for Ara_3 can be due to the lesser thermal stability of the Ara_3 when compared with the Man_3.

III.B-3.4. MALDI-MS analysis

While the oligosaccharides with low molecular weight are easily identified by ESI-MS, high molecular weight oligosaccharides are easier to access by MALDI-MS. Thus, MALDI-MS analysis was also performed for both untreated (T0) and thermally treated samples (T1).

The analysis of MALDI-MS spectra acquired for Ara_3, untreated (data not shown) and thermally treated until 200 °C (**Figure III.B.5a**), allowed concluding that the thermal treatment promotes the formation of pentose oligosaccharides with a degree of polymerization (DP) ranging from 4 to 13. These oligosaccharides were identified as sodium adduct ions occurring at *m/z* 569, 701, 833, 965, 1097, 1229, 1361, 1493, 1625, 1757, 1889, and 2021 ($[Pent_{4-15}+Na]^+$). In addition to this series of ions ($[Pent_n+Na]^+$), the derivatives of these ions belonging to the other series of ions previously identified by ESI-MS, resumed in **Table III.A.3**, were also observed. The ions corresponding to pentose oligosaccharides with a DP between 9 and 15 and their derivatives were not identified by ESI-MS.

The analysis of MALDI-MS spectra acquired for the mixture of Ara_3 and Man_3, untreated (data not shown) and thermally treated until 200 °C (**Figure III.5b**), allowed verifying that the thermal treatment promotes the formation of oligosaccharides with their sodium adduct ions occurring at higher *m/z* values than that the ion of highest *m/z* value identified in the ESI-MS spectrum, occurring at *m/z* 1055. The new ions observed at *m/z* 1127, 1259, 1391, 1523, 1655, 1787, 1919, 2051, and 2183 can be attributed to $[Pent_{7-15}Hex+Na]^+$. The ions observed at *m/z* 1025, 1157, 1289, 1421, 1553, 1685, 1817, and 1949 can be attributed $[Pent_{5-12}Hex_2+Na]^+$. The ions observed at *m/z* 1187, 1319, 1451, 1583, 1715, 1847, 1979, and 2111 can correspond to $[Pent_{5-12}Hex_3+Na]^+$. The MALDI-MS spectrum of oligosaccharide mixture treated until 200 °C (T1) also allowed to

observe a new series of ions not identified by ESI-MS, occurring at *m/z* 1145, 1277, 1409, 1541, 1673, 1805, and 1937, that can be attributed to $[Pent_nHex_6+Na]^+$, with *n* varying from 1 to 8. For all these ions belonging to $[Pent_nHex_{1-3}+Na]^+$ and $[Pent_nHex_6+Na]^+$ series were also identified in the spectrum sodiated ions that can correspond to their mono- and tri-dehydrated derivatives.

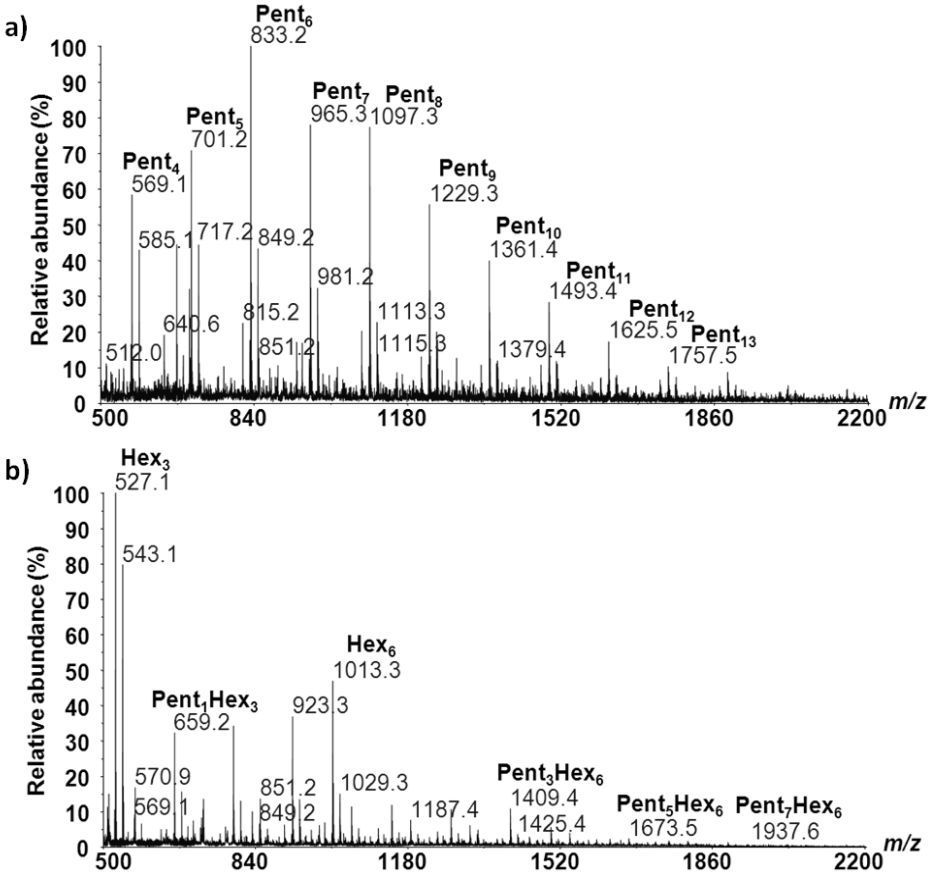

Figure III.B.5. MALDI-MS spectra of **a)** arabinotriose and **b)** arabinotriose and mannotriose mixture heated from room temperature to 200 °C (T1).

III.B-3.5. ESI-MS^n analysis

Aiming to confirm structural assignments proposed for all ions identified by ESI-MS and to find additional details about their structures, ESI-MS^n experiments were performed for all these ions. While the fragmentation of (1→4)-linked hexopyranose oligosaccharides is well reported in existing literature (*58, 92, 93, 99*), there is a only study on the MS^2 fragmentation of lithium-cationized oligosaccharides composed by (1→5)-

linked pentofuranose residues performed by liquid chromatography/tandem mass spectrometry (*103*). Thus, although arabinotriose (Ara_3) and mannotriose (Man_3) have been used in this study, only the behaviour of the $[M+Na]^+$ ion of Ara_3 (no thermally treated) under ESI-MS^n conditions is presented in detail. Also, the fragmentation of ions belonging to different series identified after T1 thermal treatment of the Ara_3 and the mixture of Ara_3 and Man_3 is described.

III.B-3.5.1. ESI-MS^n analysis of the thermally untreated arabinotriose

The MS^2 spectrum of arabinotriose (**Figure III.B.6a**), identified as a sodium adduct ion at *m/z* 437, showed two predominant fragment ions at *m/z* 377 and 347, resulting from cross-ring cleavages with the loss of 60 and 90 Da, respectively, from the precursor ion. Also, fragment ions at *m/z* 305 and 173, formed by loss of one and two pentose residues ($Pent_{res}$, -132 Da), were also observed in the spectrum. The fragment ion observed at *m/z* 419 was formed by a loss of water (-18 Da). The fragment ion observed at *m/z* 407, formed by a loss of 30 Da from the precursor ion, can be resulted from a cross-ring cleavage between two adjacent bonds with a neutral loss of CH_2O.

In order to mass-discriminate between the two possible origins of fragment ions that can be derived from either terminal of the oligosaccharide, the ^{18}O-labelling of the carbonyl group of the reducing sugar was performed. This methodology was successfully applied to study the fragmentation pathways of other oligosaccharides (*93, 99, 104, 105*). The MS^2 spectrum of ^{18}O-labelled arabinotriose (**Figure III.B.6b**), occurring at *m/z* 439, showed two predominant fragment ions at *m/z* 377 and 347, formed by a loss of 62 and 92 Da, respectively, from the precursor ion. This observation allowed concluding that cross-ring cleavages occur predominately from the reducing end. The predominance of the fragment ion at *m/z* 307, formed by a loss of 132 Da, when compared with the fragment ion at *m/z* 305, formed by a loss of 134 Da, allowed concluding that glycosidic cleavages occur preferentially on the non-reducing side of the glycosidic oxygen, as previously reported on a detailed study of the fragmentation of cellobiose (*93*) and in another study with maltopentaose alditols (*64*). Also, the predominance of the fragment ion at *m/z* 419, formed by a loss of 20 Da, when compared with the fragment ion at *m/z*

421, formed by a loss of 18 Da, indicated that the water loss occurs preferentially with cleavage of the C1-O1 bond, as previously reported for gentiobiose (*99*). The fragment ions observed at *m/z* 409 and 407, formed by loss of 30 and 32 Da, suggested that the proposed cross-ring cleavage between two adjacent bonds do not occur exclusively with a loss of anomeric carbon.

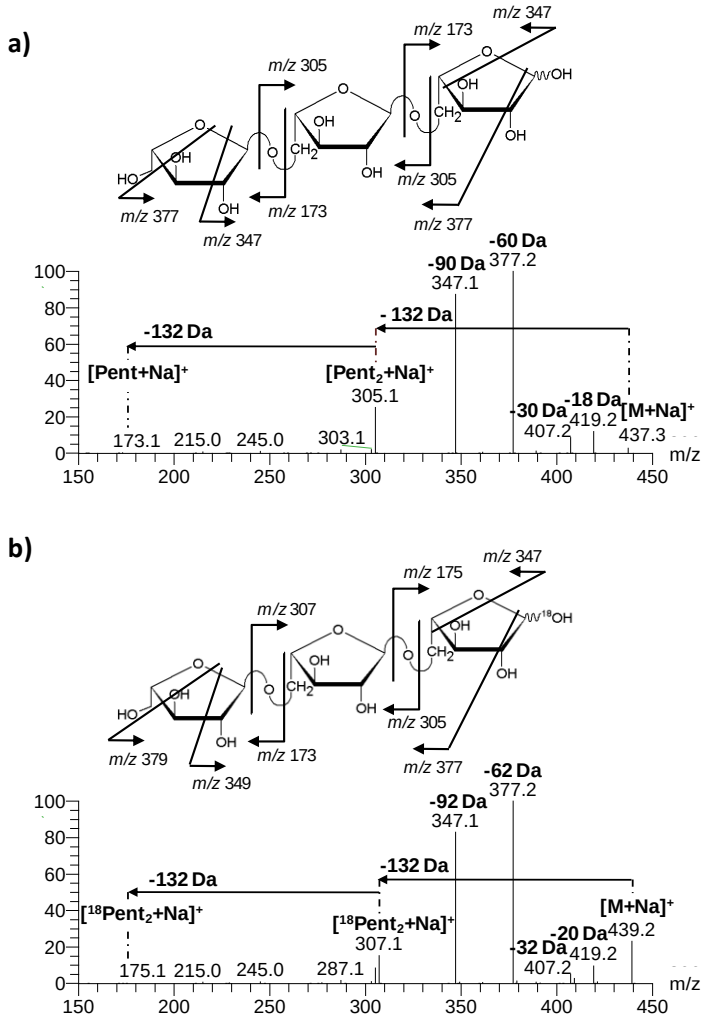

Figure III.B.6. ESI-MS^2 spectra of $[M+Na]^+$ ions from **a)** arabinotriose and **b)** ^{18}O-labelled arabinotriose.

III.B-3.5.2. ESI-MS^n analysis of the series of ions identified in the thermally treated arabinotriose

The fragment ions observed in the ESI-MS^2 spectrum of the ion at *m/z* 437, attributed to $[Pent_3+Na]^+$ (**Figure III.B.7a**), were the same than those observed in the MS^2

spectrum obtained for untreated arabinotriose (**Figure III.B.6a**). However, these spectra showed distinguishable differences in the relative abundances of some fragment ions, particularly, the fragment ions at *m/z* 377 and 347 resulting from cross-ring cleavages. Studies on lithium and sodium-cationized disaccharides have demonstrated that the patterns of cross-ring cleavage ions are linkage-dependent (*92, 93*). Thus, the change in the relative abundances of these fragment ions suggests that new types of glycosidic linkages are formed during the thermal treatment, being this observation confirmed by the results of methylation analysis. The predominant ion observed in all ESI-MS^2 spectra of the ions belonging to this series of ions ($[Pent_n+Na]^+$), except for the ion at *m/z* 305 ($[Pent_2+Na]^+$), results from a cross-ring cleavage with a loss of 90Da ($C_3H_6O_3$). The ion at *m/z* 305 presented a similar fragmentation pattern to the untreated Ara_3, suggesting that the type of glycosidic linkage present was not changed.

Figure III.B.7b shows the ESI-MS^2 spectrum of the ion at *m/z* 435, attributed to $[Pent_3-2Da+Na]^+$. The occurrence of fragment ions at *m/z* 303 and 171, formed by loss of one and two $Pent_{res}$ (-132 Da), respectively, from the precursor ion, suggests that the possible formation of the keto group occurs preferentially in the pentose residue located at the reducing end of the oligosaccharide. On other hand, the appearance of fragment ions formed by losses of 58 Da and 88 Da, resulting from cross-ring cleavages from the reducing end, suggests the location of the keto group at the C1 or C2. A predominant ion at *m/z* 403, formed by a loss of 32 Da from the precursor ion, was also observed. The fragmentation of the $[M+K]^+$ ion of thermally untreated arabinotriose (data not shown) resulted in glycosidic linkage fragment ions with low abundance, showing a predominant fragment ion also formed by a loss of 32 Da from the precursor ion. Thus, the presence of the fragment ion at *m/z* 403 in the ESI-MS^2 spectrum of the ion at *m/z* 435 suggests that this ion also should be attributed to $[Pent_3-H_2O+K]^+$. The MS^2 spectra of the other ions of this series occurring at *m/z* 567, 699, 831, and 963 (data not shown) showed a predominant fragment ion formed by loss of a $Pent_{res}$ (-132 Da) from the precursor ion and a minor fragment ion formed by a loss of 32 Da from the precursor ion, also suggesting the presence of both $[Pent_{4-7}-2Da+Na]^+$ and $[Pent_{4-7}-H_2O+K]^+$ ions.

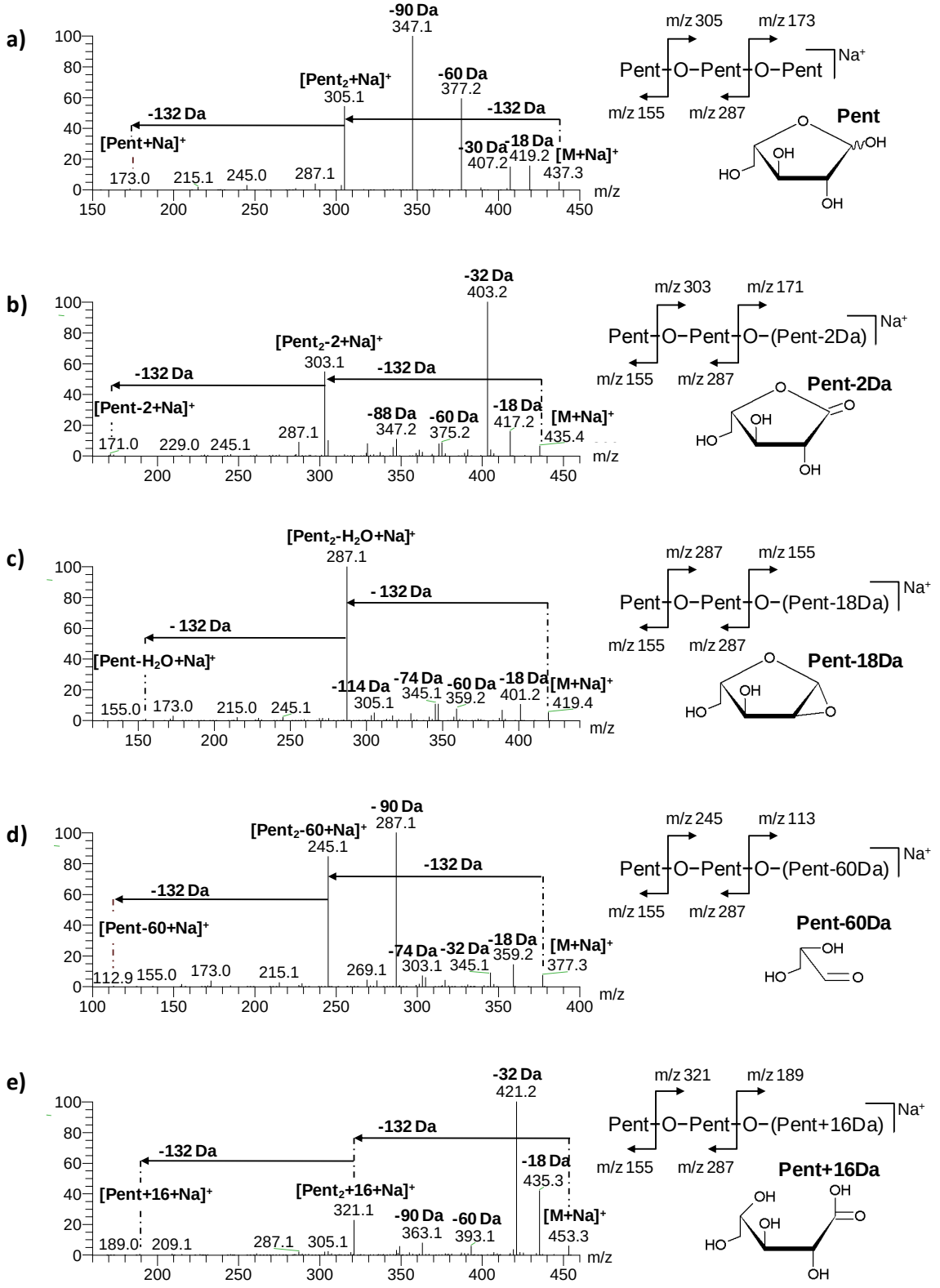

Figure III.B.7. ESI-MS^2 spectra, schematic fragmentation pathways, and tentative structures of sodium adduct ions identified after thermal treatment of the arabinotriose (Ara_3) until 200 °C (T1): **a)** $[Pent_3+Na]^+$ (*m/z* 437), **b)** $[Pent_3\text{-}2Da+Na]^+$ (*m/z* 435, **c)** $[Pent_3\text{-}H_2O+Na]^+$ (*m/z* 419), **d)** $[Pent_3\text{-}60Da+Na]^+$ (*m/z* 377), and **e)** $[Pent_3+16Da+Na]^+$ (*m/z* 453).

Figure III.B.7c shows the ESI-MS^2 spectrum of the ion at *m/z* 419, attributed to $[Pent_3\text{-}H_2O+Na]^+$. The observed fragment ion at *m/z* 305 ($[Pent_2+Na]^+$), formed by a loss of an anhydropentose residue (-114 Da) from the precursor ion, indicates that there are two pentoses linked to each other and that the dehydration occurs in a terminal residue. However, the fragment ions at *m/z* 287 ($[Pent_2\text{-}H_2O+Na]^+$) and 155 ($[Pent\text{-}H_2O+Na]^+$), resulting from the loss of one and two $Pent_{res}$ from the precursor ion, suggest that the anhydropentose unit is preferentially positioned at the reducing end of the oligosaccharide. The observed fragment ion at *m/z* 345, formed by a loss of 74 Da from the precursor ion, can be attributed to the loss of $C_3H_6O_2$, resulting from a cross-ring cleavage at the non-reducing end with the cleavage of C2-C3 and C4-O4 bonds. The dehydration occurring at the reducing end can form an epoxy group as the gas-phase water loss occurring during tandem MS experiments of oligosaccharides (*99*). The ESI-MS^2 spectra acquired for all ions belonging to this series ($[Pent_n\text{-}H_2O+Na]^+$) as well as for the ions of $[Pent_n\text{-}36+Na]^+$ and $[Pent_n\text{-}54+Na]^+$ (data not shown) allowed concluding that the dehydrations occur preferentially in the pentose residue located at the reducing end. However, the presence of other isomers formed by loss of water from the other sugar residues cannot be excluded, namely the one due to loss of one water molecule in the non-reducing end residue, supported by the presence of the fragment ion formed by a loss of 114 Da from the precursor ion.

Figure III.B.7d shows the ESI-MS^2 spectrum of the ion at *m/z* 377, attributed to $[Pent_3\text{-}60Da+Na]^+$. The fragment ions at *m/z* 245 and 113, attributed to $[Pent_{2\text{-}1}\text{-}60Da+Na]^+$, are formed by glycosidic cleavages with the loss of one and two $Pent_{res}$ (-132 Da) from the precursor ion, respectively. The observation of these fragment ions indicates that the precursor ion is constituted by two intact pentose residues linked to a modified pentose residue with 90 Da. This modified residue can result from the cleavage of the pentose residue located at the reducing end of the non-modified oligosaccharide. The ESI-MS^2 spectra acquired for all ions belonging to the $[Pent_n\text{-}60Da+Na]^+$ series as well as for the ions of $[Pent_n\text{-}72Da+Na]^+$ and $[Pent_n\text{-}90Da+Na]^+$ series (data not shown) allowed concluding that the ions belonging to these series are composed by a chain of pentose residues linked to a modified residue with 90, 78, and 60 Da, respectively. The

products formed during the thermal treatment identified in the ESI-MS spectrum as $[Pent_n\text{-}60Da+Na]^+$ and $[Pent_n\text{-}90Da+Na]^+$ ions can have a similar structure as the fragments obtained by cross-ring fragmentations that occurred in the gas-phase reactions during tandem MS of oligosaccharides formed by a loss of $C_3H_6O_3$ (-90 Da) and $C_2H_4O_2$ (-60 Da), respectively (*99*). The products identified as $[Pent_n\text{-}72Da+Na]^+$ ions can have been formed by hydration of the carbonyl group of $Pent_n$-90Da products with formation of the corresponding hydrates. The carbonyl hydrates were already found, for example, in bleached cellulosic pulps (*106*).

Figure III.B.7e shows the ESI-MS^2 spectrum of the ion at *m/z* 453, attributed to $[Pent_3+K]^+$ and $[Pent_3+16Da+Na]^+$. As observed in the fragmentation of the $[M+K]^+$ ion (*m/z* 453) of thermally untreated Ara_3 (data not shown), a predominant fragment ion occurring at *m/z* 421, formed by a loss of 32 Da from the precursor ion, was observed. However, this ESI-MS^2 spectrum showed the fragment ion at *m/z* 321, resulting from a glycosidic cleavage, with a higher relative abundance than that observed in the MS^2 spectrum of the $[Ara_3+K]^+$. This difference may be due to the presence of $[Pent_3+16Da+Na]^+$ ions that can correspond to pentose trisaccharides presenting the reducing end residue modified in the form of pentonic acid. As observed in the ESI-MS^2 spectrum of the ion at *m/z* 453, the others ions also assigned as $[Pent_n+K]^+$ and $[Pent_n+16Da+Na]^+$ showed a major fragment ion formed by a loss of 32 Da from the precursor ion.

The ions belonging to $[Pent_n+20Da+Na]^+$ and $[Pent_n+28Da+Na]^+$ series were also fragmented under ESI-MS^n conditions (data not shown). The fragmentation patterns of these ions, showing the formation of the fragment ion at *m/z* 193 ($[Pent+20Da+Na]^+$) and 201 ($[Pent+28Da+Na]^+$), respectively, suggest that they can be assigned as pentose oligosaccharides modified at the reducing end residue. However, the structures of these modified residues are still unknown.

III.B-3.5.3. ESI-MS^n analysis of the new series of ions identified in the thermally treated arabinotriose and mannotriose mixture

The ESI-MS^2 spectra (data not shown) acquired for the ions occurring at *m/z* 305, 437, 569, and 701, attributed to $[Pent_{2-5}+Na]^+$, showed a similar fragmentation pattern than that observed for the ion with the same *m/z* value identified in the ESI-MS spectrum of the thermally treated arabinotriose, confirming the proposed structural assignments for these ions. Also, the proposed structural assignments for the ions occurring at *m/z* 365 ($[Man_2+Na]^+$), 527 ($[Man_3+Na]^+$), and 1013 ($[Man_6+Na]^+$) also were confirmed. These ions showed a similar fragmentation pattern than that observed for the ions with the same *m/z* values identified in the ESI-MS spectra of the thermally treated mannotriose (T2 and T3) described in the previous study (section III.A).

The MS^2 spectrum of the ion at *m/z* 497, attributed to $[PentHex_2+Na]^+$, is shown in **Figure III.B.8a**. The major fragment ion at *m/z* 365, attributed to $[Hex_2+Na]^+$ and formed by the loss of a pentose residue ($Pent_{res}$, -132 Da) from the precursor ion, indicates that the two hexoses are linked to each other and that the pentose residue is preferentially located at the non-reducing end. The fragment ion at *m/z* 335, attributed to $[PentHex+Na]^+$ and formed by the loss of a hexose residue (Hex_{res}), can result from a glycosidic cleavage on the non-reducing side of the glycosidic oxygen. However, the occurrence of this ion can also be explained by the presence of other isomer(s), such as a disaccharide of hexose containing the reducing end residue substituted by a pentose residue. In general, all ESI-MS^2 spectra (data not shown) acquired for the ions belonging to the $[Pent_nHex_{1-3}+Na]^+$ series showed a fragmentation pattern that can be explained by the presence of more than one structure, namely linear and branching structures. For these ions composed by a variable number of pentose and hexose residues, MS^2 spectra also showed that the residues of the same type are contiguously linked.

The MS^2 spectrum of the ion at *m/z* 479, attributed to $[PentHex_2-H_2O+Na]^+$, is shown in **Figure III.B.8b**. The major fragment ion at *m/z* 347 ($[Hex_2-H_2O+Na]^+$), formed by the loss of a $Pent_{res}$ from the precursor ion, indicates the presence of an intact pentose residue located at the non-reducing end of the oligosaccharide. The fragment ion at *m/z* 185 ($[Hex-H_2O+Na]^+$), formed by the consecutive losses of a $Pent_{res}$ and a Hex_{res} from the precursor ion, suggests that the loss of a water molecule occurs in a Hex_{res} located at the reducing end of the oligosaccharide. The observed ion at *m/z* 317 can correspond to

$[PentHex_{res}+Na]^+$ resulting from the loss of the anhydrohexose. However, the occurrence of this ion can also be explained by the presence of other isomer(s), for example, having an intact hexose located at the reducing end. Also, ion at *m/z* 335 formed by the loss of an anhydrohexose residue (-144 Da) from the precursor ion is an indication that the dehydration occurs in a terminal hexose residue, as previously reported for mono-dehydrated products formed by thermal processing of mannosyl and galactomannosyl oligosaccharides. All MS^2 spectra acquired for the ions $[Pent_nHex_{1-3}-H_2O+Na]^+$ (data not shown) showed the fragment ion formed by the loss of an anhydrohexose residue (-144 Da), suggesting that the dehydration occurs in a terminal hexose residue, and most of them also showed the fragment ion at m/z 185, reinforcing that the dehydration occurs in hexose residue located at the reducing end.

The MS^2 spectrum of the ion at *m/z* 443, attributed to $[PentHex_2-3H_2O+Na]^+$, is shown in **Figure III.B.8c**. The fragment ion at *m/z* 317 ($[PentHex_{res}+Na]^+$), resulting from the loss of a trianhydrohexose (-126 Da), indicates that the loss of three water molecules occurs in a terminal hexose residue. The major fragment ion at *m/z* 311 ($[Hex_2-3H_2O+Na]^+$), formed by the loss of a $Pent_{res}$ from the precursor ion, and the ion at *m/z* 149 ($[Hex-3H_2O+Na]^+$), formed by the consecutive losses of a $Pent_{res}$ and a Hex_{res} from the precursor ion, show that an intact $Pent_{res}$ is located at the non-reducing end and that the loss of three water molecules occurs in a Hex_{res} located at the reducing end of the oligosaccharide. However, the observed fragment ion at *m/z* 281, attributed to $[PentHex-3H_2O+Na]^+$ and formed by the loss of a Hex_{res} from the precursor ion, cannot be explained by the proposed structure, indicating the occurrence of other structural isomer(s), namely a isomer containing an intact Hex_{res} located at the non-reducing end. All MS^2 spectra acquired for the ions $[Pent_nHex_{1-3}-3H_2O+Na]^+$ (data not shown) showed the fragment ion formed by the loss of a trianhydrohexose (-126 Da), suggesting that the loss of three water molecules occurs in a Hex_{res} located at the reducing end of the oligosaccharide, and most of them also showed the fragment ion at *m/z* 149, reinforcing that the loss of three water molecules occurs a in hexose residue located at the reducing end.

In the previous description of the MS^2 spectra acquired for thermally treated mixture, the fragment ions resulting from cross-ring cleavages (-60, -90, and -120 Da) were not described. As previously mentioned (section III.B-3.5.2), the patterns of cross-ring cleavage ions are linkage-dependent. Thus, the observed differences between MS^2 spectra in the patterns of cross-ring cleavage ions indicate that the thermal processing promoted the formation of new types of glycosidic linkages, confirming the results of the methylation analysis.

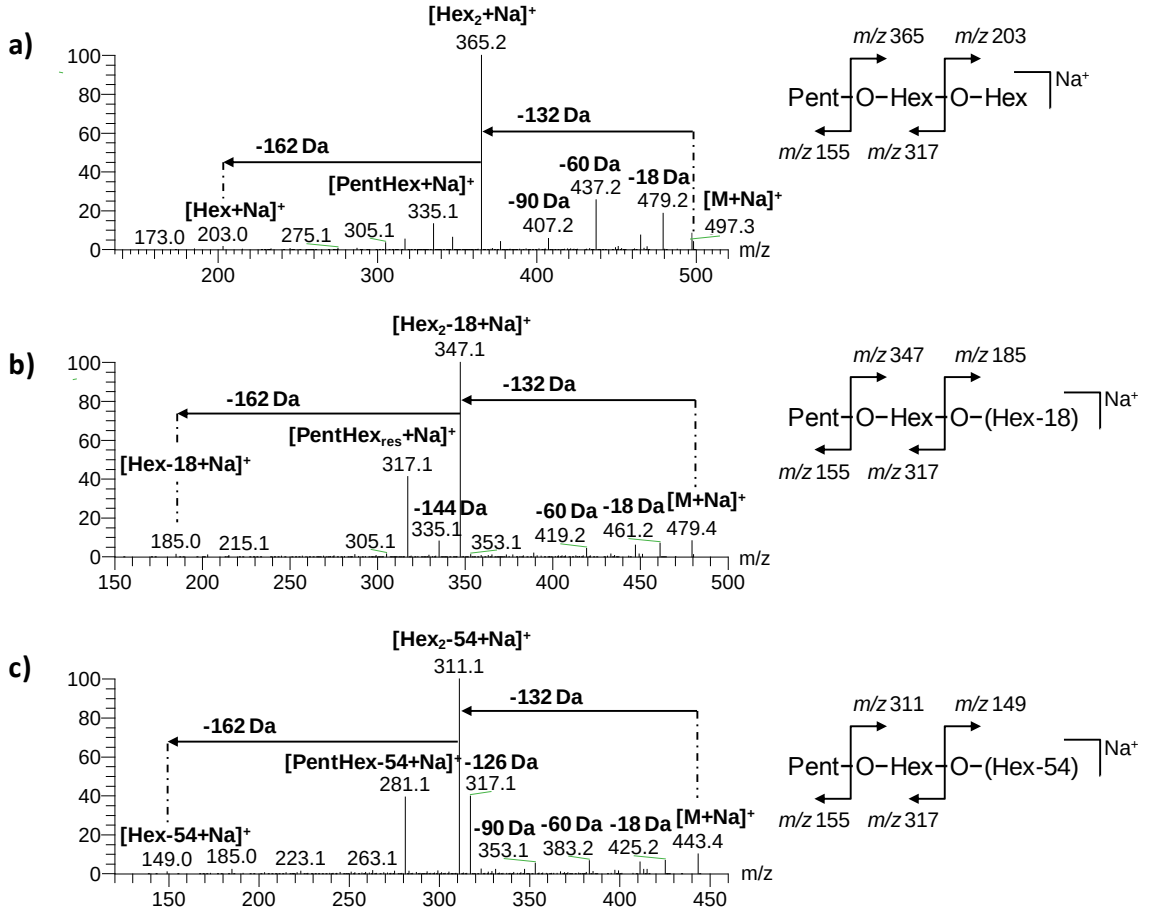

Figure III.B.8. ESI-MS^2 spectra and schematic fragmentation pathways considering a linear structure of sodium adduct ions identified after thermal treatment of the Ara_3 and Man_3 mixture until 200 °C (T1): **a)** $[PentHex_2+Na]^+$ (*m/z* 497), **b)** $[PentHex_2-18+Na]^+$ (*m/z* 479), and **c)** $[PentHex_2-54+Na]^+$ (*m/z* 443).

Aiming to obtain additional information concerning the structure of the products belonging to the $[Pent_nHex_{1-3}+Na]^+$ series, the ^{18}O-labelling of the carbonyl group of reducing sugar residues was performed. ESI-MS^2 spectra of $[PentHex_3+Na]^+$ acquired

before and after ^{18}O-labelling are shown in **Figure III.B.9**. For unlabelled sample (**Figure III.B.9a**), the major ion observed at *m/z* 527, attributed to $[Hex_3+Na]^+$, allowed to conclude that the hexose residues are contiguously linked; however, the exact location of the arabinose residue is uncertain. After ^{18}O-labelling (**Figure III.B.9b**), the MS^2 spectrum showed the presence of a fragment ion at *m/z* 205, attributed to $[^{18}Hex+Na]^+$, and the absence of the fragment ion at *m/z* 175, attributed to $[^{18}Pent+Na]^+$, allowing to conclude that the sugar at the reducing end is a hexose residue and the arabinose residue is present as a non-reducing sugar. Also, the presence of the fragment ion at *m/z* 337, attributed to $[^{18}PentHex+Na]^+$, allowed concluding ambiguously that the arabinose residue is linked to the hexose residue located at the reducing end.

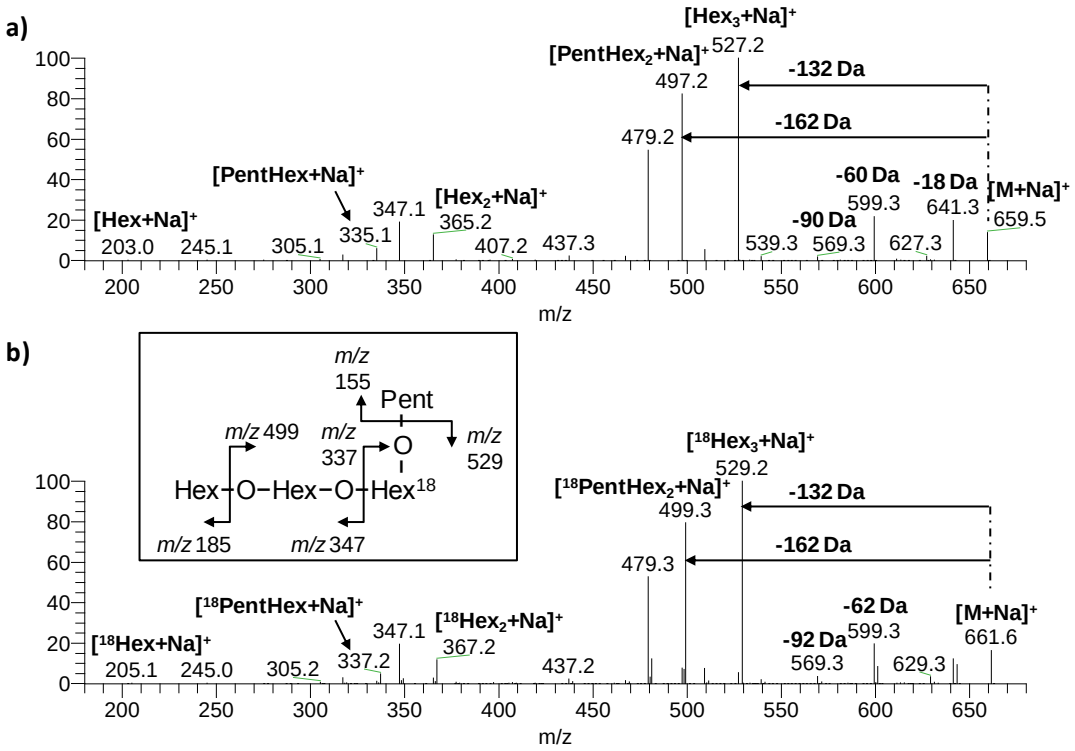

Figure III.B.9. ESI-MS^2 spectra of $[PentHex_3+Na]^+$ ion identified after thermal treatment of the arabinotriose and mannotriose mixture until 200 °C (T1): **a)** unlabelled and **b)** ^{18}O-labelled sample.

III.B.4. Conclusions

The lower thermal stability of arabinotriose than that mannotriose, suggested by analysis of DTG curves, was confirmed by the identification of new type of products

formed, not previously identified for thermally treated mannosyl oligosaccharides. Apart from dehydrated products, derivatives resulting from cleavages as well as oxidation reactions were also observed. However, for the mixture of arabinotriose and mannotriose, these products were not identified. The formation of oligosaccharides composed by arabinose and mannose residues was predominant during the thermal treatment of the oligosaccharide mixture. This observation supports the hypothesis concerning the fate of the arabinose residues resulting from the thermal degradation of arabinogalactans during the roasting process. These residues can be linked to other polysaccharides such as galactomannans.

IV. Concluding remarks and perspectives for future work

Although it is recognized that during the roasting of coffee several reaction pathways occur changing the structural features of galactomannans, the reactions that take place inside of the beans as well as the structure of the products formed are not yet completely known. Thus, the main objective of the work described in this dissertation, developed using model systems, was to set an analytical methodology that could contribute for the identification of the reactions that occur during the coffee roasting process and that are responsible for changing the structural features of coffee galactomannans.

The identification of several products formed after thermal processing of all model systems, comprising only one oligosaccharide or a mixture of manno- and arabino-oligosaccharides, allows to conclude that depolymerization, dehydration, isomerization, and polymerization reactions are taking place during the dry thermal processing. These polymerization reactions occur via transglycosylation. Also, oxidation reactions take place during thermal processing of the arabinotriose. Some of the products and/or reactions observed were never reported to occur during coffee roasting, including the occurrence of transglycosylation reactions and the formation of tri-dehydrated products. Nevertheless, although the experiments were performed in model systems, it is expected that similar reactions occur during the roasting of coffee beans modifying the structure of galactomannans. However, aiming to ascertain the reliability of the models used, similar

experiments need to be performed using polysaccharides isolated from green coffee beans. All structural modifications identified in model systems studied need to be also screened in galactomannans isolated from roasted coffee beans.

Future directions comprise also the use of model systems to study structural changes that arabinogalactanas, the second most abundant polysaccharides in coffee beans after galactomannans, undergo during the roasting process. Having in mind that polysaccharides, proteins, and phenolic compounds are involved in melanoidin formation, other model systems need to be performed in order to investigate the structure of coffee melanoidins. Aiming to understand the interactions established between coffee polysaccharides and proteins, model oligosaccharides could be mixed with selected amino acids/peptides. Also, model oligosaccharides and selected phenolic compounds could be mixed to understand the interactions established between these classes of compounds.

An overall view of the structural modifications that occur in coffee polysaccharides during the roasting is still far from being achieved. Because this knowledge can be crucial for future developments in coffee industry (namely in the area of the quality control), future studies need to be performed.

References

(1) Dumitriu, S. *Polysaccharides : structural diversity and functional versatility*. 2nd ed.; Marcel Dekker: New York 2005.

(2) Sun, D.-W. *Thermal Food Processing: new technologies and quality issues*. Taylor & Francis: Boca Raton 2006.

(3) Rufián-Henares, J. A.; Morales, F. J. Effect of in vitro enzymatic digestion on antioxidant activity of coffee melanoidins and fractions. *J. Agric. Food Chem.* **2007**, *55*, 10016-10021.

(4) Capuano, E.; Fogliano, V. Acrylamide and 5-hydroxymethylfurfural (HMF): A review on metabolism, toxicity, occurrence in food and mitigation strategies. *LWT - Food Science and Technology* **2011**, *44*, 793-810.

(5) Nunes, F. M.; Coimbra, M. A. Chemical characterization of the high molecular weight material extracted with hot water from green and roasted robusta coffees as affected by the degree of roast. *J. Agric. Food Chem.* **2002**, *50*, 7046-7052.

(6) Nunes, F. M.; Coimbra, M. A. Chemical characterization of the high molecular weight material extracted with hot water from green and roasted arabica coffee. *J. Agric. Food Chem.* **2001**, *49*, 1773-1782.

(7) Nunes, F. M.; Reis, A.; Domingues, M. R. M.; Coimbra, M. A. Characterization of galactomannan derivatives in roasted coffee beverages. *J. Agric. Food Chem.* **2006**, *54*, 3428-3439

(8) Oosterveld, A.; Harmsen, J. S.; Voragen, A. G. J.; Schols, H. A. Extraction and characterization of polysaccharides from green and roasted *Coffea arabica* beans. *Carbohydr. Polym.* **2003**, *52*, 285-296.

(9) Nunes, F. M.; Coimbra, M. A. Chemical characterization of galactomannans and arabinogalactans from two arabica coffee Infusions as affected by the degree of roast. *J. Agric. Food Chem.* **2002**, *50*, 1429-1434.

(10) Redgwell, R. J.; Trovato, V.; Curti, D.; Fischer, M. Effect of roasting on degradation and structural features of polysaccharides in Arabica coffee beans. *Carbohydr. Res.* **2002**, *337*, 421-431.

(11) Nunes, F. M.; Coimbra, M. A. Melanoidins from coffee infusions. Fractionation, chemical characterization, and effect of the degree of roast. *J. Agric. Food Chem.* **2007**, *55*, 3967-3977.

(12) Srivastava, M.; Kapoor, V. P. Seed galactomannans: an overview. *Chem. Biodivers.* **2005**, *2*, 295-317.

(13) Ahrazem, O.; Prieto, A.; Leal, J. A.; Jiménez-Barbero, J.; Bernabé, M. Fungal cell-wall galactomannans isolated from *Geotrichum* spp. and their teleomorphs, *Dipodascus* and *Galactomyces*. *Carbohydr. Res.* **2002**, *337*, 2347-2351.

(14) Carbonero, E. R.; Cordeiro, L. M. C.; Mellinger, C. G.; Sassaki, G. L.; Stocker-Wörgötter, E.; J. Gorin, P. A.; Iacomini, M. Galactomannans with novel structures from the lichen *Roccella decipiens* Darb. *Carbohydr. Res.* **2005**, *340*, 1699-1705.

(15) Omarsdottir, S.; Petersen, B. O.; Barsett, H.; Paulsen, B. S.; Duus, J. Ø.; Olafsdottir, E. S. Structural characterisation of a highly branched galactomannan from the lichen *Peltigera canina* by methylation analysis and NMR-spectroscopy. *Carbohydr. Polym.* **2006**, *63*, 54-60.

(16) Reid, J. S. G.; Edwards, M. E., Galactomannans and other cell wall storage polysaccharides in seeds. In *Food polysaccharides and their applications*, Stephen, A. M., Ed. Marcel Dekker New York, 1995; pp 155-184.

(17) Moreira, L. R. S.; Filho, E. X. F. An overview of mannan structure and mannan-degrading enzyme systems. *Appl. Microbiol. Biotechnol.* **2008**, *79*, 165-178.

(18) Kooiman, P. Structures of the galactomannans from seeds of *Annona muricata*, *Arenga saccharifera*, *Cocos nucifera*, *Convolvulus tricolor*, and *Sophora japonica*. *Carbohydr. Res.* **1971**, *20*, 329-337.

(19) Cerqueira, M. A.; Pinheiro, A. C.; Souza, B. W. S.; Lima, Á. M. P.; Ribeiro, C.; Miranda, C.; Teixeira, J. A.; Moreira, R. A.; Coimbra, M. A.; Gonçalves, M. P.; Vicente, A. A. Extraction,

purification and characterization of galactomannans from non-traditional sources. *Carbohydr. Polym.* **2009**, *75*, 408-414.

(20) Cerqueira, M. A.; Souza, B. W. S.; Simões, J.; Teixeira, J. A.; Domingues, M. R. M.; Coimbra, M. A.; Vicente, A. A. Structural and thermal characterization of galactomannans from non-conventional sources. *Carbohydr. Polym.* **2011**, *83*, 179-185.

(21) Daas, P. J. H.; Schols, H. A.; de Jongh, H. H. J. On the galactosyl distribution of commercial galactomannans. *Carbohydr. Res.* **2000**, *329*, 609-619.

(22) Chaubey, M.; Kapoor, V. P. Structure of a galactomannan from the seeds of *Cassia angustifolia* Vahl. *Carbohydr. Res.* **2001**, *332*, 439-444.

(23) Kapoor, V. P.; Chanzy, H.; Taravel, F. R. X-ray diffraction studies on some seed galactomannans from India. *Carbohydr. Polym.* **1995**, *27*, 229-233.

(24) Kapoor, V. P.; Milas, M.; Taravel, F. R.; Rinaudo, M. Rheological properties of a seed galactomannan from *Cassia siamea* Lamk. *Food Hydrocolloids* **1996**, *10*, 167-172.

(25) Singh, V.; Srivastava, A.; Tiwari, A. Structural elucidation, modification and characterization of seed gum from *Cassia javahikai* seeds: A non-traditional source of industrial gums. *Int. J. Biol. Macromol.* **2009**, *45*, 293-297.

(26) Singh, V.; Sethi, R.; Tiwari, A. Structure elucidation and properties of a non-ionic galactomannan derived from the *Cassia pleurocarpa* seeds. *Int. J. Biol. Macromol.* **2009**, *44*, 9-13.

(27) Kapoor, V. P.; Taravel, F. R.; Joseleau, J.-P.; Milas, M.; Chanzy, H.; Rinaudo, M. *Cassia spectabilis* DC seed galactomannan: Structural, crystallographical and rheological studies. *Carbohydr. Res.* **1998**, *306*, 231-241.

(28) Cunha, P. L. R.; Vieira, Í. G. P.; Arriaga, Â. M. C.; de Paula, R. C. M.; Feitosa, J. P. A. Isolation and characterization of galactomannan from *Dimorphandra gardneriana* Tul. seeds as a potential guar gum substitute. *Food Hydrocolloids* **2009**, *23*, 880-885.

(29) Bourbon, A. I.; Pinheiro, A. C.; Ribeiro, C.; Miranda, C.; Maia, J. M.; Teixeira, J. A.; Vicente, A. A. Characterization of galactomannans extracted from seeds of *Gleditsia*

triacanthos and *Sophora japonica* through shear and extensional rheology: Comparison with guar gum and locust bean gum. *Food Hydrocolloids* **2010**, *24*, 184-192.

(30) Hussein, M. M.-D.; Helmy, W. A.; Salem, H. M. Biological activities of some galactomannans and their sulfated derivatives. *Phytochemistry* **1998**, *48*, 479-484.

(31) Olennikov, D. N.; Rokhin, A. V. Galactomannan from the seeds of Ural licorice (*Glycyrrhiza uralensis* Fisch.) *Appl. Biochem. Microbiol.* **2010**, *46*, 540-544.

(32) Ganter, J. L. M. S.; Reicher, F. Water-soluble galactomannans from seeds of *Mimosaceae* spp. *Bioresour. Technol.* **1999**, *68*, 55-62.

(33) Tewari, K.; Singh, V.; Chandra Gupta, P. A non-ionic water soluble seed-gum from *Parkinsonia aculeata*. *Carbohydr. Polym.* **2005**, *59*, 393-396.

(34) Ishurd, O.; Kermagi, A.; Zgheel, F.; Flefla, M.; Elmabruk, M.; Yalin, W.; Kennedy, J. F.; Yuanjiang, P. Structural aspects of water-soluble galactomannans isolated from the seeds of *Retama raetam*. *Carbohydr. Polym.* **2004**, *58*, 41-44.

(35) Harry-O'kuru, R. E.; Wu, Y. V.; Evangelista, R.; Vaughn, S. F.; Rayford, W.; Wilson, R. F. Sicklepod (*Senna obtusifolia*) seed processing and potential utilization. *J. Agric. Food Chem.* **2005**, *53*, 4784-4787.

(36) Garti, N.; Madar, Z.; Aserin, A.; Sternheim, B. Fenugreek Galactomannans as food emulsifiers. *Lebensmittel-Wissenschaft und-Technologie* **1997**, *30*, 305-311.

(37) Ishrud, O.; Zahid, M.; Zhou, H.; Pan, Y. A water-soluble galactomannan from the seeds of *Phoenix dactylifera* L. *Carbohydr. Res.* **2001**, *335*, 297-301.

(38) Bradbury, A. G. W.; Halliday, D. J. Chemical structures of green coffee bean polysaccharides. *J. Agric. Food Chem.* **1990**, *38*, 389-392

(39) Dea, I. C. M.; Morrison, A., Chemistry and interactions of seed galactomannans. In *Advances in Carbohydrate Chemistry and Biochemistry*, Tipson, R. S.; Derek, H., Eds. Academic Press: 1975; Vol. Volume 31, pp 241-312.

(40) Oosterveld, A.; Coenen, G. J.; Vermeulen, N. C. B.; Voragen, A. G. J.; Schols, H. A. Structural features of acetylated galactomannans from green *Coffea arabica* beans. *Carbohydr. Polym.* **2004**, *58*, 427-434.

(41) Nunes, F. M.; Domingues, M. R.; Coimbra, M. A. Arabinosyl and glucosyl residues as structural features of acetylated galactomannans from green and roasted coffee infusions. *Carbohydr. Res.* **2005**, *340*, 1689-1698.

(42) Buckeridge, M. S.; Panegassi, V. R.; Rocha, D. C.; Dietrich, S. M. C. Seed galactomannan in the classification and evolution of the leguminosae. *Phytochemistry* **1995**, *38*, 871-875.

(43) Wu, Y.; Cui, W.; Eskin, N. A. M.; Goff, H. D. An investigation of four commercial galactomannans on their emulsion and rheological properties. *Food Res. Int.* **2009**, *42*, 1141-1146.

(44) Lima, D. U.; Oliveira, R. C.; Buckeridge, M. S. Seed storage hemicelluloses as wet-end additives in papermaking. *Carbohydr. Polym.* **2003**, *52*, 367-373.

(45) Franz, G., Polysaccharides in pharmacy. In *Pharmacy/Thermomechanics/Elastomers/Telechelics*, Dušek, K., Ed. Springer Heidelberg, 1986.

(46) Blackburn, R. S. Natural polysaccharides and their interactions with dye molecules: applications in effluent treatment. *Environ. Sci. Technol.* **2004**, *38*, 4905-4909.

(47) Sanghi, R.; Bhattacharya, B.; Singh, V. Seed gum polysaccharides and their grafted co-polymers for the effective coagulation of textile dye solutions. *React. Funct. Polym.* **2007**, *67*, 495-502.

(48) Martins, J. T.; Cerqueira, M. A.; Souza, B. W. S.; Avides, M. C.; Vicente, A. A. Shelf life extension of Ricotta cheese using coatings of galactomannans from nonconventional sources incorporating nisin against Listeria monocytogenes. *J. Agric. Food Chem.* **2010**, *58*, 1884-1891.

(49) Brownlee, I. A. The physiological roles of dietary fibre. *Food Hydrocolloids* **2011**, *25*, 238-250.

(50) Srichamroen, A.; Thomson, A. B.; Field, C. J.; Basu, T. K. In vitro intestinal glucose uptake is inhibited by galactomannan from Canadian fenugreek seed (*Trigonella foenum graecum* L) in genetically lean and obese rats. *Nutr. Res.* **2009**, *29*, 49-54.

(51) Jaquet, M.; Rochat, I.; Moulin, J.; Cavin, C.; Bibiloni, R. Impact of coffee consumption on the gut microbiota: A human volunteer study. *Int. J. Food Microbiol.* **2009**, *130*, 117-121.

(52) Simões, J.; Madureira, P.; Nunes, F. M.; Domingues, M. R.; Vilanova, M.; Coimbra, M. A. Immunostimulatory properties of coffee mannans. *Mol. Nutr. Food Res.* **2009**, *53*, 1036-1043.

(53) Aryaa, M.; Rao, L. J. M. An impression of coffee carbohydrates *Crit. Rev. Food Sci. Nutr.* **2007**, *47*, 51-67.

(54) Illy, A.; Viani, R. *Espresso coffee: the chemistry of quality*. Academic Press: London, 1995.

(55) Fischer, M.; Reimann, S.; Trovato, V.; Redgwell, R. J. Polysaccharides of green Arabica and Robusta coffee beans. *Carbohydr. Res.* **2001**, *330*, 93-101.

(56) Schenker, S.; Handschin, S.; Frey, B.; Perren, R.; Escher, F. Pore structure of coffee beans affected by roasting conditions. *J. Food Sci.* **2000**, *65*, 452-457.

(57) Nunes, F.; Coimbra, M. A. Role of hydroxycinnamates in coffee melanoidin formation. *Phytochem. Rev.* **2010**, *9*, 171-185.

(58) Cmelík, R.; Chmelík, J. Structural analysis and differentiation of reducing and nonreducing neutral model starch oligosaccharides by negative-ion electrospray ionization ion-trap mass spectrometry. *Int. J. Mass spectrom.* **2010**, *291*, 33-40.

(59) Fernández, L. E. M. Introduction to ion trap mass spectrometry: Application to the structural characterization of plant oligosaccharides. *Carbohydr. Polym.* **2007**, *68*, 797-807.

(60) Gonçalves, V. M. F.; Reis, A.; Domingues, M. R. M.; Lopes-da-Silva, J. A.; Fialho, A. M.; Moreira, L. M.; Sá-Correia, I.; Coimbra, M. A. Structural analysis of gellans produced by *Sphingomonas elodea* strains by electrospray tandem mass spectrometry. *Carbohydr. Polym.* **2009**, *77*, 10-19.

(61) Gullón, P.; González-Muñoz, M. J.; Gool, M. P.; Schols, H. A.; Hirsch, J.; Ebringerová, A.; Parajó, J. C. Production, refining, structural characterization and fermentability of rice husk xylooligosaccharides. *J. Agric. Food Chem.* **2010**, *58*, 3632-3641.

(62) Reis, A.; Coimbra, M. A.; Domingues, P.; Ferrer-Correia, A. J.; Domingues, M. R. M. Structural characterisation of underivatised olive pulp xylo-oligosaccharides by mass spectrometry using matrix-assisted laser desorption/ionisation and electrospray ionisation. *Rapid Commun. Mass Spectrom.* **2002**, *16*, 2124-2132.

(63) Reis, A.; Domingues, M. R. M.; Domingues, P.; Ferrer-Correia, A. J.; Coimbra, M. A. Positive and negative electrospray ionisation tandem mass spectrometry as a tool for structural characterisation of acid released oligosaccharides from olive pulp glucuronoxylans. *Carbohydr. Res.* **2003**, *338*, 1497-1505.

(64) Reis, A.; Coimbra, M. A.; Domingues, P.; Ferrer-Correia, A. J.; Domingues, M. R. M. Fragmentation pattern of underivatised xylo-oligosaccharides and their alditol derivatives by electrospray tandem mass spectrometry. *Carbohydr. Polym.* **2004**, *55*, 401-409.

(65) Reis, A.; Pinto, P.; Coimbra, M. A.; Evtuguin, D. V.; Neto, C. P.; Ferrer Correia, A. J.; Domingues, M. R. M. Structural differentiation of uronosyl substitution patterns in acidic heteroxylans by electrospray tandem mass spectrometry. *J. Am. Soc. Mass Spectrom.* **2004**, *15*, 43-47.

(66) Reis, A.; Pinto, P.; Evtuguin, D. V.; Neto, C. P.; Domingues, P.; Ferrer-Correia, A. J.; Domingues, M. R. M. Electrospray tandem mass spectrometry of underivatised acetylated xylo-oligosaccharides. *Rapid Commun. Mass Spectrom.* **2005**, *19*, 3589-3599.

(67) Zaia, J. Mass spectrometry of oligosaccharides. *Mass Spectrom. Rev.* **2004**, *23*, 161-227.

(68) Dass, C. *Fundamentals of contemporary mass spectrometry*. John Wiley & Sons: Hoboken, 2007.

(69) Hofstadler, S. A.; Bakhtiar, R.; Smith, R. D. Electrospray ionization mass spectroscopy: Part I. Instrumentation and spectral interpretation *J. Chem. Educ.* **1996**, *73*, 84-88.

(70) El-Aneed, A.; Cohen, A.; Banoub, J. Mass spectrometry, review of the basics: electrospray, MALDI, and commonly used mass analyzers. *Appl. Spectrosc. Rev.* **2009**, *44*, 210-230.

(71) Hoffmann, E. d.; Stroobant, V. *Mass spectrometry: principles and applications*. 3rd ed.; John Wiley & Sons: Chichester, 2007.

(72) Kebarle, P.; Verkerk, U. H. Electrospray: From ions in solution to ions in the gas phase, what we know now. *Mass Spectrom. Rev.* **2009**, *28*, 898-917.

(73) Hendrickson, C. Tools of the trade. http://www.magnet.fsu.edu/education/tutorials/tools/ (accessed June 6, 2011).

(74) Harvey, D. J. Matrix-assisted laser desorption/ionization mass spectrometry of carbohydrates. *Mass Spectrom. Rev.* **1999**, *18*, 349-450.

(75) Muddiman, D. C.; Bakhtiar, R.; Hofstadler, S. A.; Smith, R. D. Matrix-assisted laser desorption/ionization mass spectrometry. Instrumentation and applications. *J. Chem. Educ.* **1997**, *74*, 1288-1292.

(76) Mele, A.; Malpezzi, L. Noncovalent association phenomena of 2,5-dihydroxybenzoic acid with cyclic and linear oligosaccharides. A matrix-assisted laser desorption/ionization time-of-flight mass spectrometric and X-ray crystallographic study. *J. Am. Soc. Mass Spectrom.* **2000**, *11*, 228-236.

(77) Finke, B.; Stahl, B.; Pfenninger, A.; Karas, M.; Daniel, H.; Sawatzki, G. Analysis of high molecular weight oligosaccharides from human milk by liquid chromatography and MALDI-MS. *Anal. Chem.* **1999**, *71*, 3755-3762.

(78) Nunes, F. M.; Reis, A.; Silva, A. M. S.; Domingues, M. R. M.; Coimbra, M. A. Rhamnoarabinosyl and rhamnoarabinoarabinosyl side chains as structural features of coffee arabinogalactans. *Phytochemistry* **2008**, *69*, 1573-1585.

(79) Harvey, D. J. Analysis of carbohydrates and glycoconjugates by matrix-assisted laser desorption/ionization mass spectrometry: An update for 2003–2004. *Mass Spectrom. Rev.* **2009**, *28*, 273-361.

(80) Harvey, D. J. Collision-induced fragmentation of underivatized N-linked carbohydrates ionized by electrospray. *J. Mass Spectrom.* **2000**, *35*, 1178-1190.

(81) Domon, B.; Costello, C. E. A systematic nomenclature for carbohydrate fragmentations in FAB-MS/MS spectra of glycoconjugates *Glycoconjugate J.* **1988**, *5*, 397-409.

(82) Simões, J.; Nunes, F. M.; Domingues, M. R. M.; Coimbra, M. A. Structural features of partially acetylated coffee galactomannans presenting immunostimulatory activity. *Carbohydr. Polym.* **2010**, *79*, 397-402.

(83) Ciucanu, I.; Kerek, F. A simple and rapid method for the permethylation of carbohydrates. *Carbohydr. Res.* **1984**, *131*, 209-217.

(84) Harris, P. J.; Henry, R. J.; Blakeney, A. B.; Stone, B. A. An improved procedure for the methylation analysis of oligosaccharides and polysaccharides. *Carbohydr. Res.* **1984**, *127*, 59-73.

(85) Coimbra, M. A.; Delgadillo, I.; Waldron, K. W.; Selvendran, R. R., Isolation and analysis of cell wall polymers from olive pulp. In *Modern Methods of Plant Analysis*, Linskens, H. F.; Jackson, J. F., Eds. Springer-Verlag: Berlin - Heidelberg, 1996; Vol. 17, pp 19-44.

(86) Chen, H.; Zhao, W.; Liu, N. Thermal analysis and decomposition cinetics of Chinese forest peat under nitrogen and air atmospheres. *Energy Fuels* **2011**, *25*, 797-803.

(87) Wong, S.-S.; Kasapis, S.; Tan, Y. M. Bacterial and plant cellulose modification using ultrasound irradiation. *Carbohydr. Polym.* **2009**, *77*, 280-287.

(88) Kroh, L. W. Caramelisation in food and beverages. *Food Chem.* **1994**, *51*, 373-379.

(89) Smaniotto, A.; Bertazzo, A.; Comai, S.; Traldi, P. The role of peptides and proteins in melanoidin formation. *J. Mass Spectrom.* **2009**, *44*, 410-418.

(90) Sugisawa, H.; Edo, H. The thermal degradation of sugars I. Thermal polymerization of glucose. *J. Food Sci.* **1966**, *31*, 561-565.

(91) Tas, A. C.; Kerkenaar, A.; LaVos, G. F.; Greef, J. Pyrolysis-direct chemical ionization mass spectrometry of some biopolymers in the positive and negative ionization mode. *J. Anal. Appl. Pyrolysis* **1989**, *15*, 55-70.

(92) Simões, J.; Domingues, P.; Reis, A.; Nunes, F. M.; Coimbra, M. A.; Domingues, M. R. M. Identification of anomeric configuration of underivatized reducing glucopyranosyl-glucose

disaccharides by tandem mass spectrometry and multivariate analysis. *Anal. Chem.* **2007**, *79*, 5896-5905.

(93) Asam, M. R.; Glish, G. L. Tandem mass spectrometry of alkali cationized polysaccharides in a quadrupole ion trap. *J. Am. Soc. Mass Spectrom.* **1997**, *8*, 987-995.

(94) Kroh, L. W.; Jalyschko, W.; Häseler, J. Non-volatile reaction products by heat-induced degradation of α-Glucans. Part I: Analysis of oligomeric maltodextrins and anhydrosugars. *Starch - Stärke* **1996**, *48*, 426-433.

(95) Siljeström, M.; Björck, I.; Westerlund, E. Transglycosidation reactions following heat treatment of starch – Effects on enzymic digestibility. *Starch - Stärke* **1989**, *41*, 95-100.

(96) Helleur, R. J.; Jackman, P. Thermal fragmentation analysis of neutral polysaccharides and the presence of 1,6-anhydrooligosaccharides *Can. J. Chem.* **1990**, *68*, 1038-1043.

(97) Pouwels, A. D.; Eijkel, G. B.; Arisz, P. W.; Boon, J. J. Evidence for oligomers in pyrolysates of microcrystalline cellulose. *J. Anal. Appl. Pyrolysis* **1989**, *15*, 71-84.

(98) Lédé, J.; Blanchard, F.; Boutin, O. Radiant flash pyrolysis of cellulose pellets: products and mechanisms involved in transient and steady state conditions. *Fuel* **2002**, *81*, 1269-1279.

(99) Hofmeister, G. E.; Zhou, Z.; Leary, J. A. Linkage position determination in lithium-cationized disaccharides: tandem mass spectrometry and semiempirical calculations. *J. Am. Chem. Soc.* **1991**, *113*, 5964-5970.

(100) Guerra-Hernández, E.; Ramirez-Jiménez, A.; García-Villanova, B. Glucosylisomaltol, a new indicator of browning reaction in baby cereals and bread. *J. Agric. Food Chem.* **2002**, *50*, 7282-7287.

(101) Stick, R. V.; Williams, S. J. *Carbohydrates : the essential molecules of life* 2nd ed.; Elsevier Amsterdam 2009.

(102) Simkovic, I.; Surina, I.; Vrican, M. Primary reactions of sucrose thermal degradation. *J. Anal. Appl. Pyrolysis* **2003**, *70*, 493-504.

(103) Westphal, Y.; Kühnel, S.; Schols, H. A.; Voragen, A. G. J.; Gruppen, H. LC/CE-MS tools for the analysis of complex arabino-oligosaccharides. *Carbohydr. Res.* **2010**, *345*, 2239-2251.

(104) Fang, T. T.; Bendiak, B. The stereochemical dependence of unimolecular dissociation of monosaccharide-glycolaldehyde anions in the gas phase: a basis for assignment of the stereochemistry and anomeric configuration of monosaccharides in oligosaccharides by mass spectrometry via a key discriminatory product ion of disaccharide fragmentation, m/z 221. *J. Am. Chem. Soc.* **2007**, *129*, 9721-9736.

(105) Fang, T. T.; Zirrolli, J.; Bendiak, B. Differentiation of the anomeric configuration and ring form of glucosyl-glycolaldehyde anions in the gas phase by mass spectrometry: isomeric discrimination between m/z 221 anions derived from disaccharides and chemical synthesis of m/z 221 standards. *Carbohydr. Res.* **2007**, *342*, 217-235.

(106) Loureiro, P. E. G.; Fernandes, A. J. S.; Carvalho, M. G. V. S.; Evtuguin, D. V. The assessment of chromophores in bleached cellulosic pulps employing UV-Raman spectroscopy. *Carbohydr. Res.* **2010**, *345*, 1442-1451.